NASA/CR—2018-219880

Flow Quality Survey of the 8- by 6-Foot Supersonic Wind Tunnel (2015 Test) Prior to the 9- by 15-Foot Low-Speed Wind Tunnel Acoustic Improvement Modifications

Aaron M. Johnson
Jacobs Technology, Cleveland, Ohio

October 2018

NASA STI Program . . . in Profile

Since its founding, NASA has been dedicated to the advancement of aeronautics and space science. The NASA Scientific and Technical Information (STI) Program plays a key part in helping NASA maintain this important role.

The NASA STI Program operates under the auspices of the Agency Chief Information Officer. It collects, organizes, provides for archiving, and disseminates NASA's STI. The NASA STI Program provides access to the NASA Technical Report Server—Registered (NTRS Reg) and NASA Technical Report Server—Public (NTRS) thus providing one of the largest collections of aeronautical and space science STI in the world. Results are published in both non-NASA channels and by NASA in the NASA STI Report Series, which includes the following report types:

- TECHNICAL PUBLICATION. Reports of completed research or a major significant phase of research that present the results of NASA programs and include extensive data or theoretical analysis. Includes compilations of significant scientific and technical data and information deemed to be of continuing reference value. NASA counter-part of peer-reviewed formal professional papers, but has less stringent limitations on manuscript length and extent of graphic presentations.

- TECHNICAL MEMORANDUM. Scientific and technical findings that are preliminary or of specialized interest, e.g., "quick-release" reports, working papers, and bibliographies that contain minimal annotation. Does not contain extensive analysis.

- CONTRACTOR REPORT. Scientific and technical findings by NASA-sponsored contractors and grantees.

- CONFERENCE PUBLICATION. Collected papers from scientific and technical conferences, symposia, seminars, or other meetings sponsored or co-sponsored by NASA.

- SPECIAL PUBLICATION. Scientific, technical, or historical information from NASA programs, projects, and missions, often concerned with subjects having substantial public interest.

- TECHNICAL TRANSLATION. English-language translations of foreign scientific and technical material pertinent to NASA's mission.

For more information about the NASA STI program, see the following:

- Access the NASA STI program home page at http://www.sti.nasa.gov

- E-mail your question to help@sti.nasa.gov

- Fax your question to the NASA STI Information Desk at 757-864-6500

- Telephone the NASA STI Information Desk at 757-864-9658

- Write to:
  NASA STI Program
  Mail Stop 148
  NASA Langley Research Center
  Hampton, VA 23681-2199

NASA/CR—2018-219880

Flow Quality Survey of the 8- by 6-Foot Supersonic Wind Tunnel (2015 Test) Prior to the 9- by 15-Foot Low-Speed Wind Tunnel Acoustic Improvement Modifications

Aaron M. Johnson
Jacobs Technology, Cleveland, Ohio

Prepared under Contract NNC15BA02B

National Aeronautics and
Space Administration

Glenn Research Center
Cleveland, Ohio 44135

October 2018

This work was sponsored by the Advanced Air Vehicle Program
at the NASA Glenn Research Center

Level of Review: This material has been technically reviewed by expert reviewer(s).

Available from

NASA STI Program
Mail Stop 148
NASA Langley Research Center
Hampton, VA 23681-2199

National Technical Information Service
5285 Port Royal Road
Springfield, VA 22161
703-605-6000

This report is available in electronic form at http://www.sti.nasa.gov/ and http://ntrs.nasa.gov/

Flow Quality Survey of the 8- by 6-Foot Supersonic Wind Tunnel (2015 Test) Prior to the 9- by 15-Foot Low-Speed Wind Tunnel Acoustic Improvement Modifications

Aaron M. Johnson
Jacobs Technology
Cleveland, Ohio 44135

Summary

A flow quality survey (FQS) was conducted in November 2015 to characterize the flow quality of the 8- by 6-Foot Supersonic Wind Tunnel (8×6 SWT) test section and facility air dryer prior to the start of significant structural and acoustic modifications to the 9- by 15-Foot Low-Speed Wind Tunnel (9×15 LSWT). The data from this FQS will be compared with FQS data collected after completion of the 9×15 LSWT acoustic improvement modifications. This document contains only the FQS data collected in November 2015 using the 16-in.-diameter cone cylinder and a set of 20 air dryer bed wind anemometers. The ability to reach the extents of the 8×6 SWT operating envelope with a large blockage model was verified through the 16-in.-diameter cone cylinder tests. The flow uniformity and angularity at the entrance of the facility air dryer was assessed and quantified using the air dryer bed wind anemometers.

Introduction

The tests described in this report document the flow quality survey (FQS) completed at a single axial station in the 8- by 6-Foot Supersonic Wind Tunnel (8×6 SWT) prior to structural and acoustic modifications to the 9- by 15-Foot Low-speed Wind Tunnel (9×15 LSWT). These tests are referred to in this report as the "9×15 LSWT acoustic improvement modifications." This entry is considered the ninth test section characterization entry (TSC9) in the 8×6 SWT. The data from these tests will be compared with data collected following the completion of the acoustic improvement modifications to determine if Jacobs Technology has met the aerothermal flow quality acceptance criteria defined in the facility modification project requirements.

The following are the flow quality criteria for the 9×15 LSWT acoustic improvement modifications related to the 8×6 SWT:

(1) The 8×6 SWT can reach Mach 2.0, nominally, with substantial model blockage.[1]
(2) Corner 1 static pressure stays within the allowable structural range over the 8×6 SWT operating range ($\Delta P_{S,C1} \leq 75.5$ psf).
(3) The uniformity of the flow through the air dryer beds following the 9×15 LSWT acoustic improvement modifications is less than or equal to 125 percent of the uniformity measured prior to the facility modifications for open- and closed-loop operation:

$$\sigma\left(V/\overline{V}\right)_{post} \leq 125\% \bullet \sigma\left(V/\overline{V}\right)_{pre}$$

[1]At a nominal test section Mach number of 2.0, the actual freestream Mach number is typically 1.982 (according to Table I in Ref. 1).

The acceptance criteria were developed by Jacobs Technology, 8×6 SWT and 9×15 LSWT facility engineers and manager, and the NASA Glenn Research Center wind tunnel calibration team. The tests and data in this document pertain only to the 2015 FQS entry. Where appropriate, descriptions and figures of the facility, hardware, instrumentation, etc., have been reproduced from the 1996 to 1997 test entry calibration report (Ref. 1), as this FQS repeats similar tests with the same or similar hardware and instrumentation.

Nomenclature

Symbols

M	Mach number
P	pressure
V	velocity
$\bar{V}$	mean velocity in the air dryer bed inlet plane
X	distance or position in the axial or streamwise direction
x/D	ratio of axial distance to model diameter; typically used for cone cylinder models
β	yaw flow angle
σ	standard deviation

Subscripts

avg	denotes the mean value of a set of data
axial	refers to a measured or calculated parameter (e.g., velocity) moving in the axial or streamwise direction
*C*1	refers to a measurement taken in corner 1 of the 8×6 SWT and 9×15 LSWT loop
cone	refers to a parameter using only the pressures measured or Mach number calculated on the cone surface of the cone cylinder model
cyl	refers to a parameter using only the pressures measured or Mach number calculated on the cylinder of the cone cylinder model
DBA	refers to a value pertaining to measurements taken by an air dryer bed anemometer
fs	refers to a local freestream parameter, typically calculated through theoretical relationships (e.g., $M_{fs,cone}$)
i	typically refers to the i^{th} probe in a set or array of probes
lateral	refers to a measured or calculated parameter (e.g., velocity) moving perpendicularly to the axial or streamwise direction in the X-Y plane
model	refers to a measurement taken by the model in the test section, such as the 16-in.-diameter cone cylinder model
post	refers to measurement or value obtained following the completion of the 9×15 LSWT acoustic improvement modifications
pre	refers to measurement of value obtained before the start of the 9×15 LSWT acoustic improvement modifications
S	static condition of a given parameter (e.g., P_S = static pressure)
T	stagnation condition of a given parameter (e.g., P_T = stagnation pressure)
TS	refers to a calibrated test section parameter

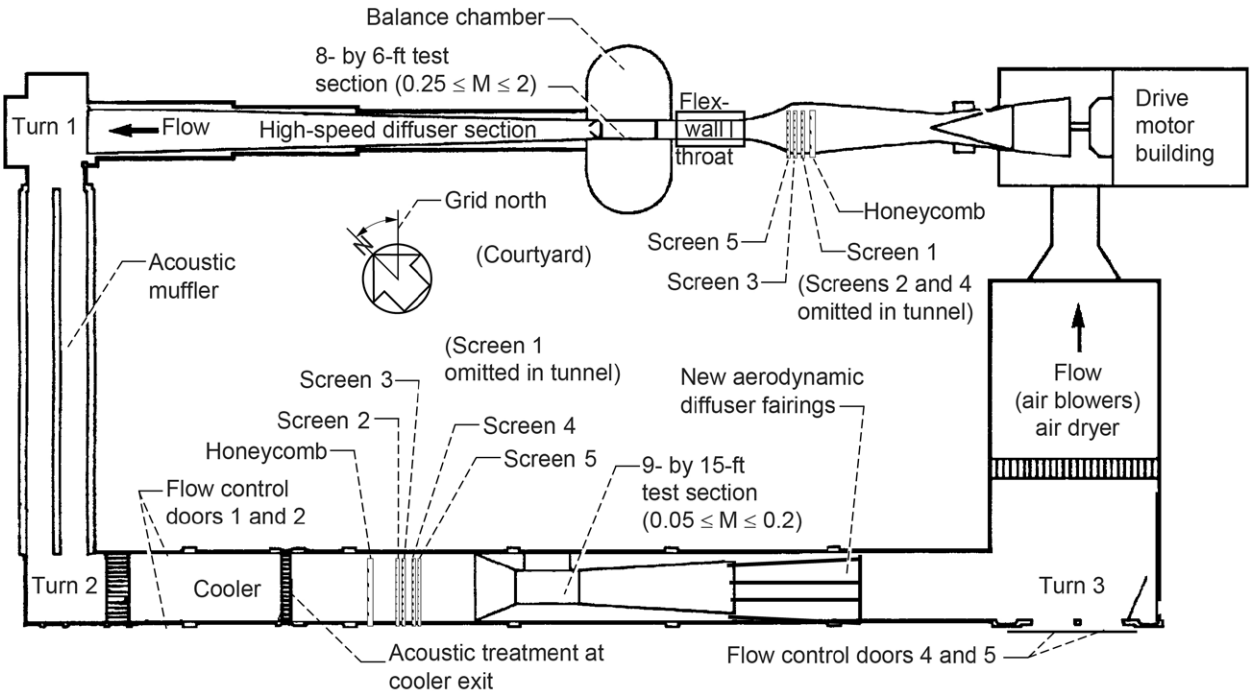

Figure 1.—Plan view of 8- by 6-Foot Supersonic and 9- by 15-Foot Low-speed Wind Tunnel facility (Ref. 1).

Description of Facility[2]

The 8- by 6-Foot Supersonic and 9- by 15-Foot Low-Speed Wind Tunnel complex, shown in Figure 1, is an atmospheric-pressure, continuous-flow propulsion wind tunnel. The airflow is driven through the facility by a seven-stage axial compressor (18-ft inlet diam.) powered by three 29,000-hp electric motors. The 8- by 6-ft test section is a porous-wall-type transonic test section with a Mach number range of 0.25 to 2.0. The 9- by 15-ft test section is located in the return leg of the 8- by 6-ft wind tunnel loop. The 8- by 6-ft test section walls, floor, and ceiling have no divergence over the 23-ft, 6-in. length of the test section. The test section consists of a solid-wall supersonic flow region (9-ft, 1-in. length) followed by a porous-wall transonic region (14 ft, 5 in.). The Mach number range in the transonic test section is 0.36 to 2.0 for standard operation using all three drive motors. There are six configurations for the transonic test section based on the length of the porous area used and the open area of the test section surfaces:

(1) 14 ft, 5.8-percent porosity
(2) 8 ft, 6.2-percent porosity
(3) 8 ft, 3.1-percent porosity
(4) 8 ft, 6.2-percent porosity modified
(5) 8 ft, 3.1-percent porosity modified
(6) 14 ft, schlieren windows installed

The 14-ft transonic test section uses the entire length of the porous area; the 8-ft test section is the aft 8 ft of the porous test section (Figure 2). The tunnel can be operated in either an aerodynamic (closed-loop) or propulsion (open-loop) cycle (for propulsion cycle, flow control doors 1 and 2 are open so that the airflow is exhausted from the tunnel).

[2]Adapted from Reference 1.

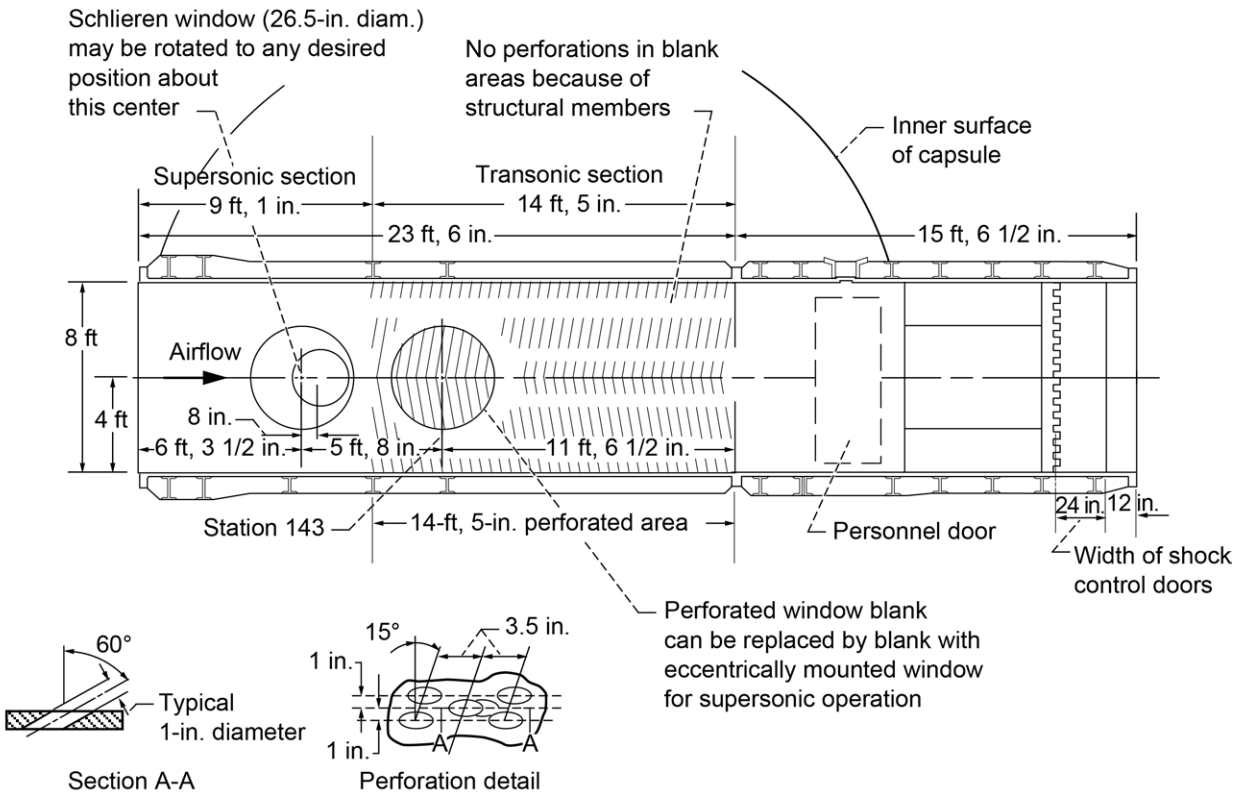

Figure 2.—Elevation view of 8- by 6-Foot Supersonic Wind Tunnel test section (Ref. 1).

The conditions in the 8- by 6-ft test section were set by controlling compressor speed, flexible wall position, balance chamber pressure (test section bleed), and shock door (second throat) position. For standard operation of the drive system, the test section Mach number range is 0.36 to 2.0. In order to reduce the test section Mach number below 0.36, it was necessary to slow the compressor speed. This was done by powering the compressor using only one of the three electric drive motors. By operating in this mode, it was possible to expand the operational envelope of the facility by reducing the low-end Mach number to 0.25. Very low speed conditions (below Mach 0.1) can be achieved in the 8- by 6-ft test section by using only the air dryer building air circulation fans (the eight fans are used to pull air through the air dryer building to cool the desiccant beds; by properly configuring the tunnel and air dryer flow control doors, the fans will push air through the 8- by 6-ft test section).

Flow quality improvements were installed in the facility in 1992. The improvements that affect the 8- by 6-ft test section are a flow-straightening honeycomb and three 10-mesh turbulence reduction screens in the settling chamber upstream of the test section as well as an aerodynamically contoured compressor exit tailcone fairing. A more complete description of the 8×6 SWT is found in Reference 2.

Instrumentation and Test Hardware[3]

Existing and newly acquired hardware and instrumentation were used for the 2015 FQS. The 16-in.-diameter cone cylinder model has been used in previous 8×6 SWT characterization test entries, and the wind anemometers were acquired specifically for the pre- and post-construction test entries to assess flow

[3]Adapted from Reference 1.

uniformity in the facility air dryer inlet. Each of the instruments, their associated support systems, and their locations are described below.

16-in. Cone Cylinder

The cone cylinders are used to measure the axial static pressure and Mach number distributions. The 16-in. cone cylinder was chosen for this test entry from the family of cone cylinder models available for use in the 8×6 SWT. The family of cone cylinder models consists of 4-, 8-, 12-, 16-, and 20-in.-diameter models. The 4-in.-diameter model is typically used to provide empty test-section calibration data; the larger diameter models provide blockage effect data. The 16-in. model (2.91-percent blockage) is approximately 120 in. long and has a total of 226 static pressure taps. See Figure 3 for details on the 16-in. cone cylinder and instrumentation layout.

Each cone cylinder model consists of a 10° half-angle cone with base diameter as noted above, which extends into a constant-diameter cylinder. Each model is instrumented with static taps arranged in four axial rows spaced 90° apart. The cone cylinder models are sting mounted into the tunnel transonic strut. Axial position changes of the model in the tunnel are accomplished by means of a split sting section, which can be added to or removed from the model assembly without disconnecting the instrumentation lines. The split sting section allows for an axial position change of 34 in. The tip of the cone cylinders can be positioned at either the inlet of the 8-ft test section or the centerline of the schlieren window blanks in the 14-ft test section. For the 2015 FQS, the 16-in. cone cylinder did not use the split sting, positioning the cone cylinder tip at the inlet of the 8-ft test section; the tip of the cone cylinder was located at test section station (TSTA) 177.375 during the 2015 FQS entry. See Figure 4 showing the 16-in. cone cylinder installed during this entry.

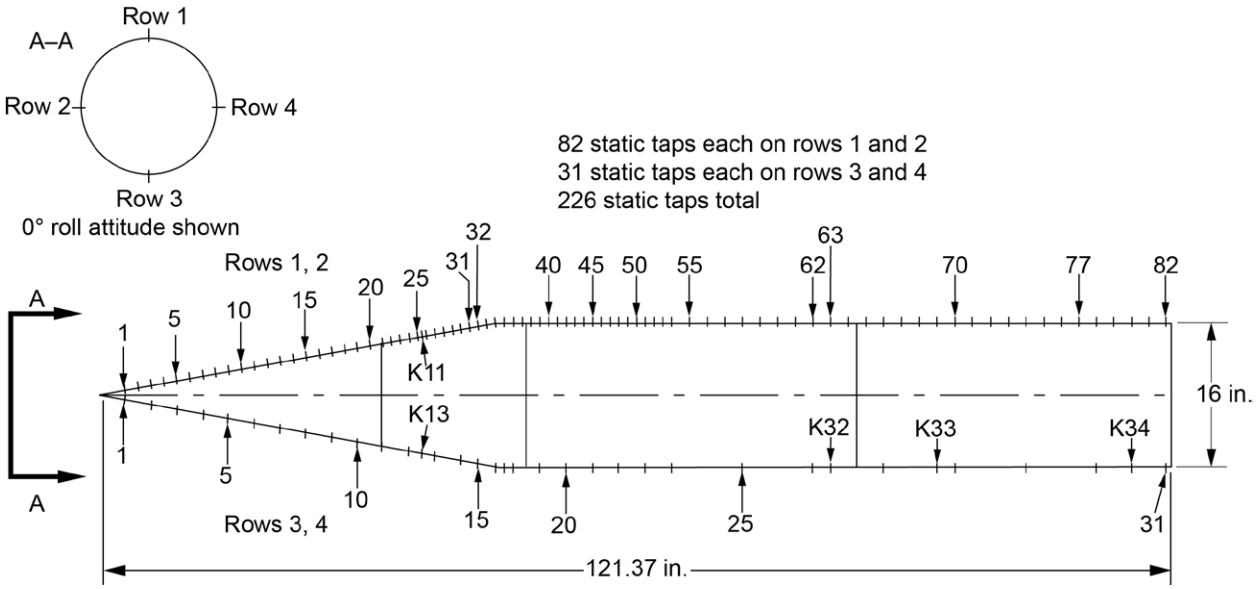

Figure 3.—Diagram of 16-in.-diameter cone cylinder model showing static pressure port locations and general dimensions, in.

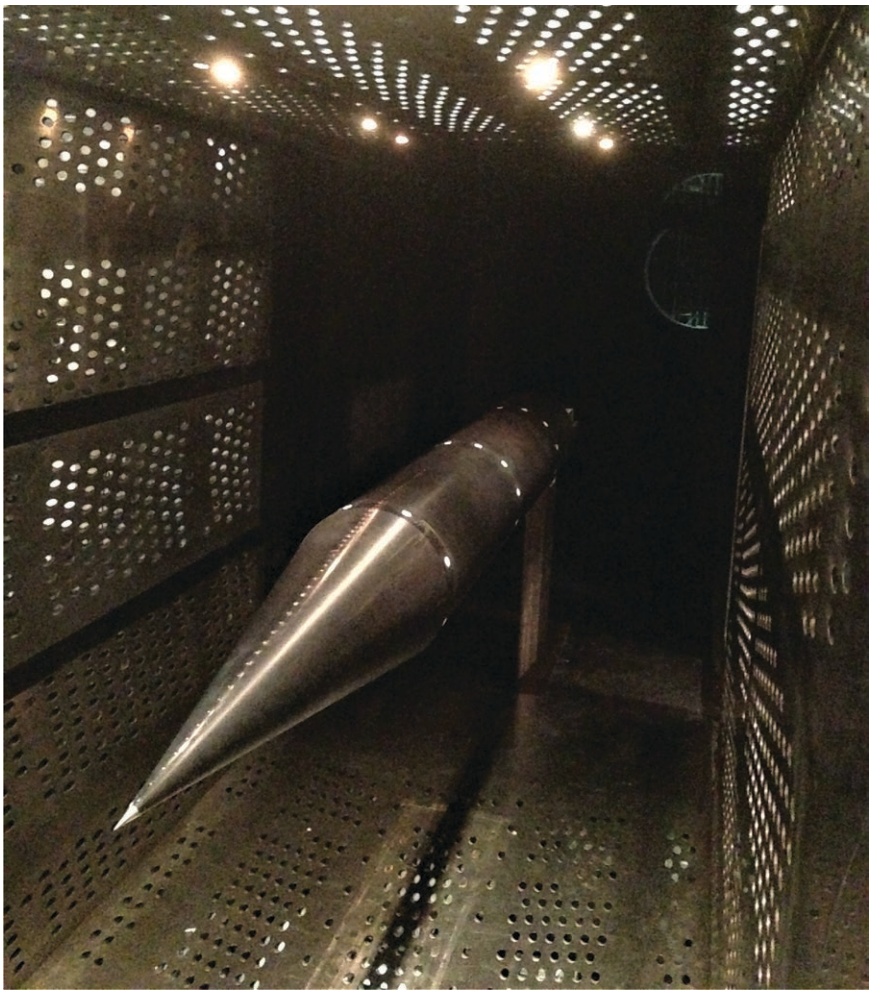

Figure 4.—16-in. cone cylinder installed at inlet of 8-ft test section in 8- by 6-Foot Supersonic Wind Tunnel for ninth test section characterization entry (TSC9).

Air Dryer Bed Wind Anemometers

Twenty Davis 7911 wind anemometers were purchased for use in the air dryer beds as part of the 2015 FQS of the 8×6 SWT. These anemometers are capable of measuring wind speeds up to 200 mph and wind direction (0° to 360°) in a plane. The anemometers were oriented such that the weather vane on the top of the unit could measure the component of flow angle in the yaw direction (as opposed to pitch direction). Figure 5 shows a diagram of the anemometers installed in the dryer building. The anemometers were installed such that the anemometers were located at the center of each of the 20 openings in the air dryer bed building (5 high by 4 across) at the entrance plane on the upstream side of the air dryer beds. The air dryer building is approximately 47.75 ft tall by 70 ft wide. A pipe that vertically spans the entrance to each of the 20 air dryer bed openings is used as a mounting point for each anemometer. The anemometers are cantilevered away from these pipes perpendicular to the approaching flow such that the pipe is neither upstream nor downstream of the anemometer and the anemometer is closer to the center of the air dryer bed building than the pipe to which it is mounted. Air dryer bed anemometer number 1 is located at the top left of the building if standing upstream of the air dryer bed openings looking downstream. The anemometer number increases monotonically from left to right in each row (e.g., anemometer number 20 is in the bottom right corner of the building).

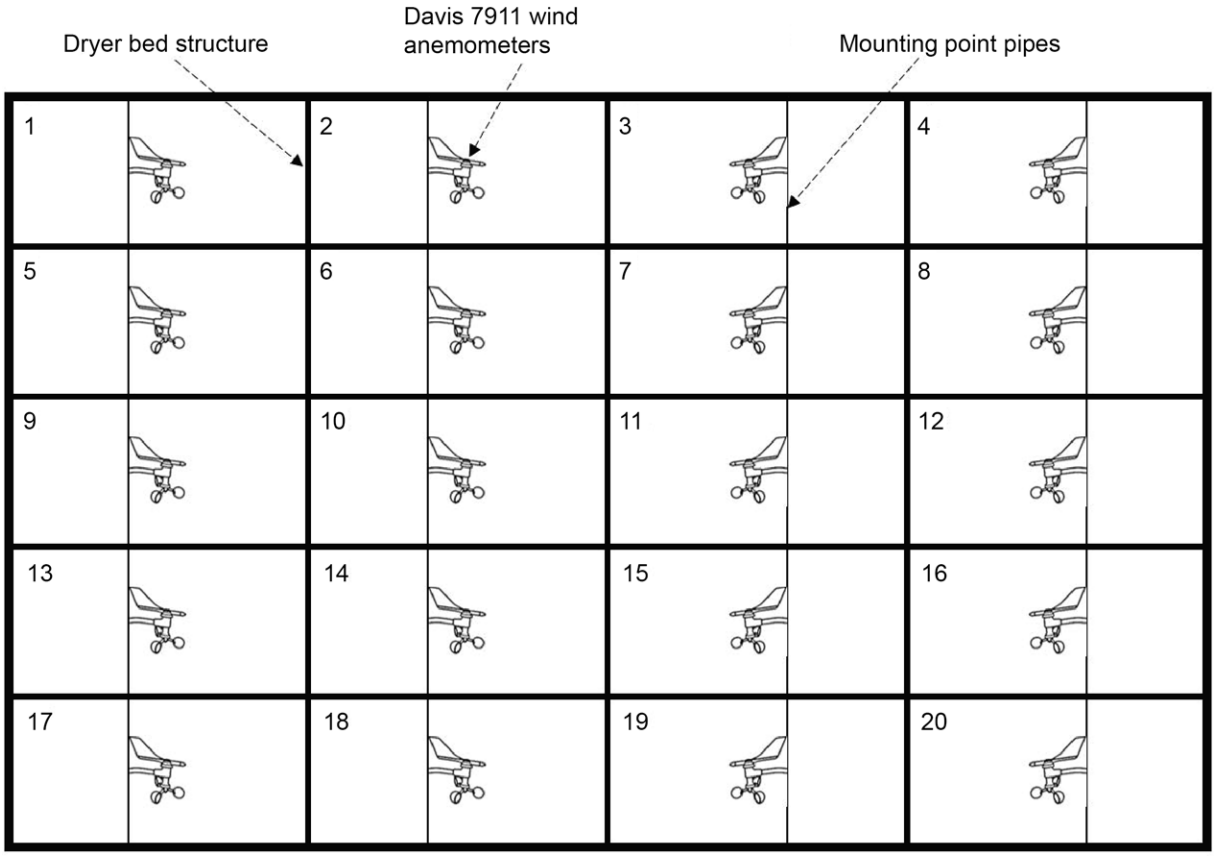

Figure 5.—Air dryer bed wind anemometer layout at inlet to 8×6 and 9×15 facility air dryer beds if standing upstream of air dryer bed openings looking downstream.

Facility Instrumentation

The following permanent facility instrumentation was used during the 2015 FQS:

Bellmouth Rakes

Two wall-mounted rakes are located near the exit of the bellmouth upstream of the test section. One rake is mounted to the north tunnel wall and the other to the south tunnel wall at approximately the tunnel centerline (the rakes are designated “north” and “south”; see Figure 6). The instrumentation mounted on each rake consists of four total pressure and two total temperature probes. Each rake has a fifth pitot tube devoted to the tunnel control system, and one of the four total temperature probes is devoted to the tunnel control system. During the 2015 FQS, the total temperature probes on the bellmouth rakes were Type K ball-joint thermocouples without shielding or aspirated tips.

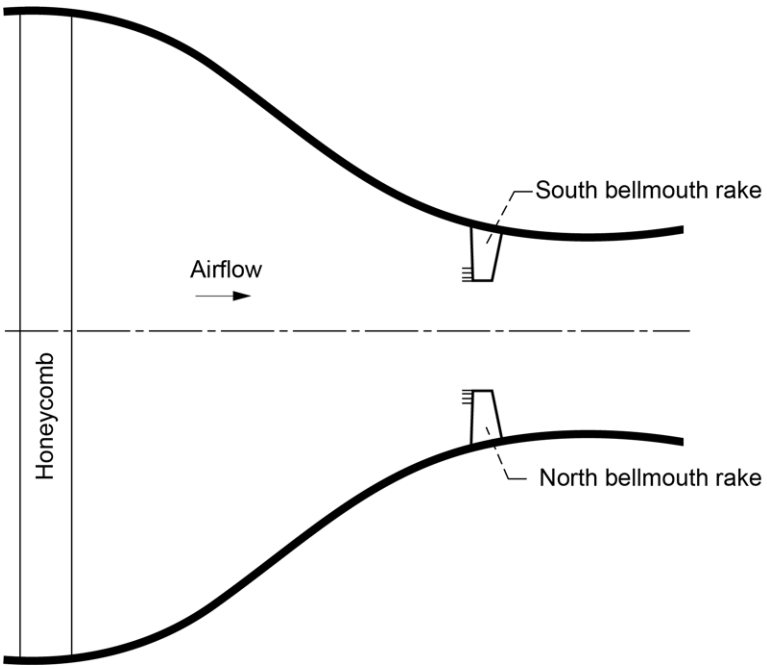

Figure 6.—Installation of bellmouth total pressure, total temperature rakes upstream of 8- by 6-Foot Supersonic Wind Tunnel test section and flexwall (Ref. 1).

Facility Static Pressures

Figure 7 shows the location of all static pressure taps located on the ceiling of the 8- by 6-ft test section and high-speed diffuser section.

Data Systems

The standard tunnel data system was used for the 2015 FQS entry. Steady-state pressure data was acquired with an electronically scanned pressure (ESP) system. The ESP system uses plug-in modules, each containing 32 individual transducers, which can be addressed and scanned at a rate of 10,000 ports per second. On-line calibration of all ESP transducers can be performed automatically every 2 hr or at the discretion of the test engineer. Calibration is carried out by the operation of a pneumatic valve in each module that allows three pressures, measured with precision digital quartz transducers, to be applied. Throughout the test entry, the ESP transducers were calibrated every 2 hr or when convenient between Mach number settings. For this test entry, ±15-psid rack-mounted modules were used.[4]

Real-time data acquisition and display was provided by Escort D+, the standard data system used in the large test facilities at the NASA Glenn Research Center. This system accommodates the ESP inputs as well as all steady-state analog and digital signals used, including facility thermocouples and pertinent tunnel control parameters such as compressor speed, shock door positions, and positions of flow control doors 1 and 2. The Escort D+ facility microcomputer acquires these data, converts them to engineering units, executes calculations, checks limits on selected channels, and displays the information in alphanumeric and graphical form with a 1-sec update rate. For this test, each collected data reading was the average of 100 scans (100 sec) of data.

[4]A 64-port, ±5-psid mini-module was used to scan the solid-walled, supersonic test section static pressure taps for the preliminary supersonic test section calibration entry, which occurred immediately after the removal of the 16-in. cone cylinder and installation of the transonic array. Results of this test are not included in this document.

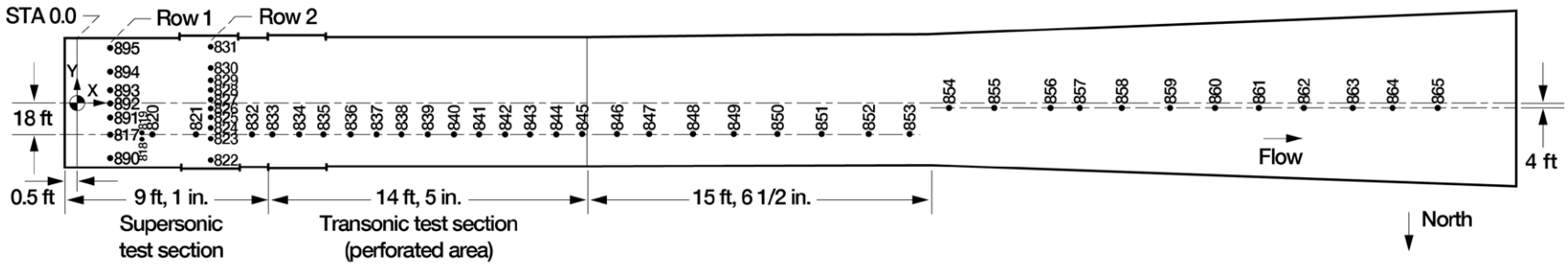

Static tap location	Axial station, X, in.	Distance from centerline, Y, in.	Static tap location	Axial station, X, in.	Distance from centerline, Y, in.
817	17.00	–18.00	838	169.25	–18.00
890	17.00	–30.63	839	183.25	–18.00
891	17.00	–7.50	840	197.50	–18.00
892	17.00	0.00	841	211.50	–18.00
893	17.00	7.56	842	225.50	–18.00
894	17.00	18.06	843	239.50	–18.00
895	17.00	25.78	844	253.38	–18.00
818	32.88	–19.56	845	267.63	–18.00
819	32.88	– 16.56	846	286.50	–18.00
820	39.31	–18.00	847	303.75	–18.00
821	63.31	–18.00	848	327.50	–18.00
822	72.25	–31.50	849	350.50	–18.00
823	72.25	–19.50	850	374.06	–18.00
824	72.25	–13.50	851	398.75	–18.00
825	72.25	–7.50	852	422.63	–18.00
826	72.25	–2.50	853	446.00	–18.00
827	72.25	2.50	854	473.38	–4.00
828	72.25	7.50	855	497.44	–4.00
829	72.25	13.50	856	528.19	–4.00
830	72.25	19.50	857	543.31	–4.00
831	72.25	31.50	858	567.19	–4.00
832	87.50	–18.00	859	593.25	–4.00
833	99.25	–18.00	860	617.31	–4.00
834	113.25	–18.00	861	641.25	–4.00
835	127.25	–18.00	862	665.25	–4.00
836	141.38	–18.00	863	692.31	–4.00
837	155.75	–18.00	864	713.25	–4.00
			865	736.94	–4.00

Figure 7.—Ceiling static tap locations in test section and diffuser of 8- by 6-Foot Supersonic Wind Tunnel. All dimensions are in inches unless otherwise noted (Ref. 1).

Test Setup and Procedures

The test procedures specific to each piece of characterization hardware are described in the following sections.

16-in. Cone Cylinder

End-to-end checks of all instrumentation lines were conducted following installation of the cone cylinder model in the test section. Any issues were resolved prior to testing and noted in the test log. Prior to each run, the cone cylinder was positioned such that the tip was at the test section centerline and leveled in the pitch using a digital inclinometer. During a typical tunnel run, the highest Mach number condition was set first to preserve air dryer capacity, and then the Mach number was reduced incrementally to cover the planned test matrix. Due to issues with drive motor 1 during the test entry, several conditions were approached from below: Mach 1.3 to 2.0 in closed-loop operating mode and Mach 1.6 in open-loop operating mode.

Air Dryer Bed Wind Anemometers

Prior to installation, the 20 wind anemometers were calibrated by facility electrical engineers for voltage output at given angles of the weather vanes. The calibration was completed for ±60° with 0° representing flow approaching the air dryer beds perpendicularly to the air dryer bed inlet plane. First-order curve fits were applied to all anemometer flow angle calibrations; therefore, all angles measured outside of ±60° are extrapolated, although the performance of the anemometers' weather vanes is typically linear at all angles. The wind speed is proportional to the number of revolutions of the cups per hour; the wind speed is computed using the relationship 1 mph = 1600 r/hr.

Prior to each run that involved the use of dry air, a reactivation of the air dryer beds was completed. During a reactivation, the air dryer bed wind anemometers were removed due to the high temperatures in the air dryer building and installed during the shift before the run. Each anemometer was checked for operability and continuity with the DEWETRON data system before each run. Data were acquired by the air dryer bed anemometers continuously during the 2015 FQS runs. The data were collected at a rate of 1 kHz and then averaged to 1-sec samples for ease of processing and comparison to the steady-state data acquired by Escort D+.

Test Matrix

The FQS in the 8×6 SWT intended to cover the full operating envelope of the facility: Mach 0.25 to 2.0 in both open- and closed-loop operating mode. In open-loop (propulsion) operating mode, air is brought into the tunnel circuit through facility doors 4 and 5 and exhausted through doors 1 and 2 (refer to Figure 1). Operating the facility in open-loop versus closed-loop (aerodynamic) operating mode has been shown not to have an effect on the test section operating conditions in terms of flow quality or operating condition; however, there is a potential for reduced operating time on dry air when in open-loop operating mode.

Due to issues with drive motor 1 during the test entry, the whole operating envelope was not completed. Data at the following conditions were collected:

- Mach 1.3 to 2.0 in 0.1 increments; closed loop (three drive motor operation)[5]

[5]Mach 1.3 in closed-loop operating mode was completed with facility doors 4 and 5 partially open, a mode commonly referred to as "modified closed loop."

- Mach 1.6 to 0.4 in 0.1 decrements; open loop (three drive motor operation)
- Mach 0.5, 0.4, 0.3, and 0.25; open loop (one drive motor operation)

All conditions at and above Mach 1.2 were completed with the air dryer beds enabled, referred to as "dry air." All conditions below Mach 1.2 were completed without use of the air dryer beds, referred to as "wet air." The test section was set to configuration 6 (14-ft test section, all porosity holes open with solid schlieren windows installed in transonic test section) for the duration of this test entry. At each condition, a single 100-sec reading was recorded. For all testing, a detailed log was maintained to track test points, collected data reading numbers, hardware and instrumentation problems, etc. Online data monitoring was used to ensure data quality.

Data Reduction[6]

The data analysis methodology used for each part of the calibration tests is described in the following sections. The information presented here applies to the general treatment of the data; for some specific applications, details of the data reduction are included in the discussion section.

The first step of the data reduction and analysis was a thorough review of the data to ensure data quality. While most instrumentation and data problems were detected and resolved either prior to or during the testing, there were instances where bad or questionable data were collected and editing of the data was required (e.g., bad data points were flagged and therefore not used in subsequent steps of the analysis). Notes taken during the testing as part of the test engineers' log proved invaluable in troubleshooting problems with data channels and test configurations. At the completion of the test entry, the data were reprocessed using programs that mimicked the online data reduction. This step corrected any errors in the data from instrumentation problems or test setup errors. A majority of the post-test analyses were performed by custom scripts in MATLAB (The MathWorks, Inc.).

During a leak check of the 16-in. cone cylinder pressure tubing following this test entry, the NASA Glenn Research Center instrumentation shop determined that several pressure tubes were unable to hold vacuum. A majority of these pressure tubes that were found to have leaks were located on the aft portion of the cylinder. All measurements from the pressure ports shown to be compromised were removed from the analysis to avoid biasing the results.

16-in. Cone Cylinder

A detailed description of the development of the cone cylinder data analysis methodology is contained in Reference 3, but an abbreviated explanation is included here. The average static pressure on the cone portion of the model was used to determine the local freestream Mach number and static pressure for supersonic conditions; a theoretical relationship between a cone cylinder model's cone surface static pressure and the freestream Mach number exists for supersonic conditions (see Ref. 3 for details). The average static pressure over the aft portion of the cylinder provides a reasonable measurement of the freestream static pressure for all Mach number settings; however, it is assumed that the static pressure has not fully recovered at any point along the length of the 16-in.-diameter model due to the expansion over the cone's shoulder.

The following were computed to assess the freestream Mach number:

$M_{cyl,avg}$ Average Mach number over the aft 40 in. of the cylinder using cylinder static pressure and test section freestream total pressure.

[6]Adapted from Reference 1.

$M_{fs,cone}$ Freestream Mach number computed from the theoretical relationship between the average cone pressure ratio ($P_{S,cone}/P_{T,TS}$) and the freestream Mach number (refer to Table V(a) in Ref. 3; only valid for supersonic test section conditions). $P_{S,cone}$ is the average pressure measured on the cone.

The following were computed to assess the freestream static pressure:

$P_{S,cyl,avg}$ Average pressure measured along the aft 40 in. of the cylinder.

$P_{S,fs,cone}$ Freestream static pressure computed from the theoretical Mach number, $M_{fs,cone}$, based on the average of the cone pressure measurements (only valid for supersonic test section conditions).

Air Dryer Bed Wind Anemometers

In post processing, the time stamps from the anemometer samples were compared with those of the Escort D+ readings taken to match the proper air dryer bed measurements to the corresponding facility/8×6 test section operating conditions. A positive yaw flow angle (+$\beta_{i,DBA}$, where *DBA* represents an air dryer bed anemometer measurement) measured by the anemometers is defined as follows: when upstream looking aft, flow pointing toward the outer wall of the dryer building. In Figure 5, a positive yaw flow angle would indicate that air travels from left to right. Using the measured yaw flow angle and the magnitude of the airspeed, the airspeed (V_i) can be decomposed into axial (streamwise) and lateral (side-to-side) velocity components using the following equations:

$$V_{i,axial} = V_i * \cos\left(\beta_{i,DBA}\right) \tag{1}$$

$$V_{i,lateral} = V_i * \sin\left(\beta_{i,DBA}\right) \tag{2}$$

where V_i is the magnitude of the airspeed (or velocity) measured at air dryer bed anemometer *i* and β_i is the yaw flow angle measured at air dryer bed anemometer *i*. As part of the acceptance criteria set by Jacobs Technology and NASA for the 9×15 LSWT acoustic improvement modifications, the flow uniformity through the air dryer beds across the operating envelope of the 8×6 SWT needed to be quantified for comparison of pre- and post-construction results. The axial velocity is assessed for uniformity by taking a standard deviation of the 20 anemometer axial velocity measurements normalized by the mean axial velocity at that condition across the 20 anemometers, $\bar{V}$.

$$\sigma\left(V/\bar{V}\right) = \sqrt{\frac{\sum_{i=1}^{20}\left(V_i/\bar{V} - \overline{\left(V_i/\bar{V}\right)}\right)^2}{20}} \tag{3}$$

The lateral uniformity of the velocity was not assessed. The mean lateral velocity is typically near zero because the yaw flow angle, and thus the lateral velocity at the air dryer bed inlet, tends to be symmetrical. This results in large values of $V_i/\bar{V}$, which does not necessarily indicate poor uniformity. Additionally, the lateral velocity does not have a large impact on the performance of the air dryer bed; the axial velocity through the different sections of the air dryer bed is of greater importance in determining the relative efficiency of the air dryer beds' sections. As a measure of the degree of lateral airflow, the root mean square (RMS) of the yaw flow angle was calculated for each test section/facility condition.

$$\mathrm{RMS}\left(\beta_{DBA}\right)=\sqrt{\frac{\sum_{i=1}^{20}\left(\beta_{i,DBA}\right)^2}{20}} \tag{4}$$

Discussion of Results

Data were acquired for 8×6 test section conditions of Mach 2.0 to 1.3 in closed-loop (aerodynamic) operating mode and Mach 1.6 to 0.25 in open-loop (propulsion) operating mode. All conditions at Mach 1.2 and above were in "dry-air" mode (air dryer beds enabled), and conditions at Mach 1.1 and below were in "wet-air" mode.[7] Due to issues with the facility drive system and the resulting schedule delays during the 2015 FQS testing, a full survey of open- and closed-loop operation across the full 8×6 SWT operating envelope was not completed as desired.

16-in. Cone Cylinder

The cone cylinder static pressure profile along the length of the model normalized by the test section total pressure, $P_{T,TS}$, is shown in Figure 8 to Figure 14 for each test section condition completed during the test entry. These profile plots display the average pressure ratio at each static pressure port axial station along the cone cylinder model, which is either the average of two or four static pressure measurements. For supersonic conditions, the figures show the theoretical pressure ratio along the length of the model for a given freestream Mach number, using the test section calibrated Mach number, M_{TS}, as the freestream Mach number (refer to Table VI(a) in Ref. 3). In the pressure ratio profiles, those that display data collected at supersonic test section conditions show $P_{S,cyl,avg}$ and $P_{S,fs,cone}$ located arbitrarily aft of the last cylinder measurements for easy comparison. The value of $P_{S,cyl,avg}$ is shown for subsonic conditions as well. These values are normalized by the test section total pressure, $P_{T,TS}$, in Figure 8 to Figure 14.

The Mach number profile on the cone cylinder model, computed using the freestream total pressure, is shown in Figure 15 to Figure 21. For supersonic conditions, the figures show the theoretical Mach number along the length of the model for a given freestream Mach number, using the test section calibrated Mach number, M_{TS}, as the freestream Mach number (refer to Table VI(a) in Ref. 3). As with the pressure ratio profile figures, additional Mach number information ($M_{cyl,avg}$ and $M_{fs,cone}$) is located aft of the last cylinder measurements for comparison.

For calibration of the static pressure in the 8×6 SWT transonic test section, the 4-in. cone cylinder model is typically used. The static pressures downstream of $x/D = 10$ on a cone cylinder model (10 times the model diam.) are considered constant. Past analyses of 4-in. cone cylinder data used pressure data aft of $x/D = 11.5$ for freestream static pressure measurements (Ref. 3). The location of $x/D = 10$ for the 16-in. cone cylinder model falls past the end of the model, so true freestream static pressure measurements cannot be confidently made with this model; the static pressure measured at the aftmost pressure taps of the 16-in. cone cylinder model is assumed not to have fully recovered to freestream static pressure after expanding over the shoulder of the model. The choice to use the aft 40 in. of the cylinder's data for an average cylinder pressure measurement (e.g., $P_{S,cyl,avg}$) was made to match the length of the model over which the 4-in. cone cylinder averages its static pressure data. That being said, this data set will not be used to create any test section calibration relationships; however, it will be used to compare the pre- and post-construction FQS results.

[7]Mach 1.3 closed-loop data were acquired with facility doors 4 and 5 open. Mach 0.5 and 0.4 were repeated for both three-motor and one-motor operation with all Mach numbers above Mach 0.5 using three motors and all below Mach 0.4 using only drive motor 1.

Corner 1 Static Pressure

During operation of the 8×6 SWT, the difference in corner 1 static pressure and atmospheric pressure is monitored. The full operating envelope of both the 8×6 SWT and the 9×15 LSWT needs to be accomplished with this delta pressure below 75.5 psf due to structural limitations in this region of the tunnel. During this test entry, the delta pressure in corner 1 was monitored and recorded by the tunnel control system for each of the test conditions completed. Table I shows the corner 1 static pressure delta at each operating condition, and all values fall below 75.5 psf.[8]

TABLE I.—TABULATED AIR DRYER BED WIND ANEMOMETER AXIAL VELOCITY STANDARD DEVIATIONS, YAW FLOW ANGLE ROOT MEAN SQUARE VALUES, AND CORNER 1 STATIC PRESSURE DIFFERENTIALS FOR EVERY 8×6 SUPERSONIC WIND TUNNEL TEST SECTIONCONDITION PERFORMED DURING 2015 FLOW QUALITY SURVEY (NINTH TEST SECTION CHARACTERIZATION ENTRY)[a]

	Nominal 8×6 SWT Mach number	M_{TS}	$\sigma\left(V/\bar{V}\right)$	RMS(β_{DBA}), deg	$\Delta P_{S,C1}$, psf
Closed loop	2.00	1.970	0.476	32.606	54.570
	1.90	1.881	0.487	33.190	57.168
	1.80	1.779	0.485	33.209	62.885
	1.70	1.676	0.478	32.596	66.004
	1.60	1.568	0.481	33.155	68.602
	1.50	1.467	0.475	32.595	69.122
	1.40	1.363	0.481	32.975	68.602
	1.30[b]	1.262	0.478	32.658	70.161
Open loop	1.60	1.574	0.300	18.346	10.914
	1.50	1.469	0.300	18.197	10.914
	1.40	1.364	0.302	18.791	10.914
	1.30	1.264	0.302	18.260	10.914
	1.20	1.195	0.306	20.594	10.914
	1.10	1.081	0.698	44.613	10.914
	0.90	0.900	0.698	40.422	10.914
	0.80	0.799	0.696	44.046	10.914
	0.70	0.701	0.701	43.128	10.914
	0.60	0.600	0.705	47.428	7.796
	0.50	0.500	0.726	45.053	7.796
	0.40	0.400	0.756	44.680	5.197
	0.50	0.500	0.741	46.830	5.197
	0.40	0.401	0.767	44.424	5.197
	0.30	0.300	0.814	42.987	2.599
	0.25	0.250	0.840	41.928	2.599

[a]"Dry air" is only used at nominal Mach numbers greater than or equal to Mach 1.20.

[b]Facility doors 4 and 5 partially open during test condition (modified closed loop).

[8]Facility engineers noted in the run log notes that the corner 1 pressure differential reached 13.9 in. of water (72.3 psf), which is still below the 75.5 psf limit; partially opening doors 4 and 5 relieved some of the pressure when at Mach 1.3 closed loop.

Air Dryer Bed Wind Anemometers

Table I also shows the tabulated standard deviation of the axial velocity component through the air dryer beds, $\sigma\left(V/\bar{V}\right)$, and RMS of the yaw flow angle, β_{DBA}, for each tunnel setting completed during the entry. Figure 22 to Figure 45 show contour maps of the yaw flow angle at the air dryer bed inlet if upstream looking aft for all 8×6 SWT test section conditions completed during the test entry. The axial and lateral airspeed contour maps are shown in Figure 46 to Figure 69. Lastly, the yaw flow angle, axial airspeed, and lateral airspeed measurements for each anemometer are shown in Figure 70 to Figure 93.

Concluding Remarks

The flow quality survey (FQS) of the 8- by 6-Foot Supersonic Wind Tunnel (8×6 SWT) was completed in a single test entry in 2015. This entry was necessary to capture the state of the flow quality in the 8×6 SWT prior to the start of the 9- by 15-Foot Low-Speed Wind Tunnel (9×15 LSWT) acoustic improvement modifications.

The data acquired during the 2015 FQS were used to create a quantitative measurement of the facility air dryer flow quality, including uniformity and flow angularity. Additionally, the data are evidence of the facility's ability to operate over its full operating range with a relatively large blockage model in the test section; the corner 1 static pressure differential remained below structural limits across the operating envelope of the 8×6 SWT and the test section was able to reach a maximum Mach number of 2.0, nominally. This flow quality data are to be compared to FQS data collected following completion of the 9×15 LSWT acoustic improvement modifications.

References

1. Arrington, E. Allen: Calibration of the NASA Glenn 8- by 6-Foot Supersonic Wind Tunnel (1996 and 1997 Tests), NASA/CR—2012-217270, 2012. http://ntrs.nasa.gov
2. Soeder, Ronald H.: NASA Lewis 8- By 6-Foot Supersonic Wind Tunnel User Manual. NASA TM–105771, 1993. http://ntrs.nasa.gov
3. Arrington, E. Allen; Pickett, Mark T.; and Soeder, Ronald H.: Baseline Calibration of the NASA Lewis Research Center 8- by 6-Foot Supersonic Wind Tunnel (1991 and 1992 Tests). NASA/TM—97-107431, 1998. Available from the NASA STI Program.

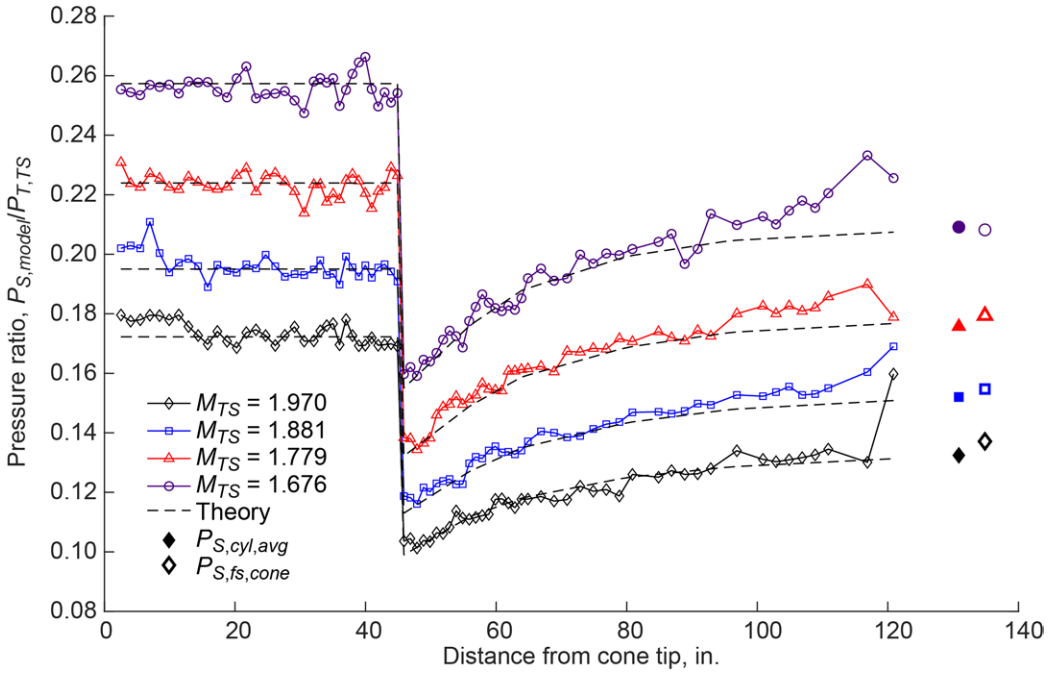

Figure 8.—Axial pressure ratio profiles along 16-in.-diameter cone cylinder with cone tip positioned at test section station 177.375 for Mach 1.970, 1.881, 1.779, and 1.676 (three-motor, closed-loop operating mode).

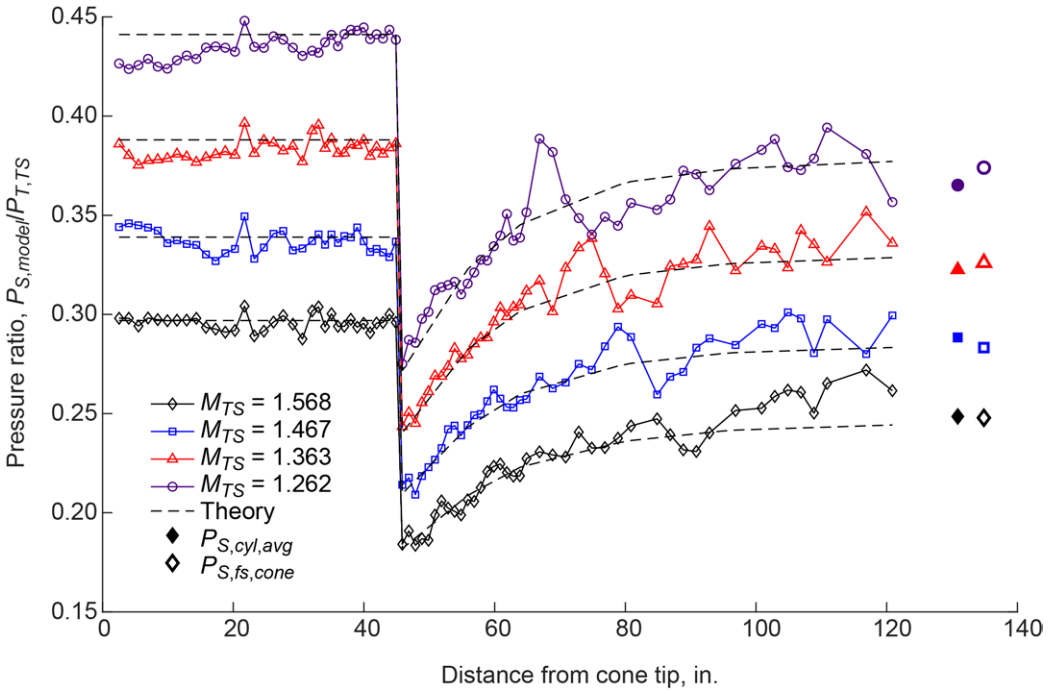

Figure 9.—Axial pressure ratio profiles along 16-in.-diameter cone cylinder with cone tip positioned at test section station 177.375 for Mach 1.568, 1.467, 1.363, 1.262 (three-motor, closed-loop operating mode).

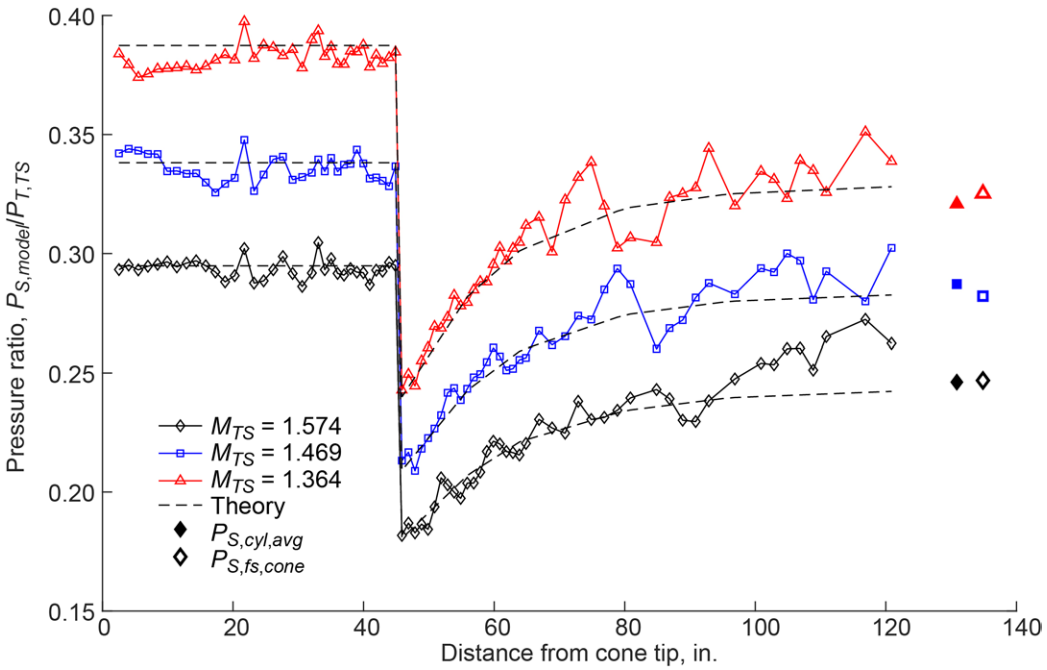

Figure 10.—Axial pressure ratio profiles along 16-in.-diameter cone cylinder with cone tip positioned at test section station 177.375 for Mach 1.574, 1.469, and 1.364 (three-motor, open-loop operating mode).

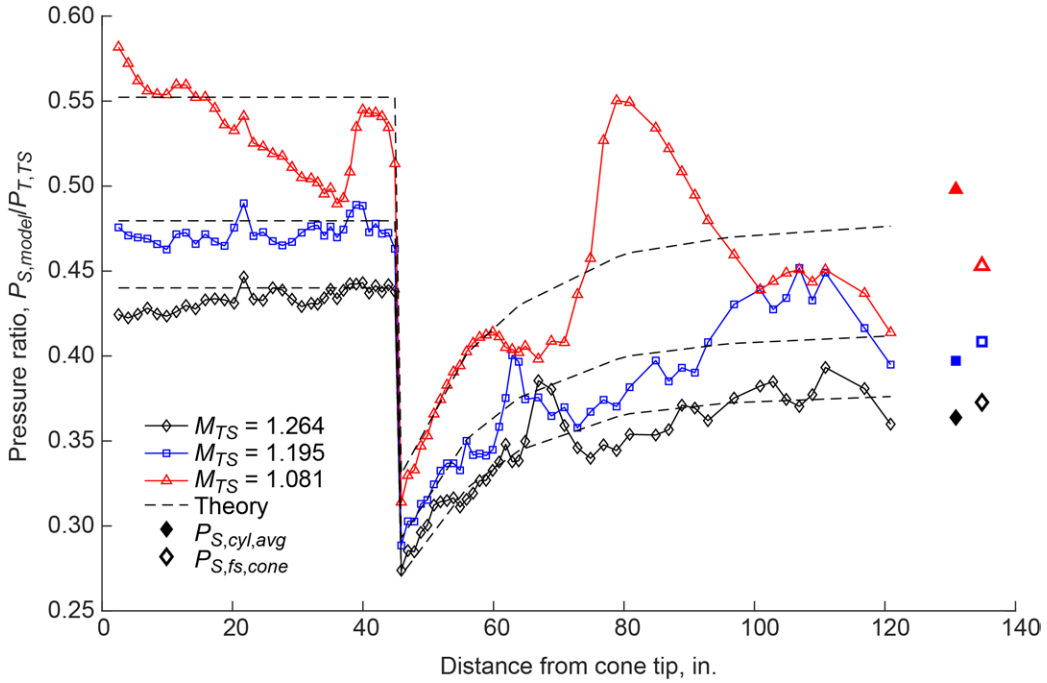

Figure 11.—Axial pressure ratio profiles along 16-in.-diameter cone cylinder with cone tip positioned at test section station 177.375 for Mach 1.264, 1.195, and 1.081 (three-motor, open-loop operating mode).

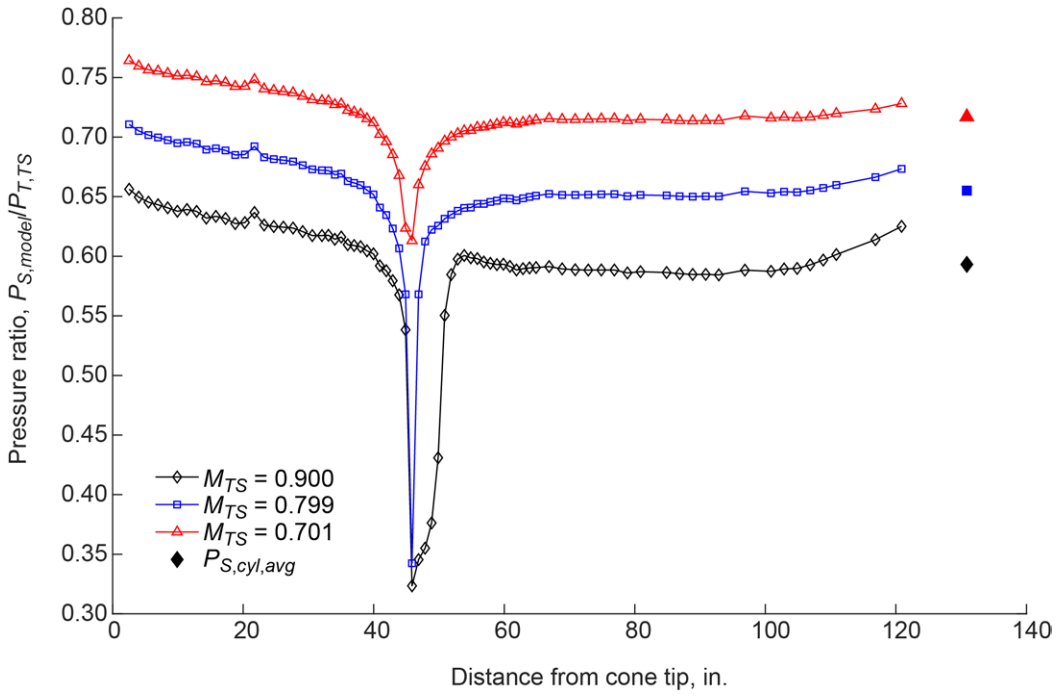

Figure 12.—Axial pressure ratio profiles along 16-in.-diameter cone cylinder with cone tip positioned at test section station 177.375 for Mach 0.900, 0.799, and 0.701 (three-motor, open-loop operating mode).

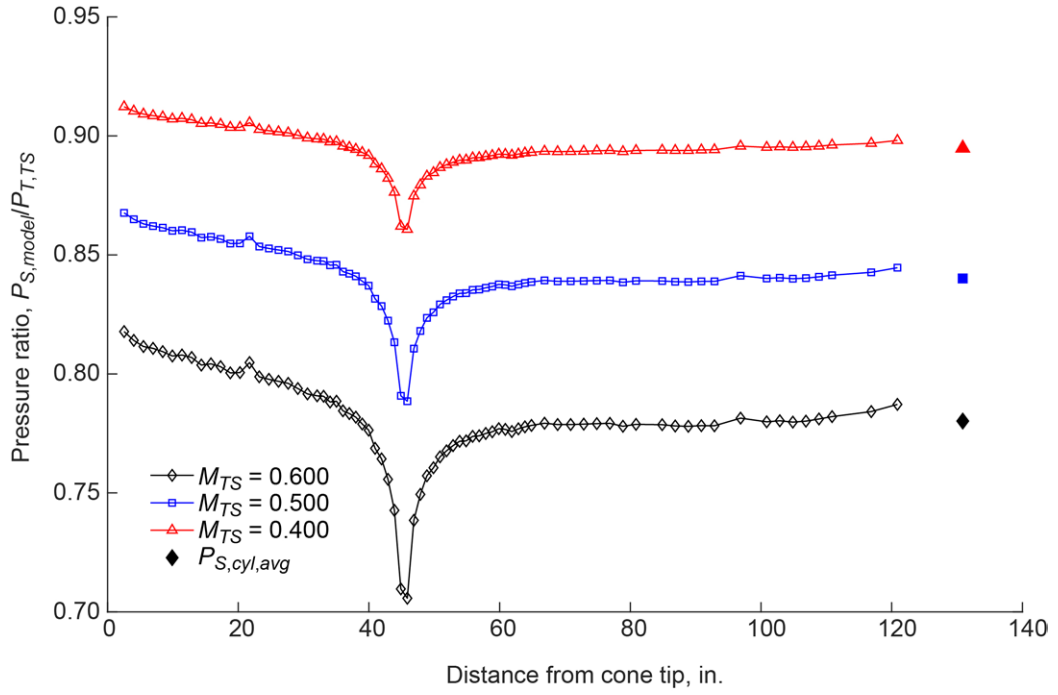

Figure 13.—Axial pressure ratio profiles along 16-in.-diameter cone cylinder with cone tip positioned at test section station 177.375 for Mach 0.600, 0.500, and 0.400 (three-motor, open-loop operating mode).

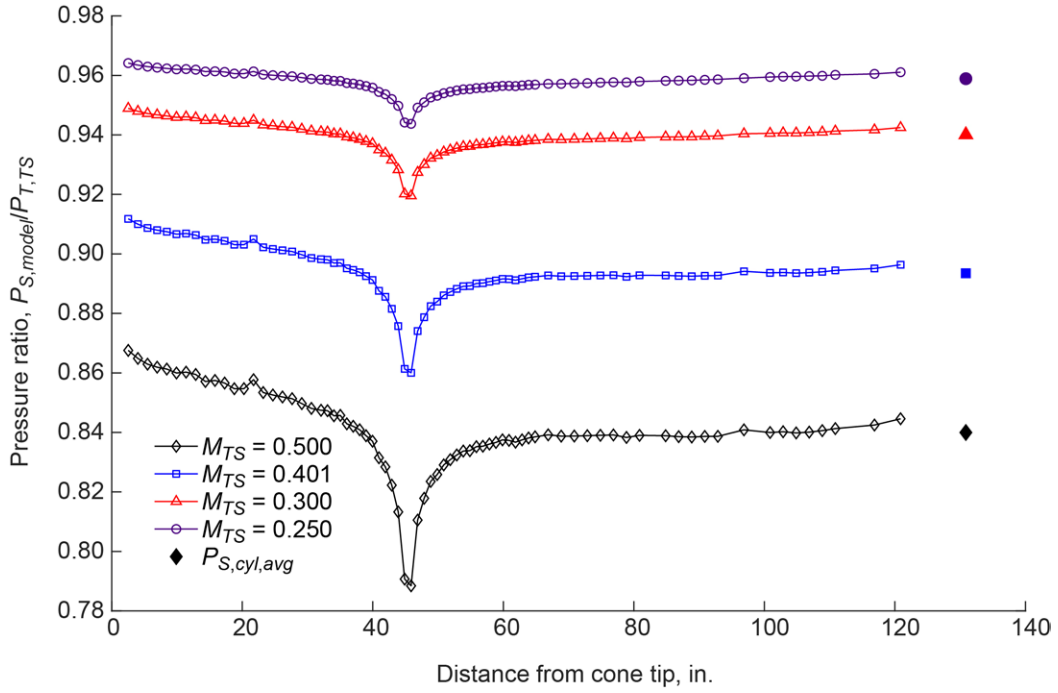

Figure 14.—Axial pressure ratio profiles along 16-in.-diameter cone cylinder with cone tip positioned at test section station 177.375 for Mach 0.500, 0.401, 0.300, and 0.250 (one-motor, open-loop operating mode).

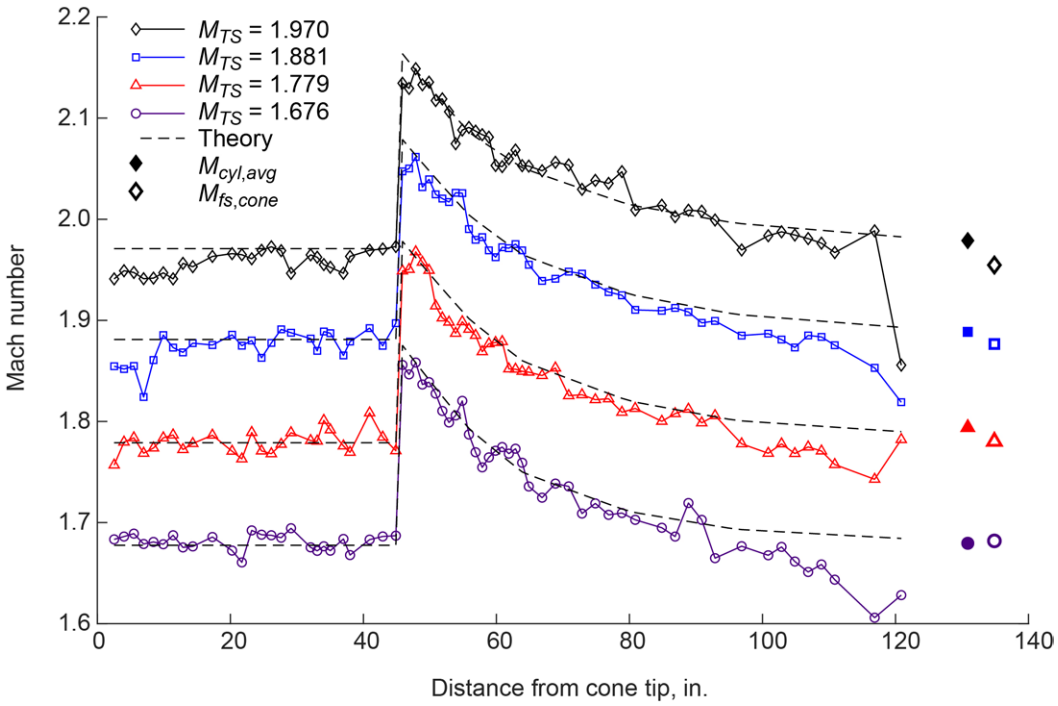

Figure 15.—Axial Mach number distribution along 16-in.-diameter cone cylinder with cone tip positioned at test section station 177.375 for Mach 1.970, 1.881, 1.779, and 1.676 (three-motor, closed-loop operating mode). Test section total pressure $P_{T,TS}$ used for calculating local Mach number.

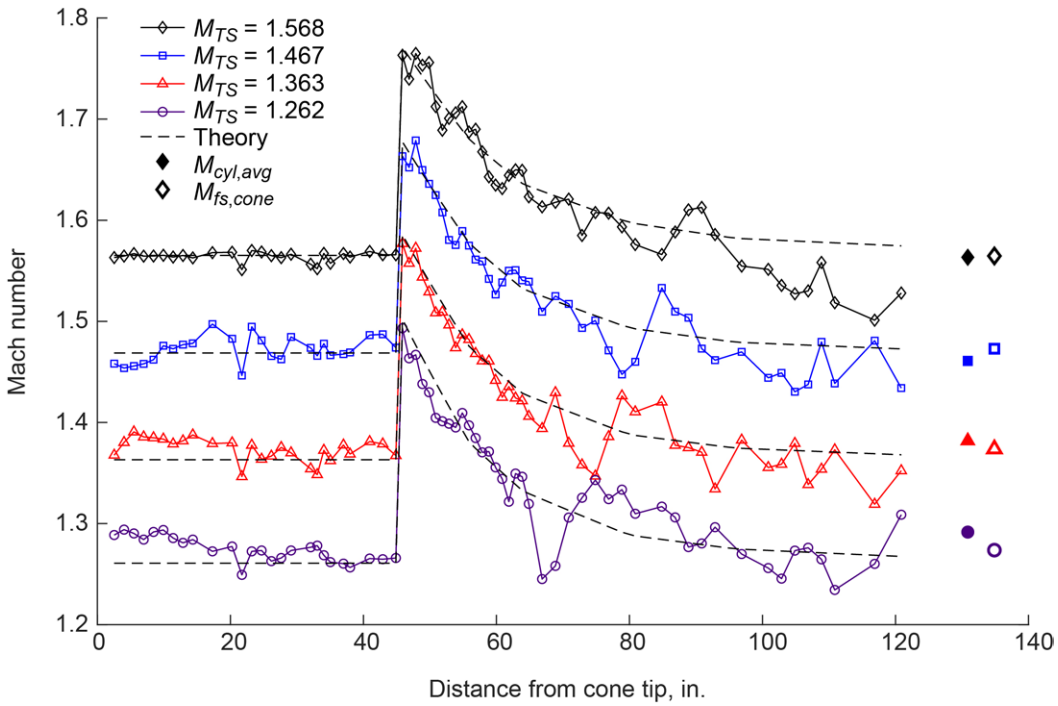

Figure 16.—Axial Mach number distribution along 16-in.-diameter cone cylinder with cone tip positioned at test section station 177.375 for Mach 1.568, 1.467, 1.363, and 1.262 (three-motor, closed-loop operating mode). Test section total pressure $P_{T,TS}$ used for calculating local Mach number.

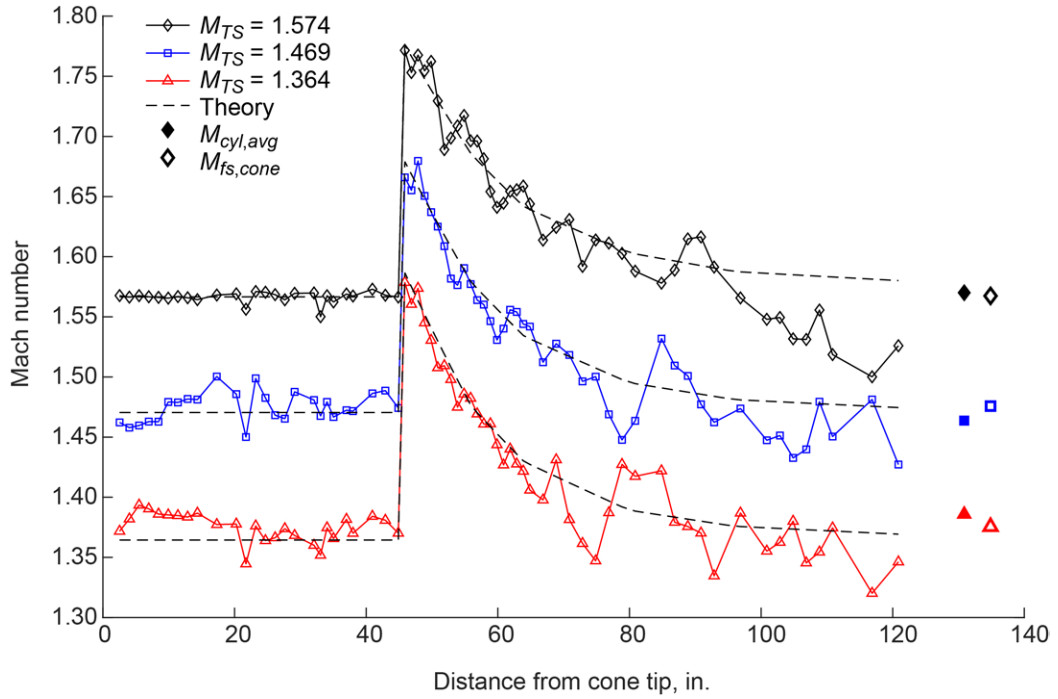

Figure 17.—Axial Mach number distribution along 16-in.-diameter cone cylinder with cone tip positioned at test section station 177.375 for Mach 1.574, 1.469, and 1.364 (three-motor, open-loop operating mode). Test section total pressure $P_{T,TS}$ used for calculating local Mach number.

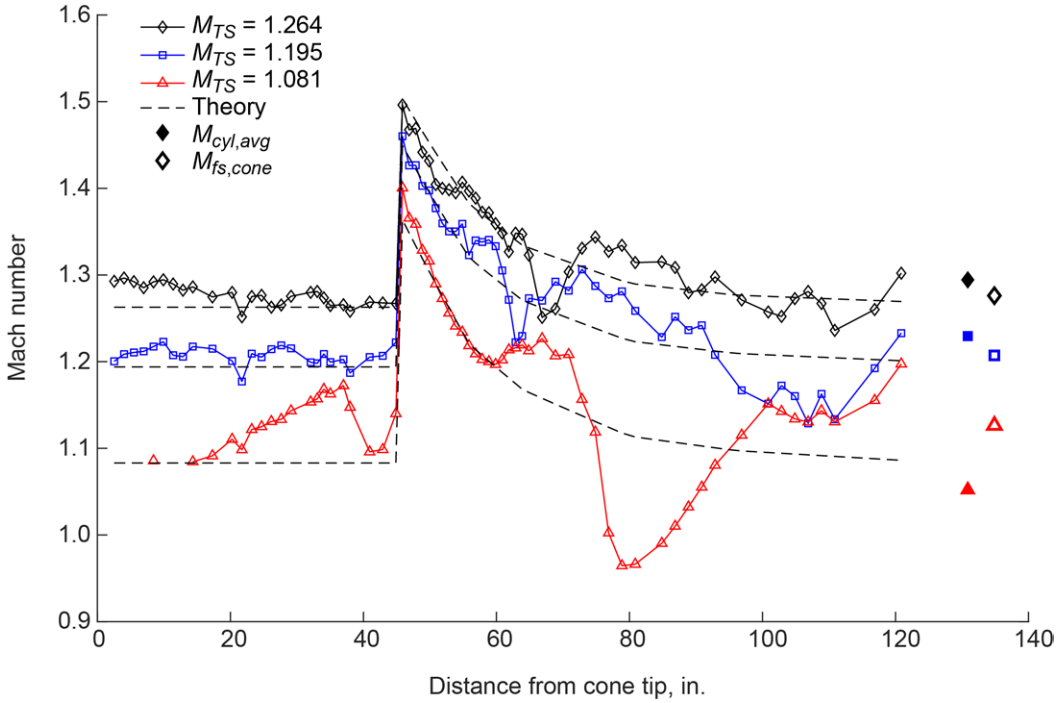

Figure 18.—Axial Mach number distribution along 16-in.-diameter cone cylinder with cone tip positioned at test section station 177.375 for Mach 1.264, 1.195, and 1.081 (three-motor,open-loop operating mode). Test section total pressure $P_{T,TS}$ used for calculating local Mach number.

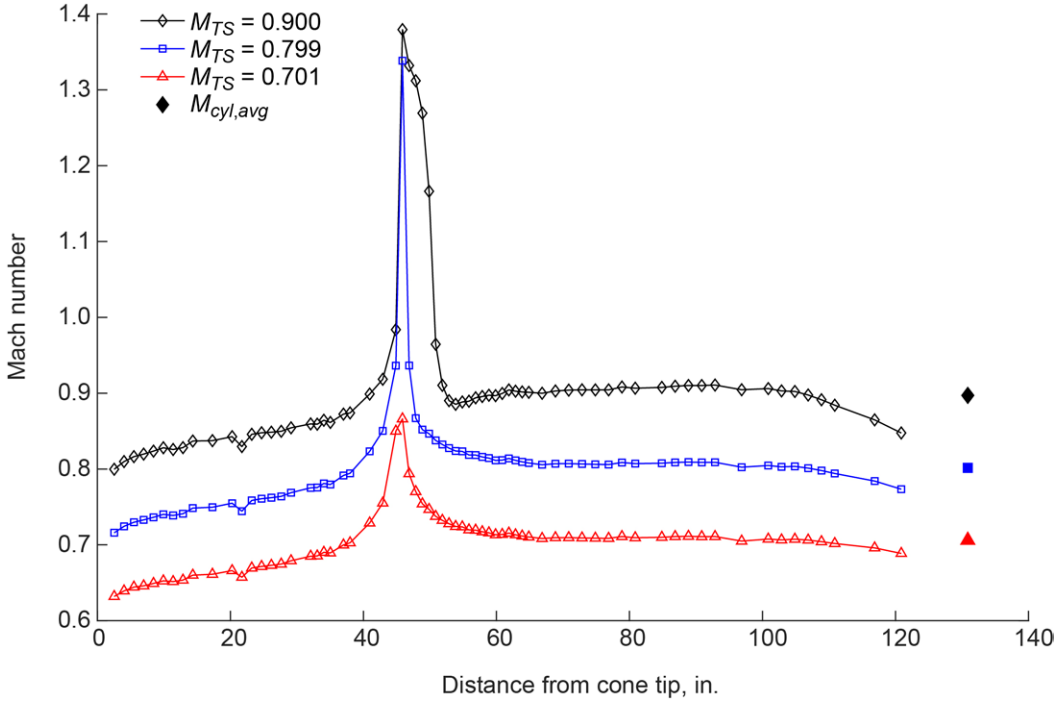

Figure 19.—Axial Mach number distribution along 16-in.-diameter cone cylinder with cone tip positioned at test section station 177.375 for Mach 0.900, 0.799, and 0.701 (three-motor, open-loop operating mode). Test section total pressure $P_{T,TS}$ used for calculating local Mach number.

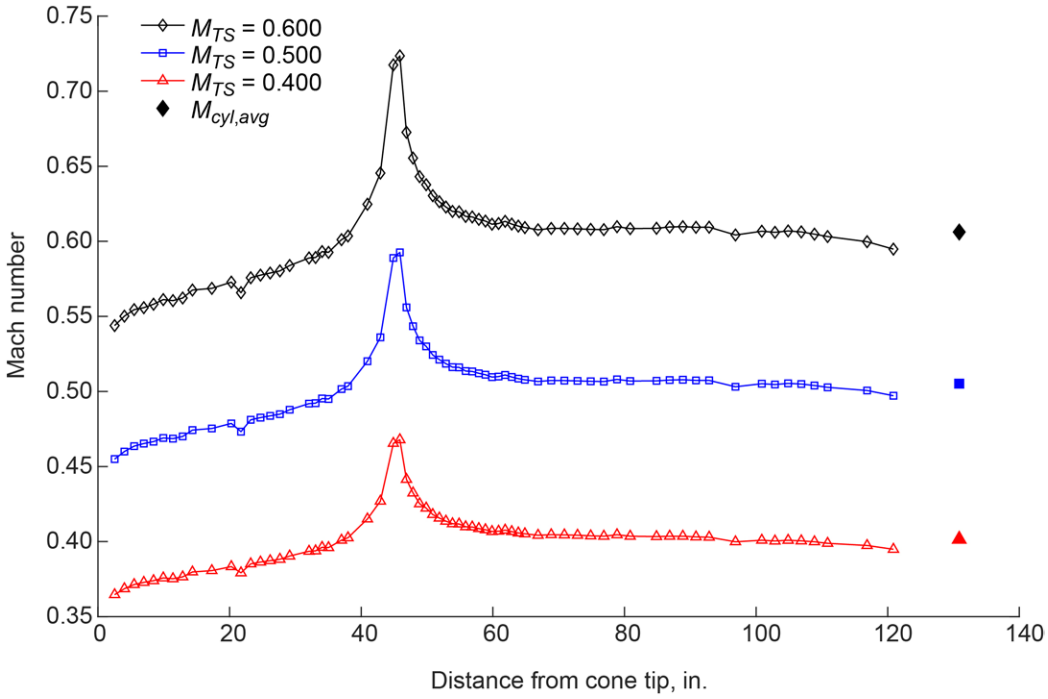

Figure 20.—Axial Mach number distribution along 16-in.-diameter cone cylinder with cone tip positioned at test section station 177.375 for Mach 0.600, 0.500, and 0.400 (three-motor, open-loop operating mode). Test section total pressure $P_{T,TS}$ used for calculating local Mach number.

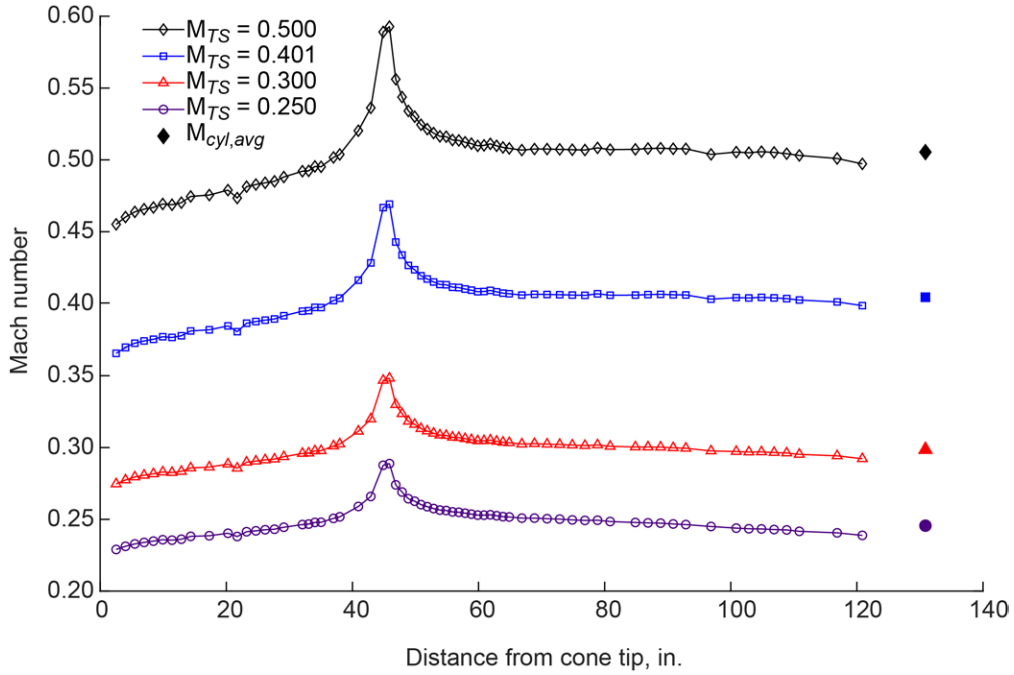

Figure 21.—Axial Mach number distribution along 16-in.-diameter cone cylinder with cone tip positioned at test section station 177.375 for Mach 0.500, 0.401, 0.300, and 0.250 (one-motor, open-loop operating mode). Test section total pressure $P_{T,TS}$ used for calculating local Mach number.

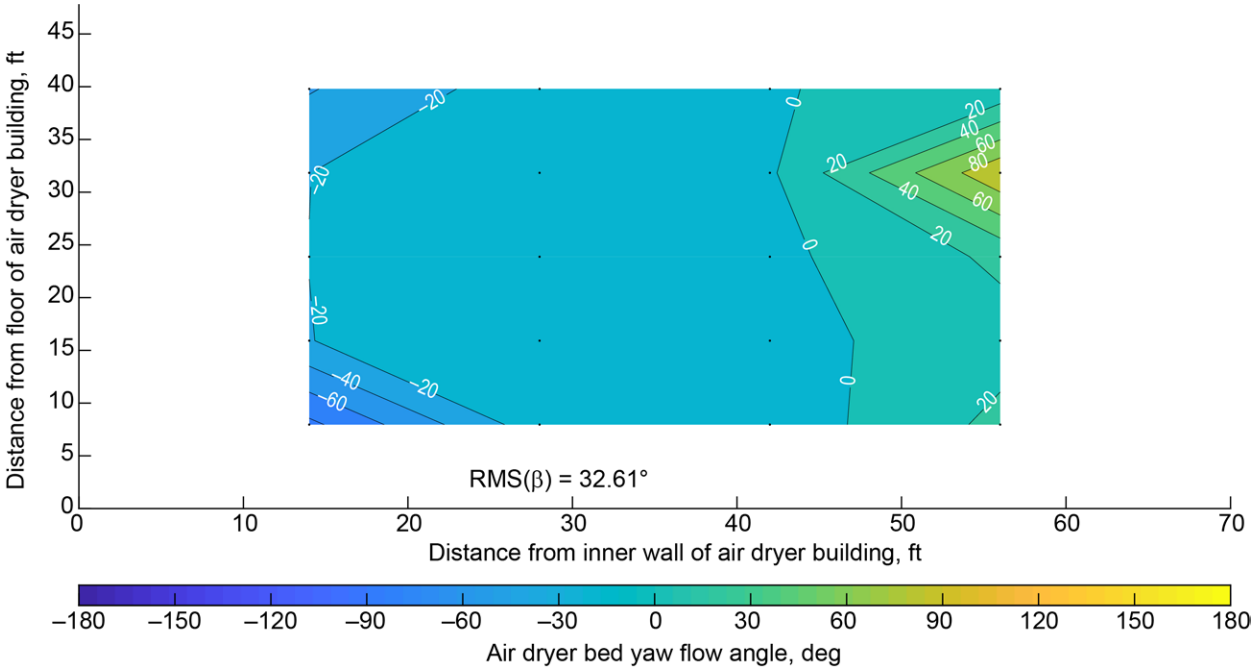

Figure 22.—Contour plot of air dryer bed inlet plane yaw flow angle during operation of 8- by 6-Foot Supersonic Wind Tunnel (upstream looking aft). Nominally Mach 2.00 (three-motor, closed-loop operating mode).

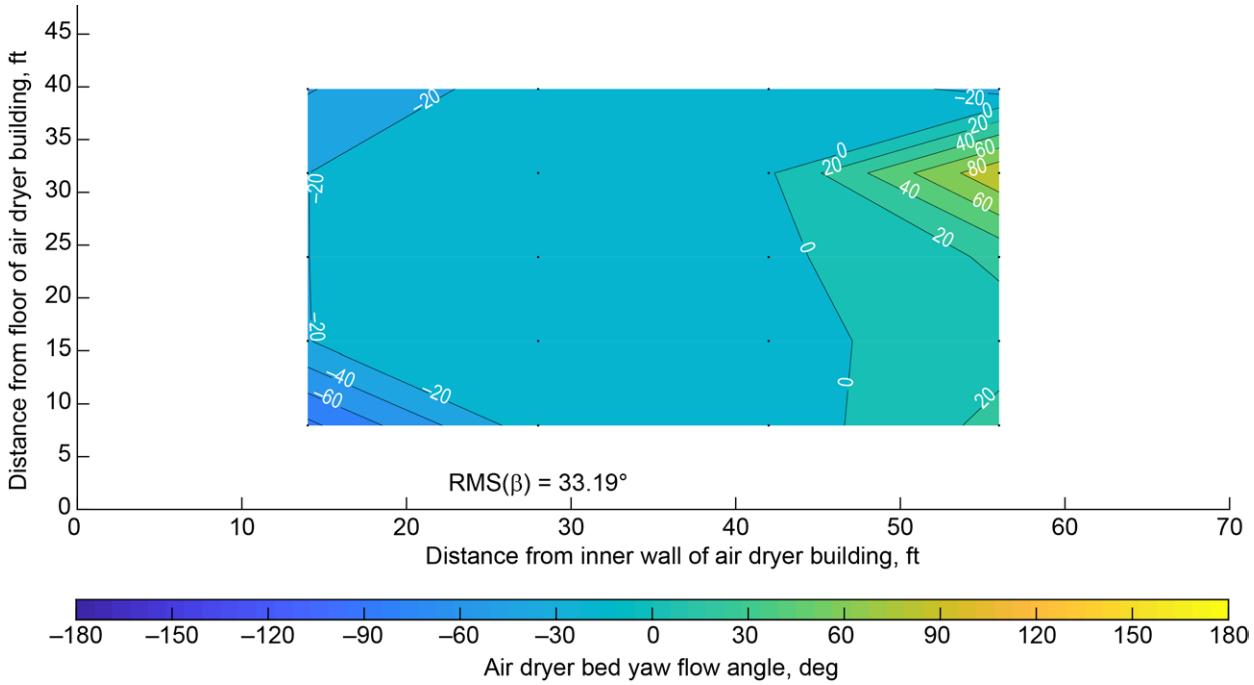

Figure 23.—Contour plot of air dryer bed inlet plane yaw flow angle during operation of 8- by 6-Foot Supersonic Wind Tunnel (upstream looking aft). Nominally Mach 1.90 (three-motor, closed-loop operating mode).

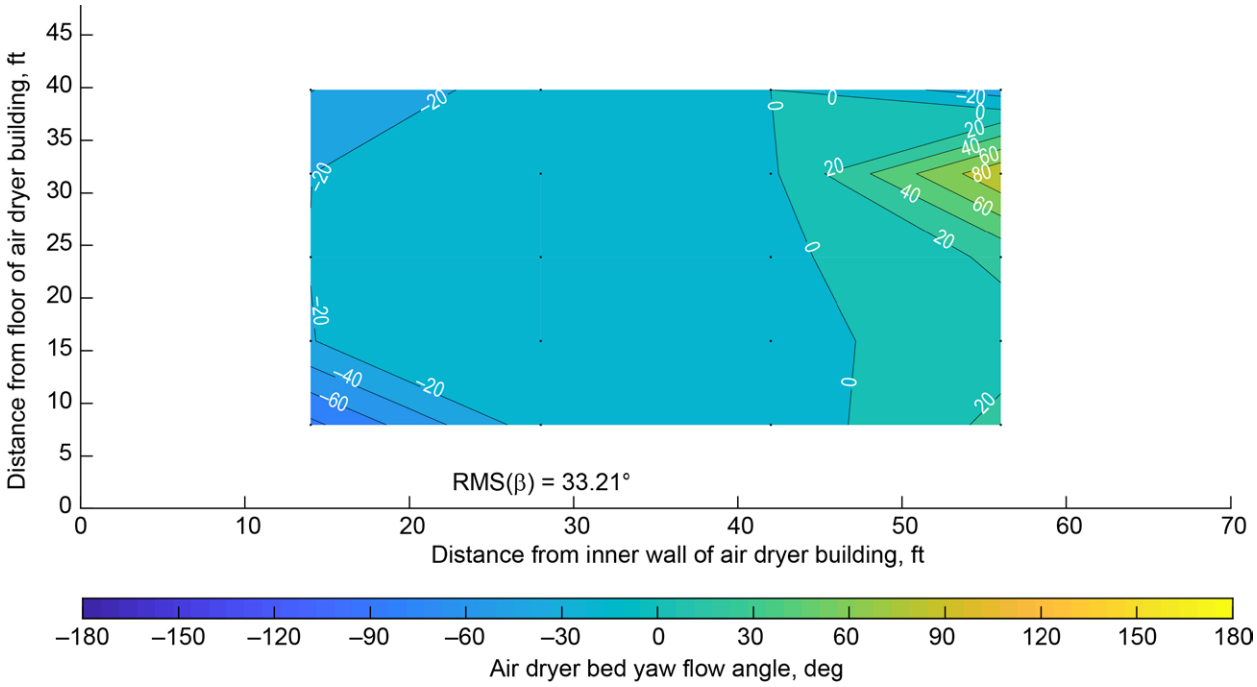

Figure 24.—Contour plot of air dryer bed inlet plane yaw flow angle during operation of 8- by 6-Foot Supersonic Wind Tunnel (upstream looking aft). Nominally Mach 1.80 (three-motor, closed-loop operating mode).

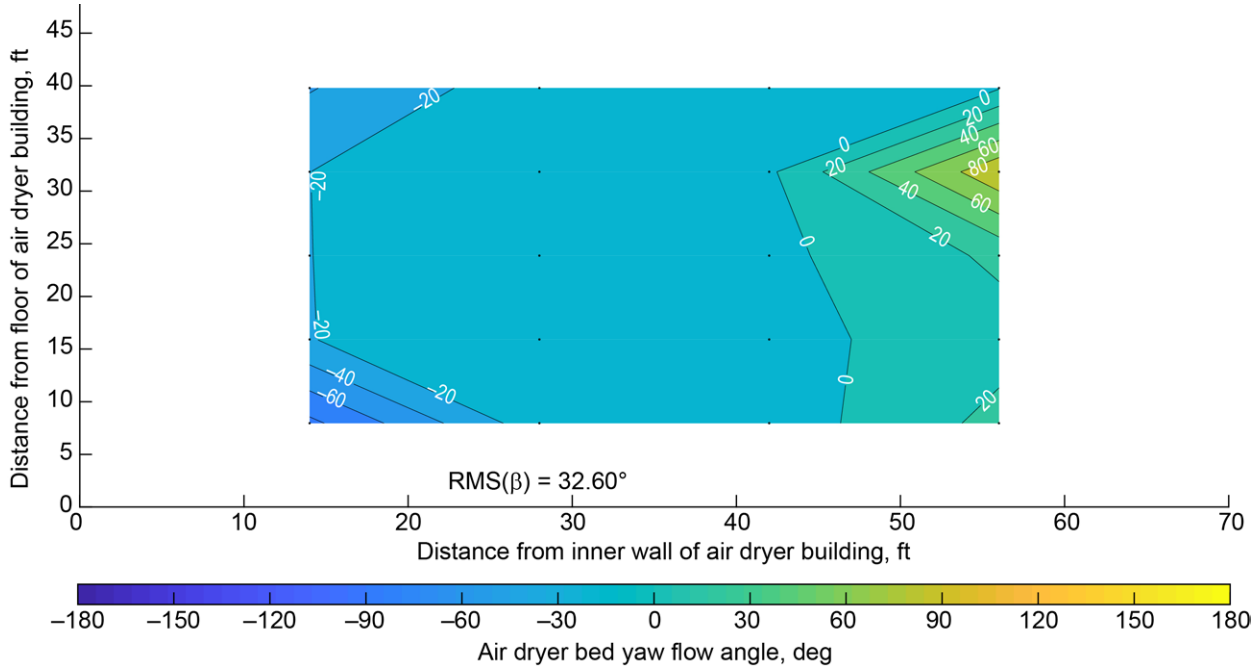

Figure 25.—Contour plot of air dryer bed inlet plane yaw flow angle during operation of 8- by 6-Foot Supersonic Wind Tunnel (upstream looking aft). Nominally Mach 1.70 (three-motor, closed-loop operating mode).

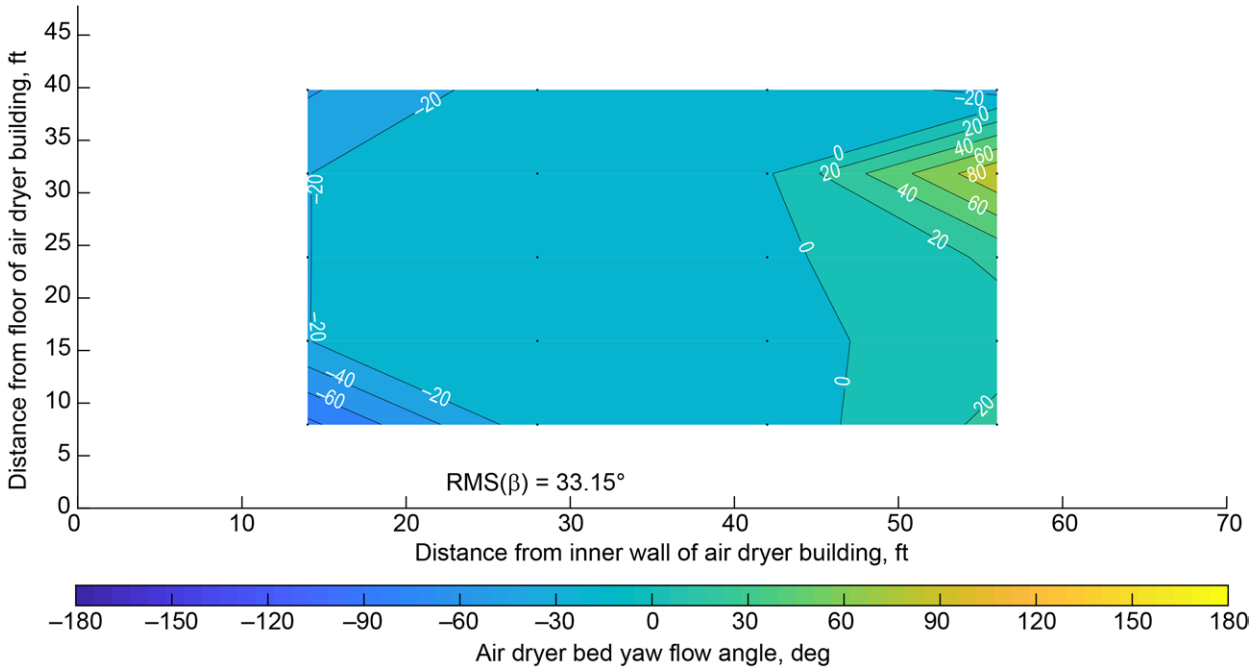

Figure 26.—Contour plot of air dryer bed inlet plane yaw flow angle during operation of 8- by 6-Foot Supersonic Wind Tunnel (upstream looking aft). Nominally Mach 1.60 (three-motor, closed-loop operating mode).

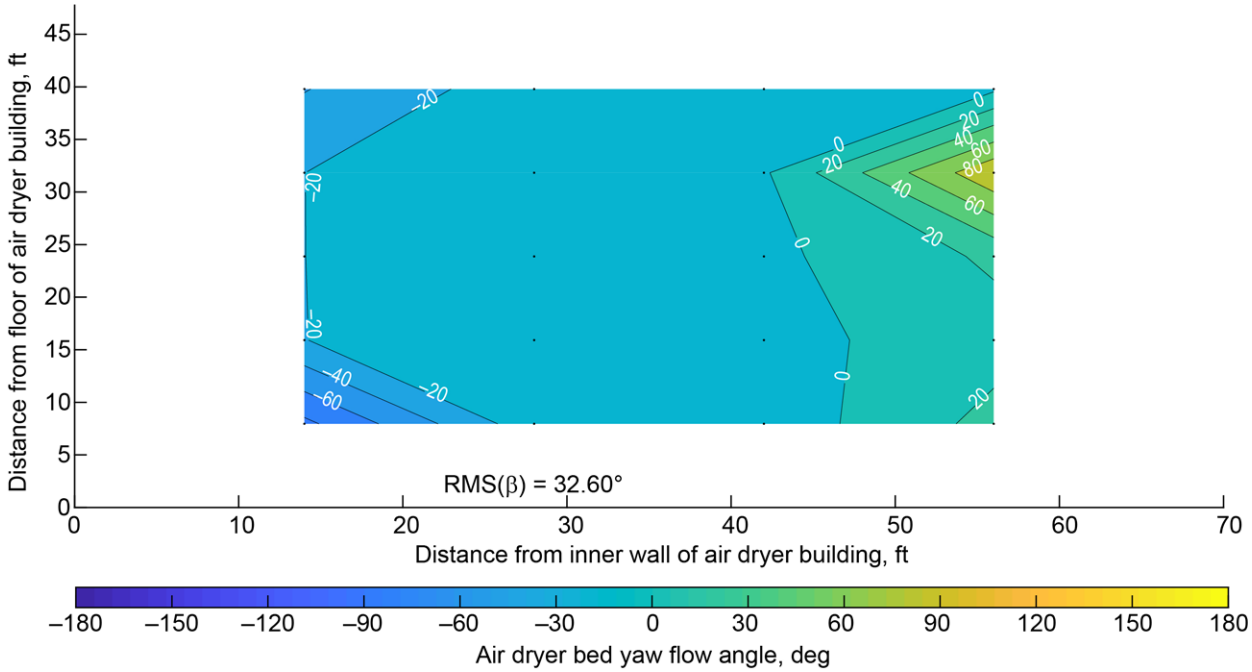

Figure 27.—Contour plot of air dryer bed inlet plane yaw flow angle during operation of 8- by 6-Foot Supersonic Wind Tunnel (upstream looking aft). Nominally Mach 1.50 (three-motor, closed-loop operating mode).

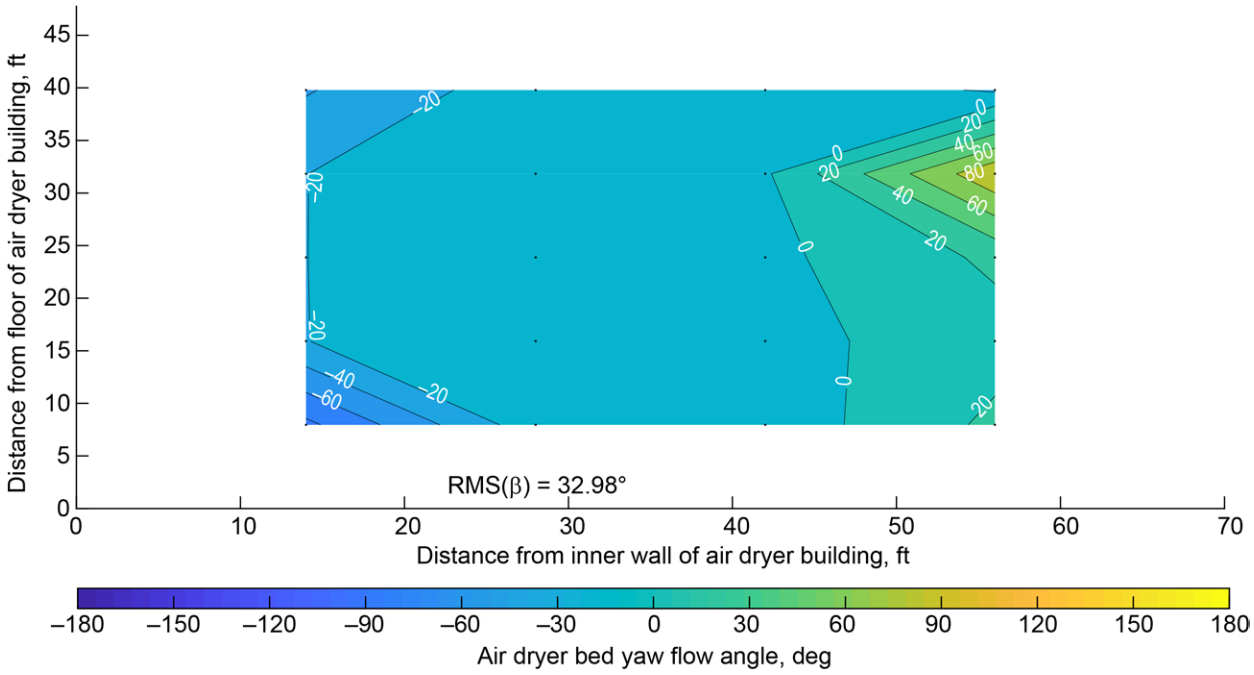

Figure 28.—Contour plot of air dryer bed inlet plane yaw flow angle during operation of 8- by 6-Foot Supersonic Wind Tunnel (upstream looking aft). Nominally Mach 1.40 (three-motor, closed-loop operating mode).

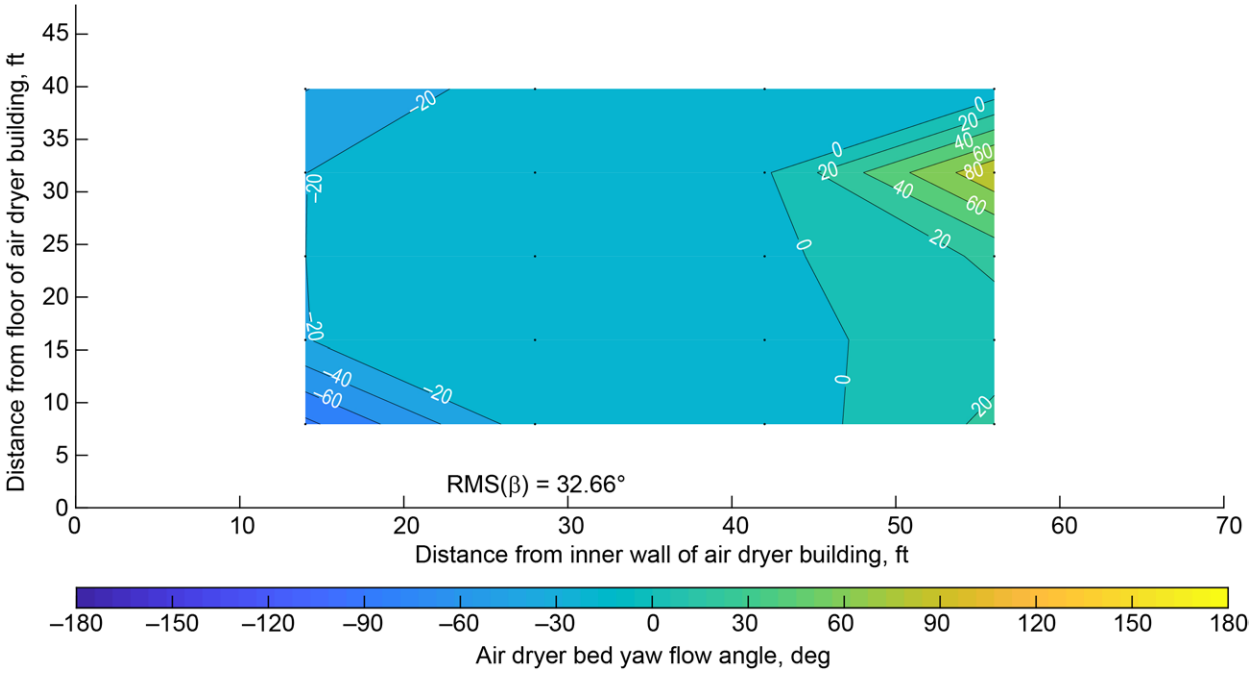

Figure 29.—Contour plot of air dryer bed inlet plane yaw flow angle during operation of 8- by 6-Foot Supersonic Wind Tunnel (upstream looking aft). Nominally Mach 1.30 (three-motor, closed-loop operating mode with doors 4 and 5 open).

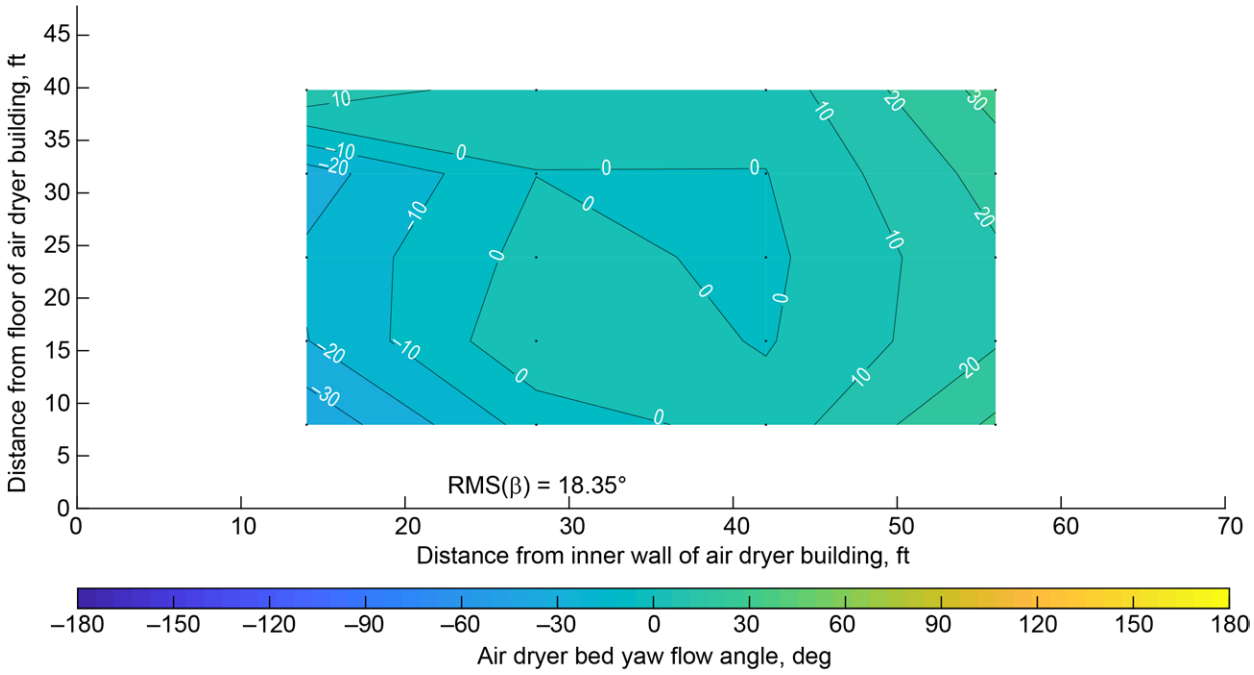

Figure 30.—Contour plot of air dryer bed inlet plane yaw flow angle during operation of 8- by 6-Foot Supersonic Wind Tunnel (upstream looking aft). Nominally Mach 1.60 (three-motor, open-loop operating mode).

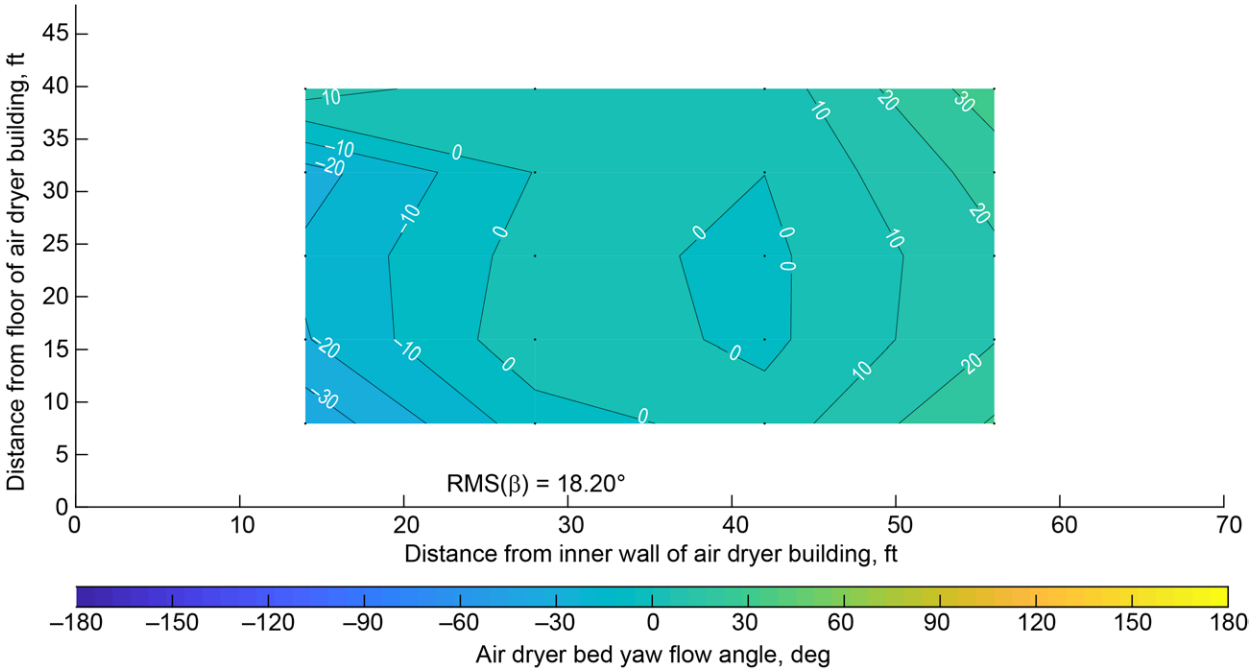

Figure 31.—Contour plot of air dryer bed inlet plane yaw flow angle during operation of 8- by 6-Foot Supersonic Wind Tunnel (upstream looking aft). Nominally Mach 1.50 (three-motor, open-loop operating mode).

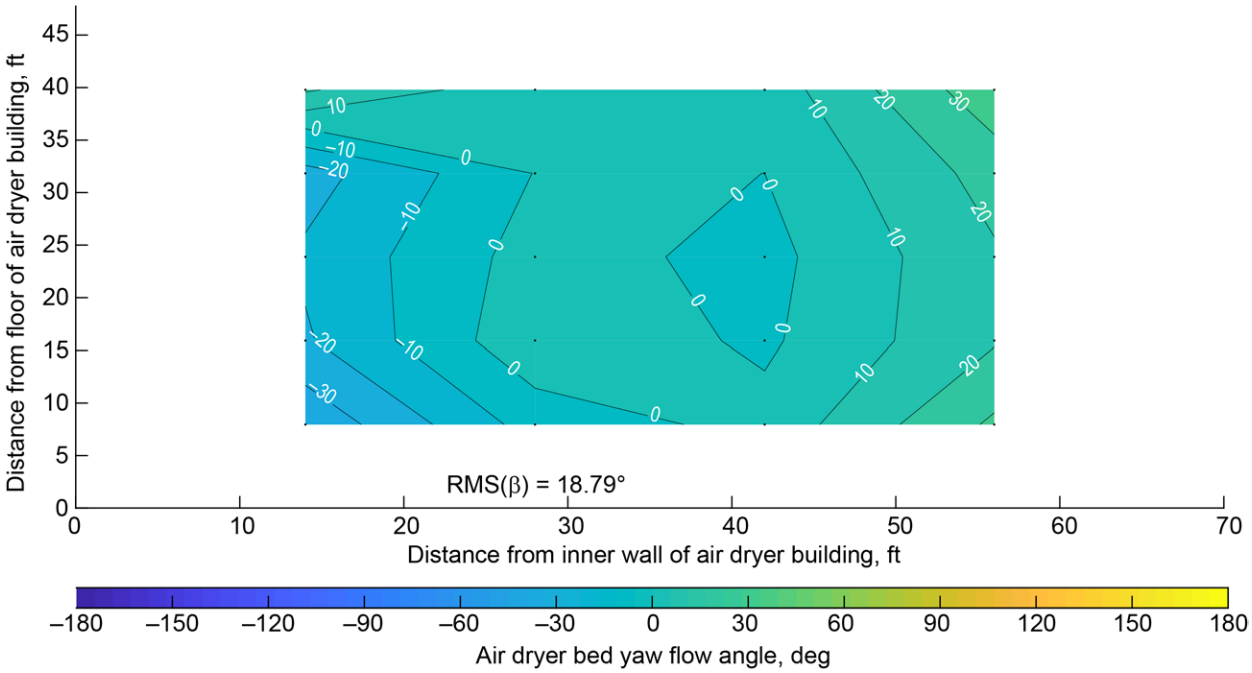

Figure 32.—Contour plot of air dryer bed inlet plane yaw flow angle during operation of 8- by 6-Foot Supersonic Wind Tunnel (upstream looking aft). Nominally Mach 1.40 (three-motor, open-loop operating mode).

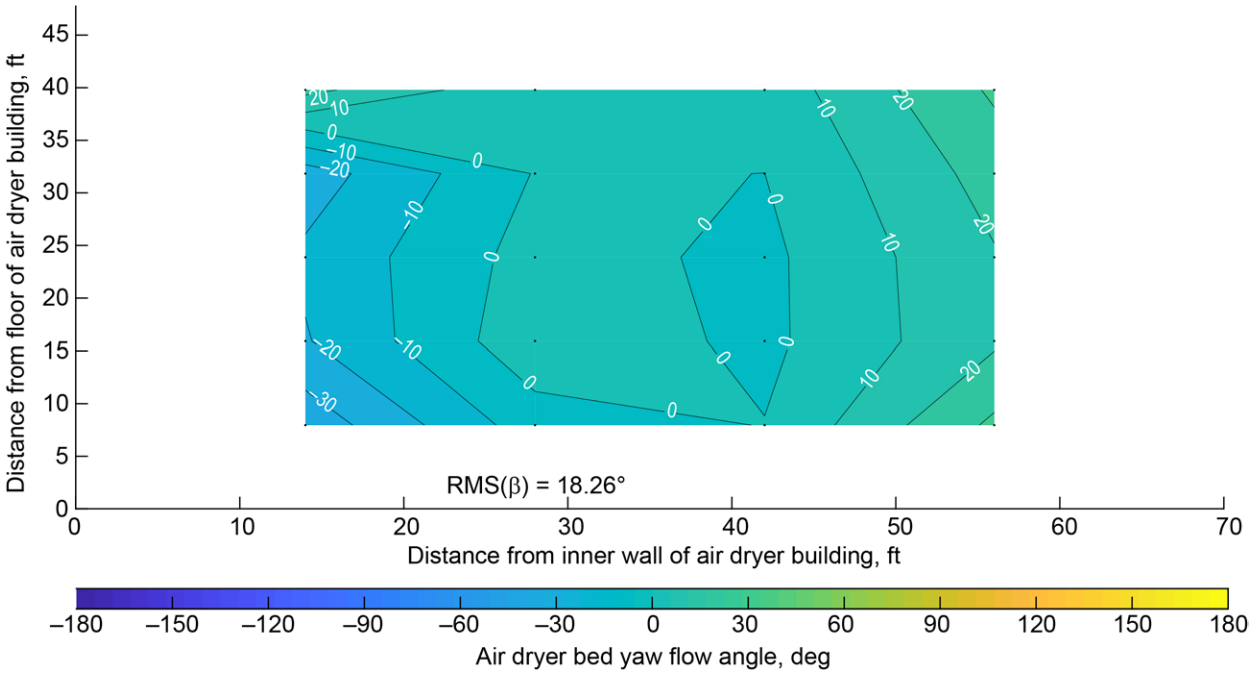

Figure 33.—Contour plot of air dryer bed inlet plane yaw flow angle during operation of 8- by 6-Foot Supersonic Wind Tunnel (upstream looking aft). Nominally Mach 1.30 (three-motor, open-loop operating mode).

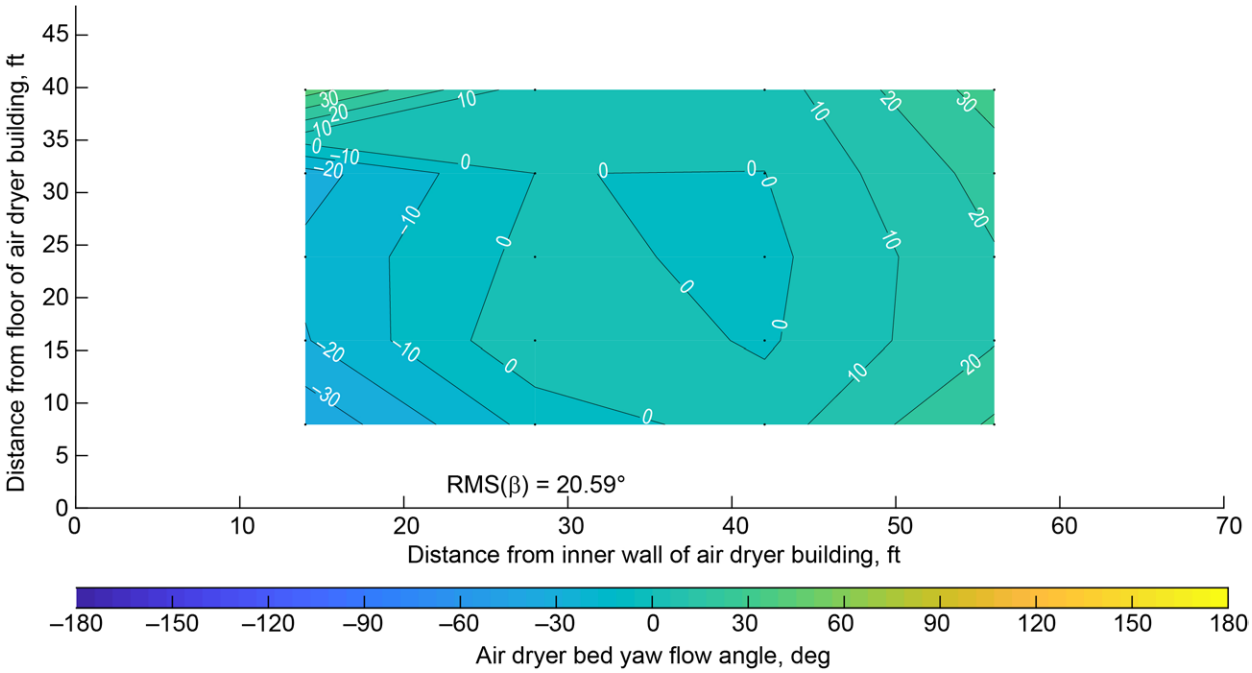

Figure 34.—Contour plot of air dryer bed inlet plane yaw flow angle during operation of 8- by 6-Foot Supersonic Wind Tunnel (upstream looking aft). Nominally Mach 1.20 (three-motor, open-loop operating mode).

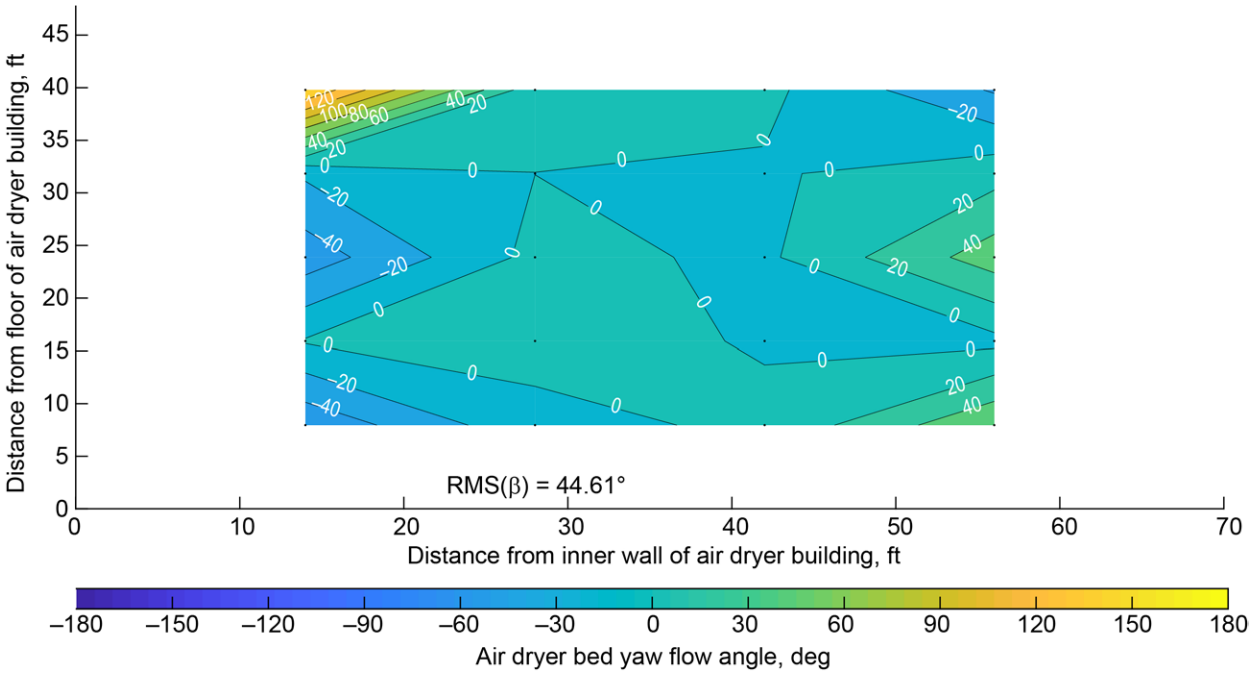

Figure 35.—Contour plot of air dryer bed inlet plane yaw flow angle during operation of 8- by 6-Foot Supersonic Wind Tunnel (upstream looking aft). Nominally Mach 1.10 (three-motor, open-loop operating mode).

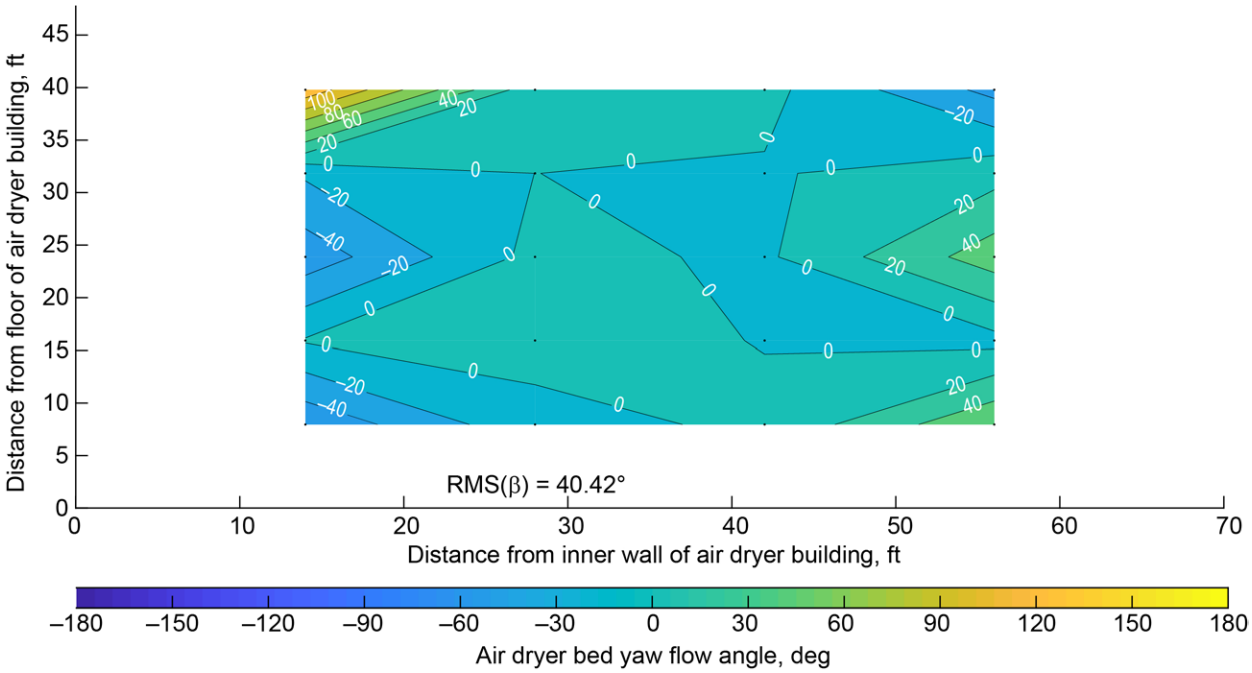

Figure 36.—Contour plot of air dryer bed inlet plane yaw flow angle during operation of 8- by 6-Foot Supersonic Wind Tunnel (upstream looking aft). Nominally Mach 0.90 (three-motor, open-loop operating mode).

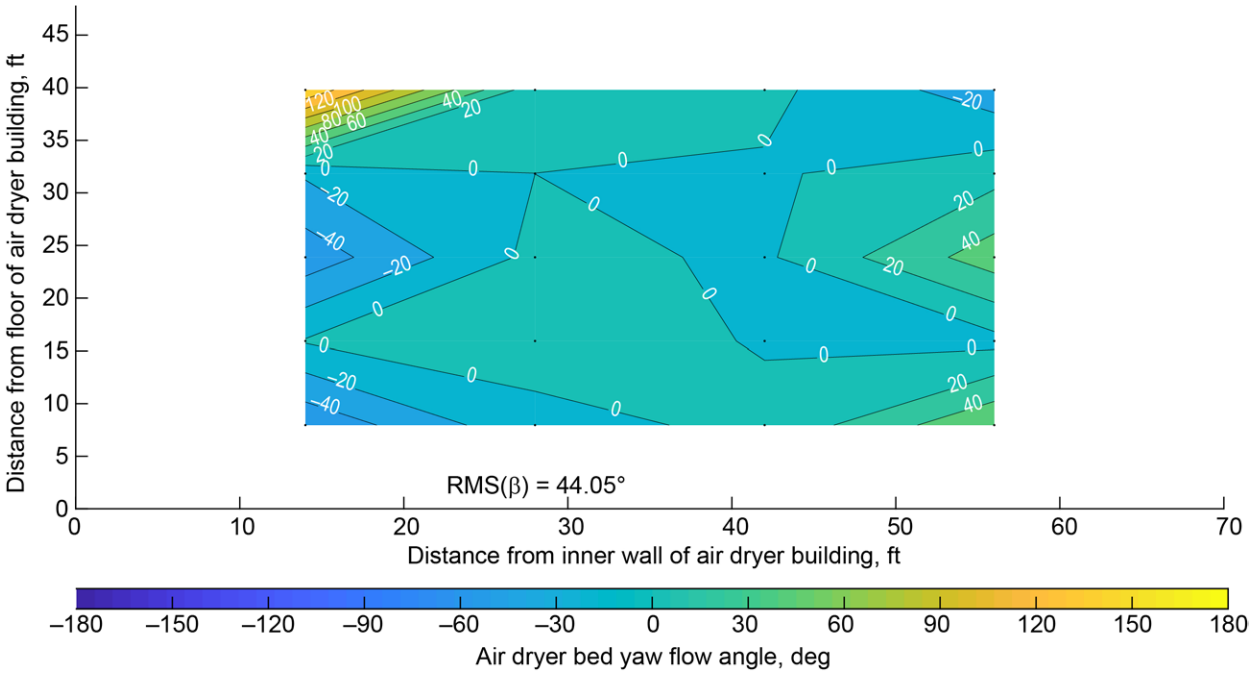

Figure 37.—Contour plot of air dryer bed inlet plane yaw flow angle during operation of 8- by 6-Foot Supersonic Wind Tunnel (upstream looking aft). Nominally Mach 0.80 (three-motor, open-loop operating mode).

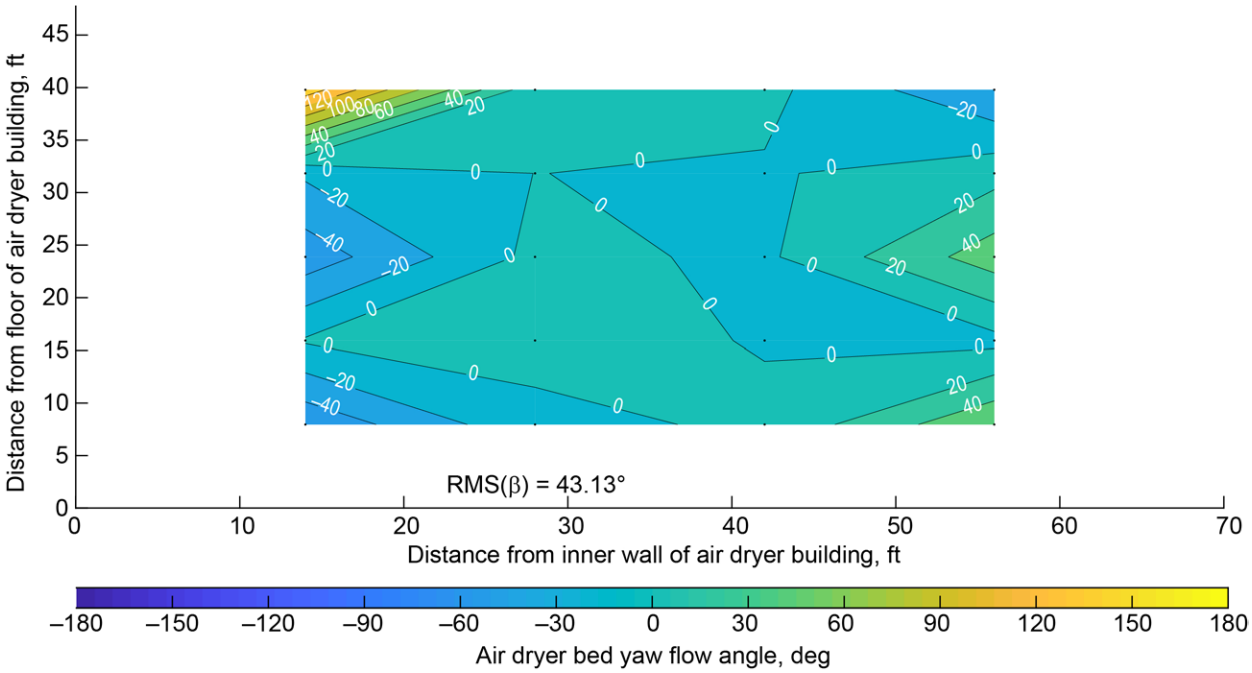

Figure 38.—Contour plot of air dryer bed inlet plane yaw flow angle during operation of 8- by 6-Foot Supersonic Wind Tunnel (upstream looking aft). Nominally Mach 0.70 (three-motor, open-loop operating mode).

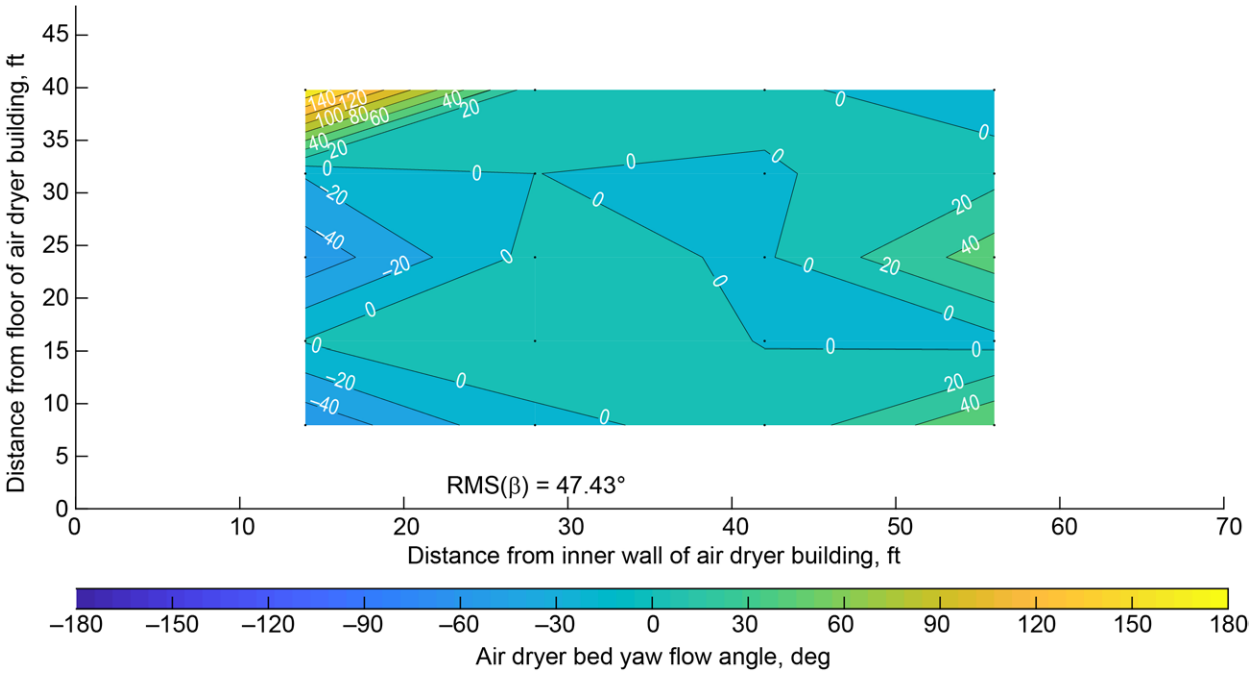

Figure 39.—Contour plot of air dryer bed inlet plane yaw flow angle during operation of 8- by 6-Foot Supersonic Wind Tunnel (upstream looking aft). Nominally Mach 0.60 (three-motor, open-loop operating mode).

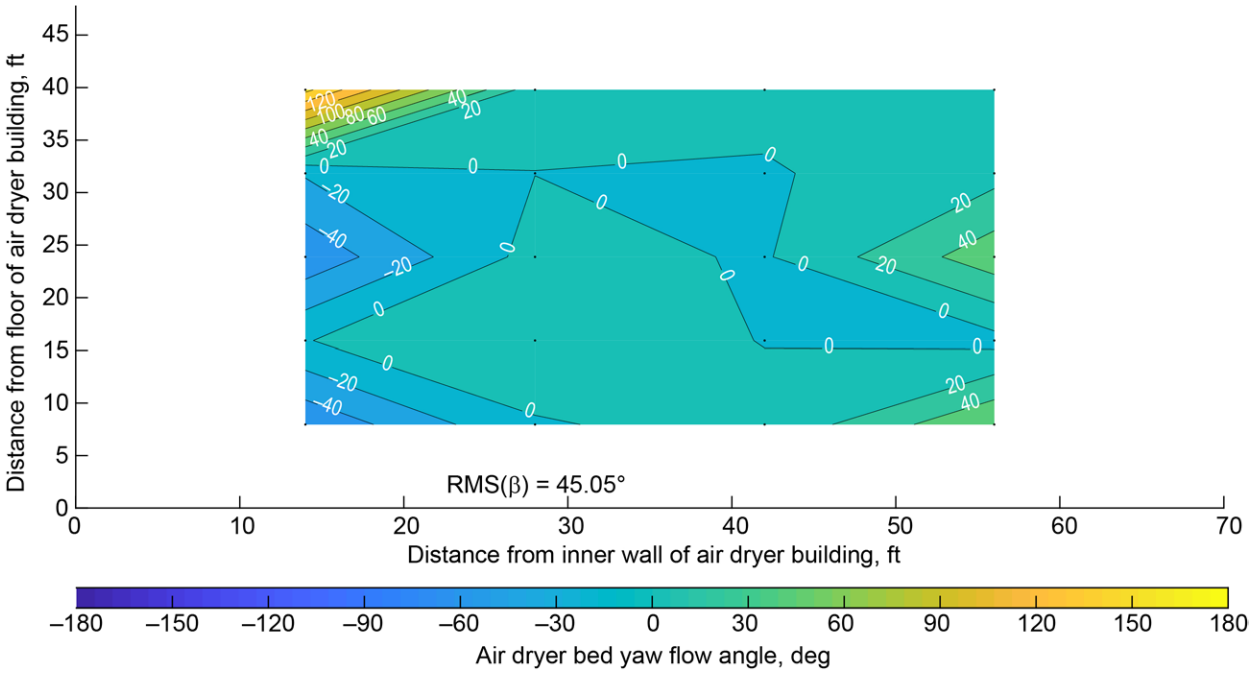

Figure 40.—Contour plot of air dryer bed inlet plane yaw flow angle during operation of 8- by 6-Foot Supersonic Wind Tunnel (upstream looking aft). Nominally Mach 0.50 (three-motor, open-loop operating mode).

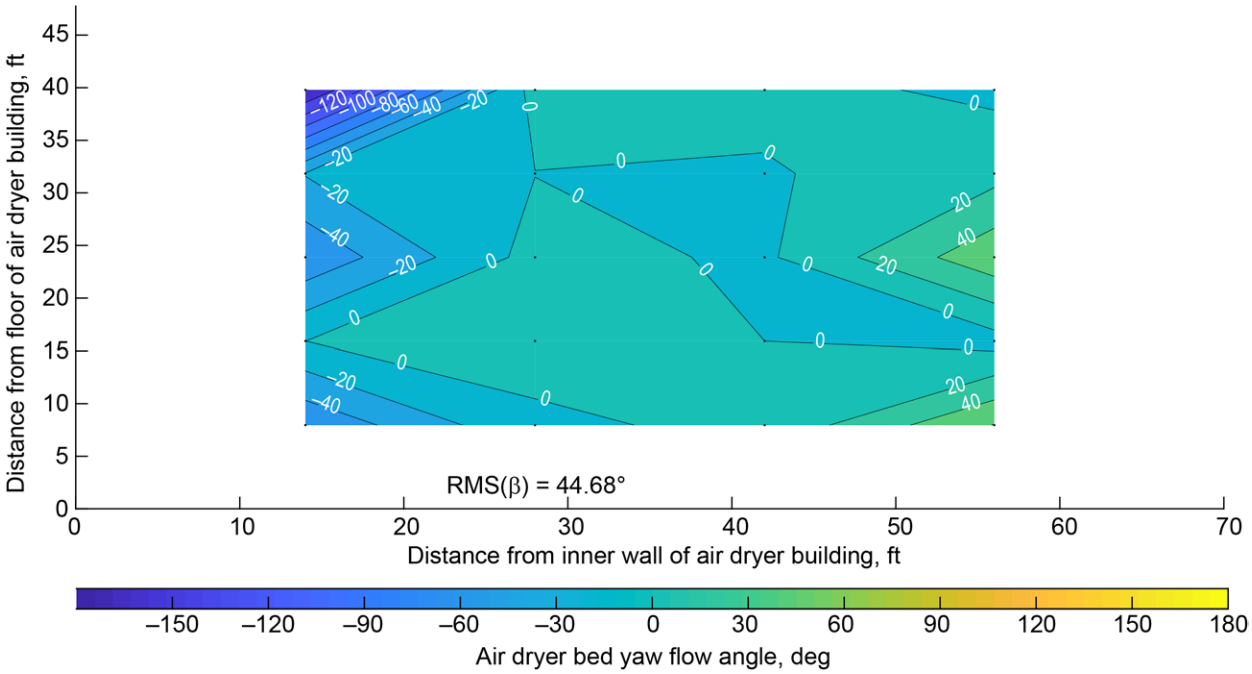

Figure 41.—Contour plot of air dryer bed inlet plane yaw flow angle during operation of 8- by 6-Foot Supersonic Wind Tunnel (upstream looking aft). Nominally Mach 0.40 (three-motor, open-loop operating mode).

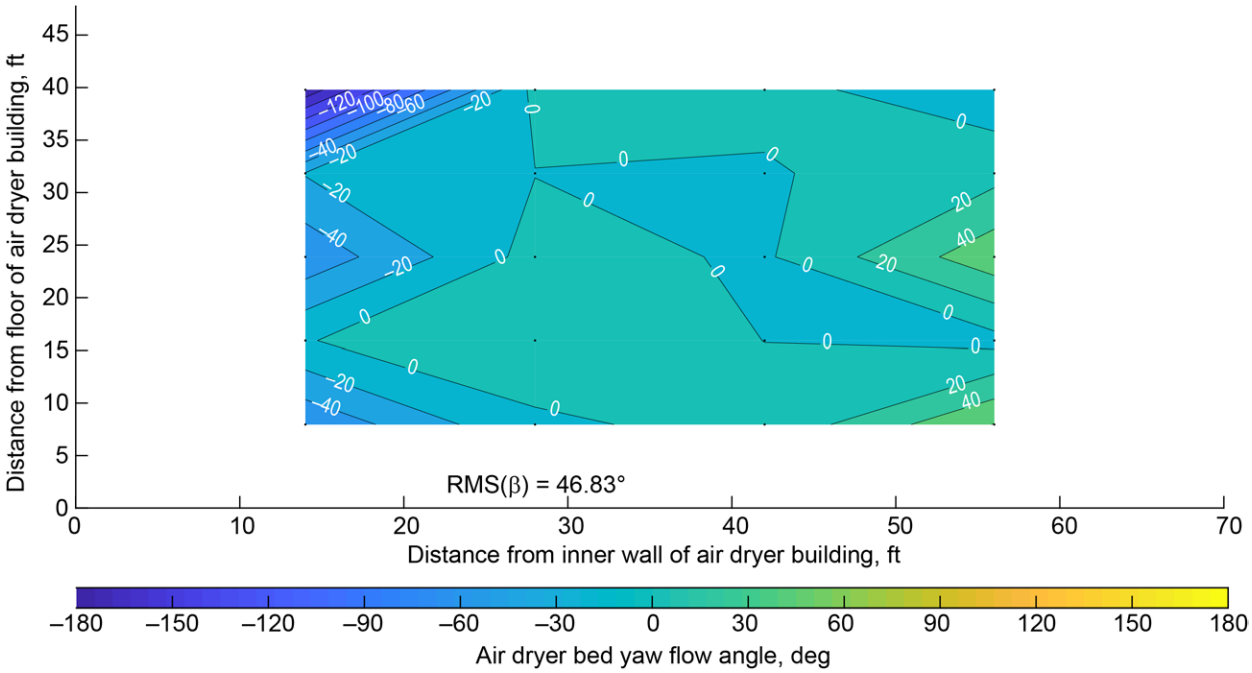

Figure 42.—Contour plot of air dryer bed inlet plane yaw flow angle during operation of 8- by 6-Foot Supersonic Wind Tunnel (upstream looking aft). Nominally Mach 0.50 (one-motor, open-loop operating mode).

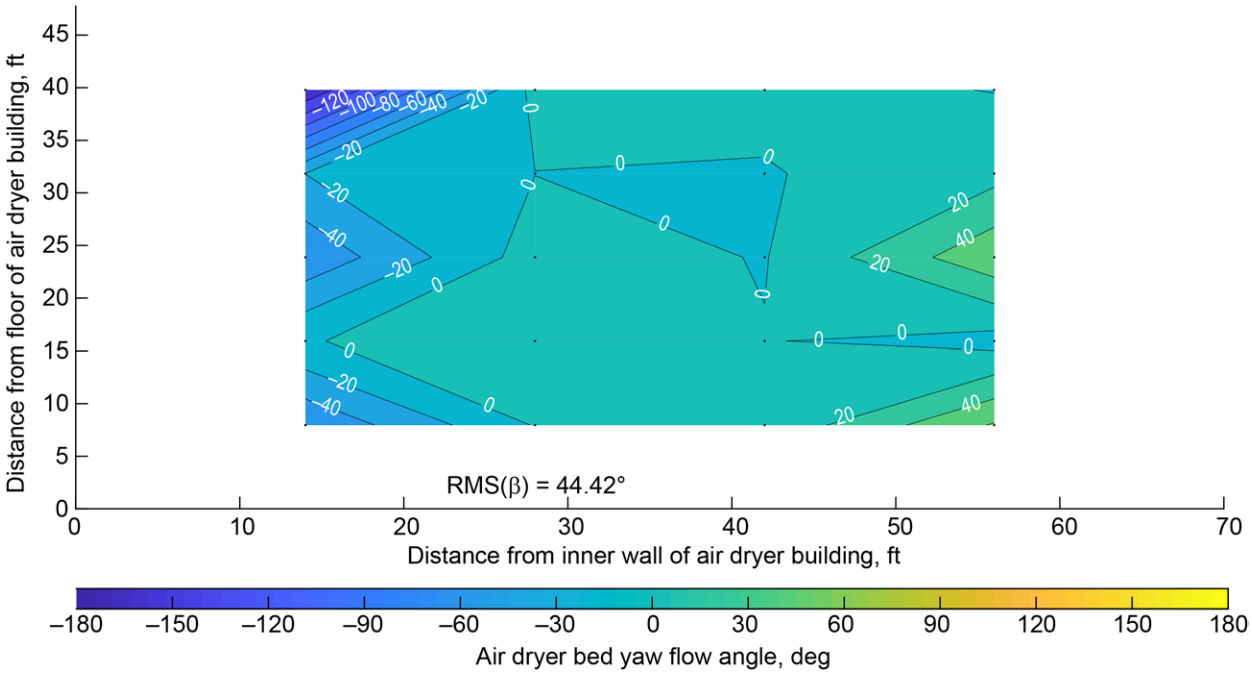

Figure 43.—Contour plot of air dryer bed inlet plane yaw flow angle during operation of 8- by 6-Foot Supersonic Wind Tunnel (upstream looking aft). Nominally Mach 0.40 (one-motor, open-loop operating mode).

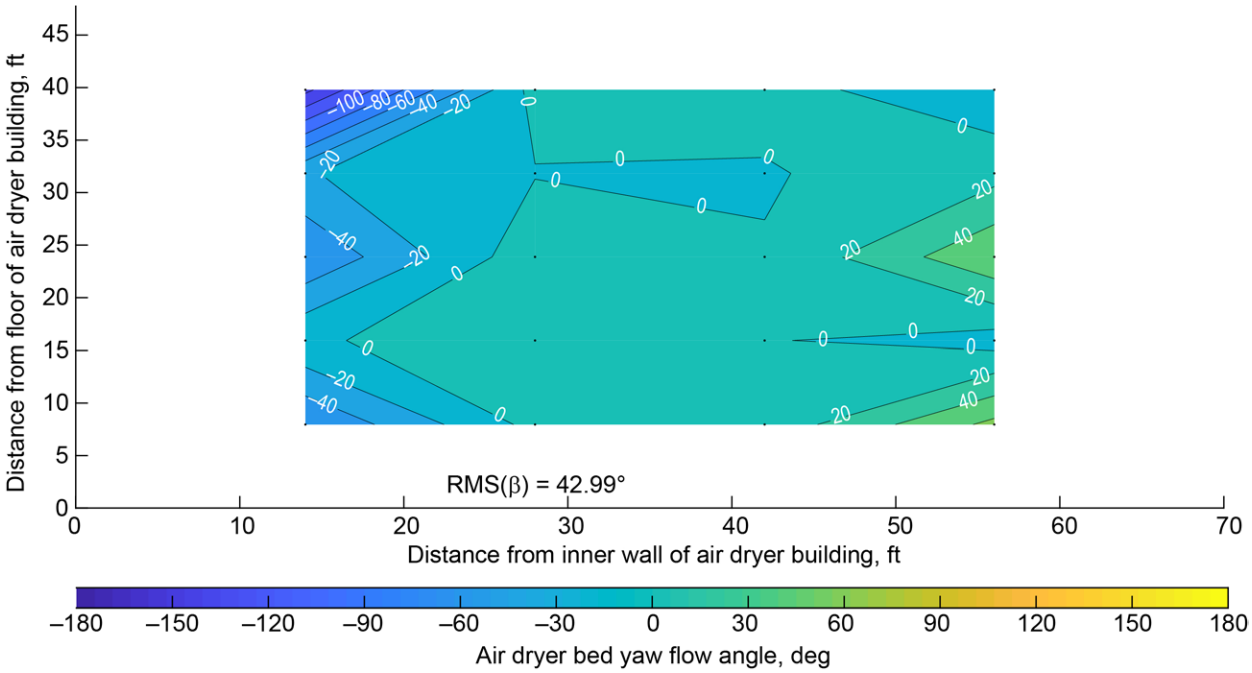

Figure 44.—Contour plot of air dryer bed inlet plane yaw flow angle during operation of 8- by 6-Foot Supersonic Wind Tunnel (upstream looking aft). Nominally Mach 0.30 (one-motor, open-loop operating mode).

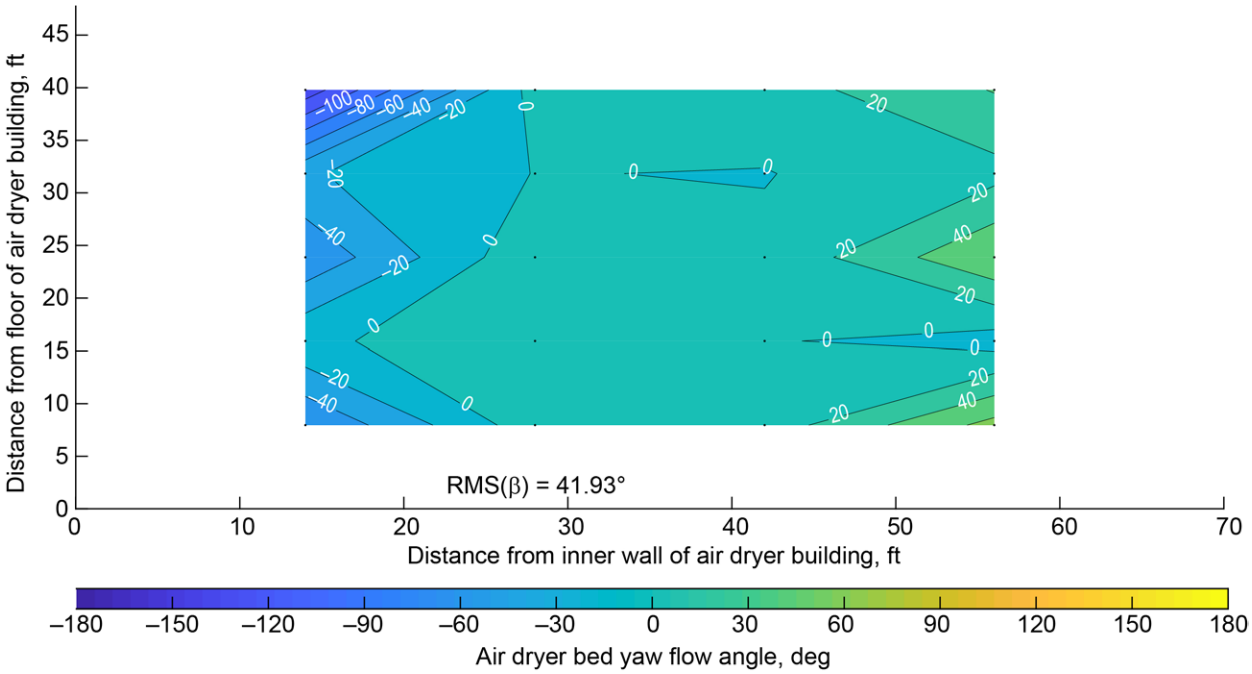

Figure 45.—Contour plot of air dryer bed inlet plane yaw flow angle during operation of 8- by 6-Foot Supersonic Wind Tunnel (upstream looking aft). Nominally Mach 0.25 (one-motor, open-loop operating mode).

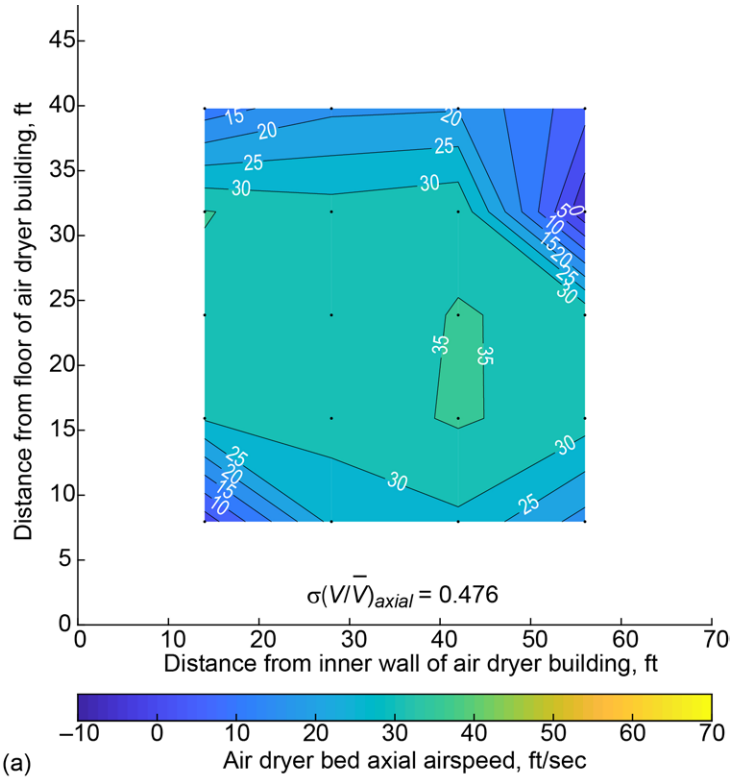

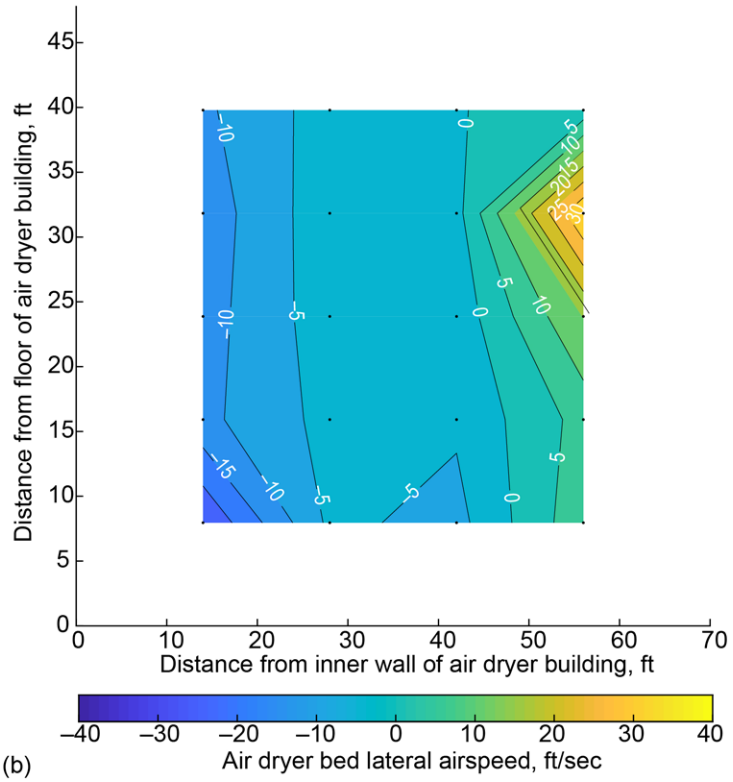

Figure 46.—Contour plot of airspeed at air dryer bed inlet plane during operation of 8- by 6-Foot Supersonic Wind Tunnel (upstream looking aft). Nominally Mach 2.00 (three-motor, closed-loop operating mode). (a) Axial airspeed. (b) Lateral airspeed.

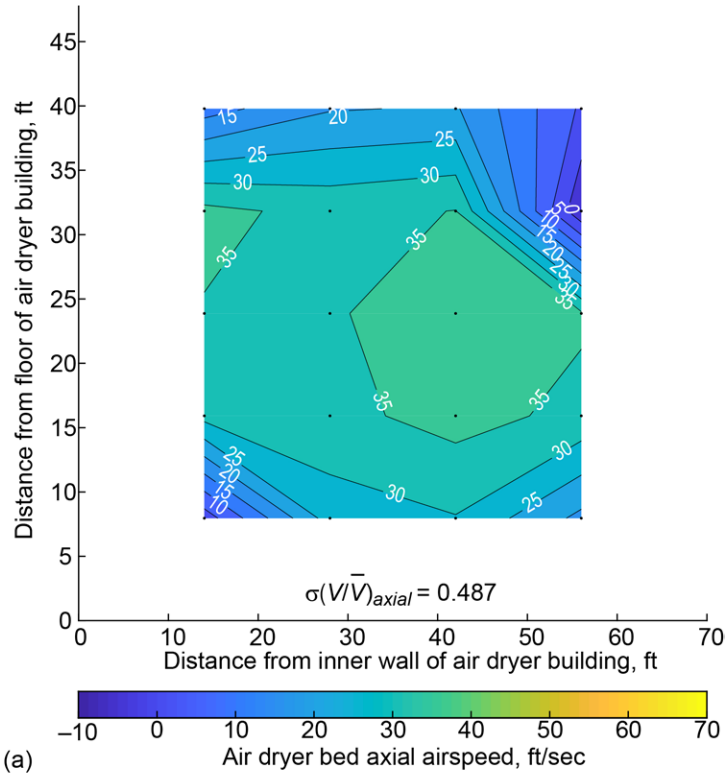

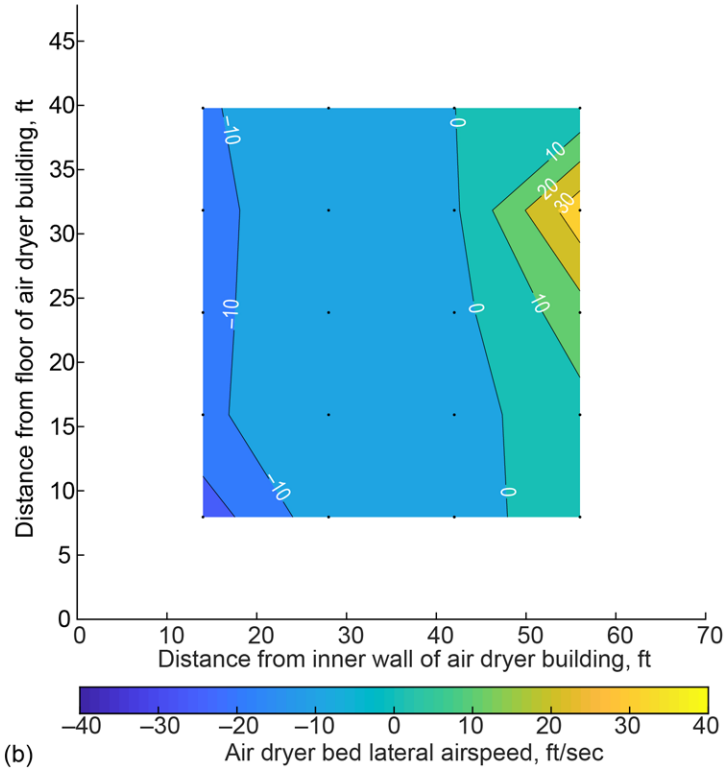

Figure 47.—Contour plot of airspeed at air dryer bed inlet plane during operation of 8- by 6-Foot Supersonic Wind Tunnel (upstream looking aft). Nominally Mach 1.90 (three-motor, closed-loop operating mode). (a) Axial airspeed. (b) Lateral airspeed.

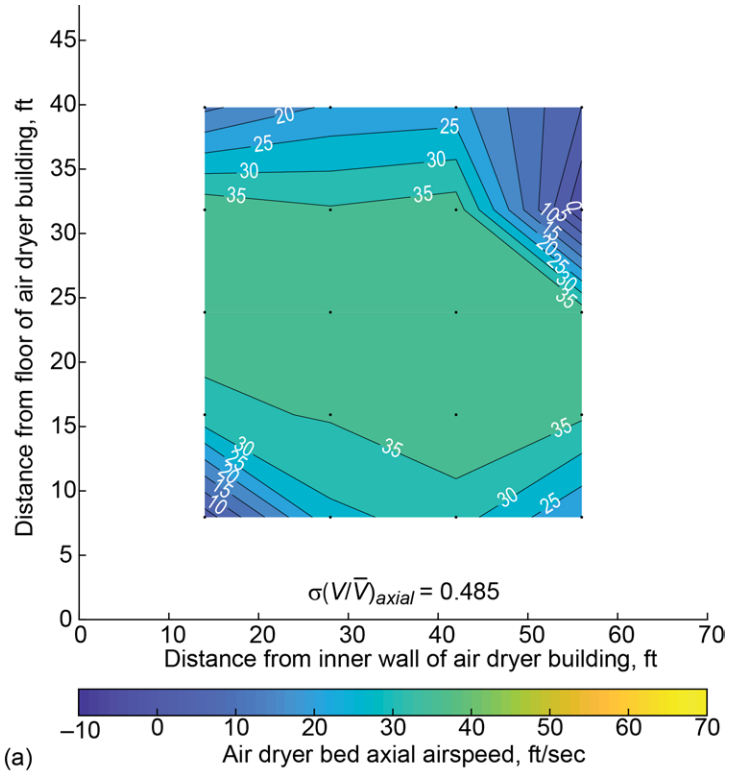

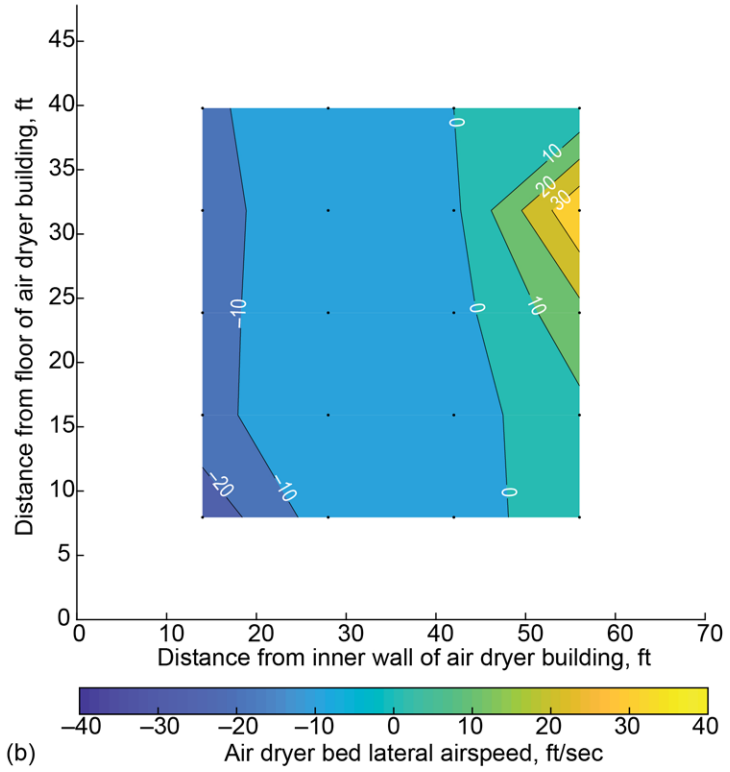

Figure 48.—Contour plot of airspeed at air dryer bed inlet plane during operation of 8- by 6-Foot Supersonic Wind Tunnel (upstream looking aft). Nominally Mach 1.80 (three-motor, closed-loop operating mode). (a) Axial airspeed. (b) Lateral airspeed.

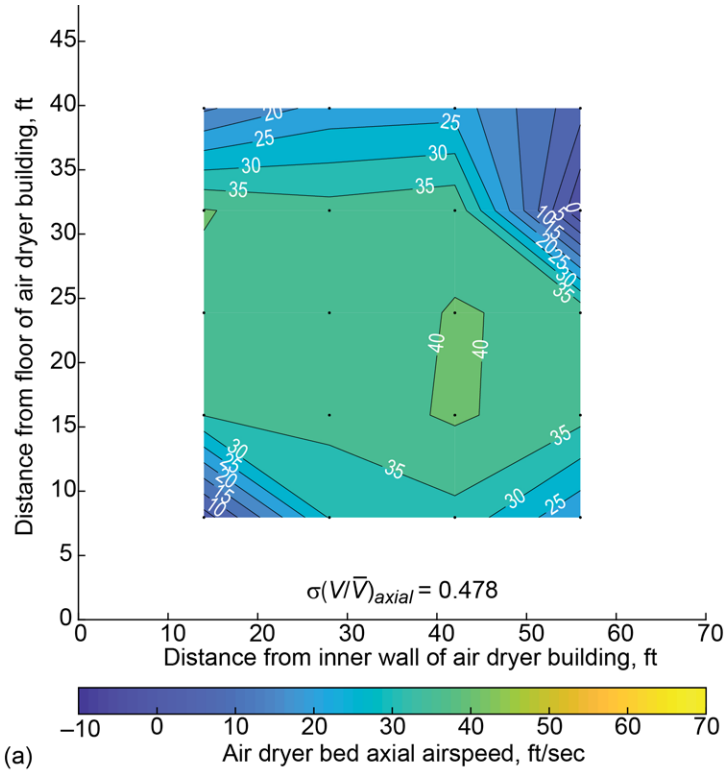

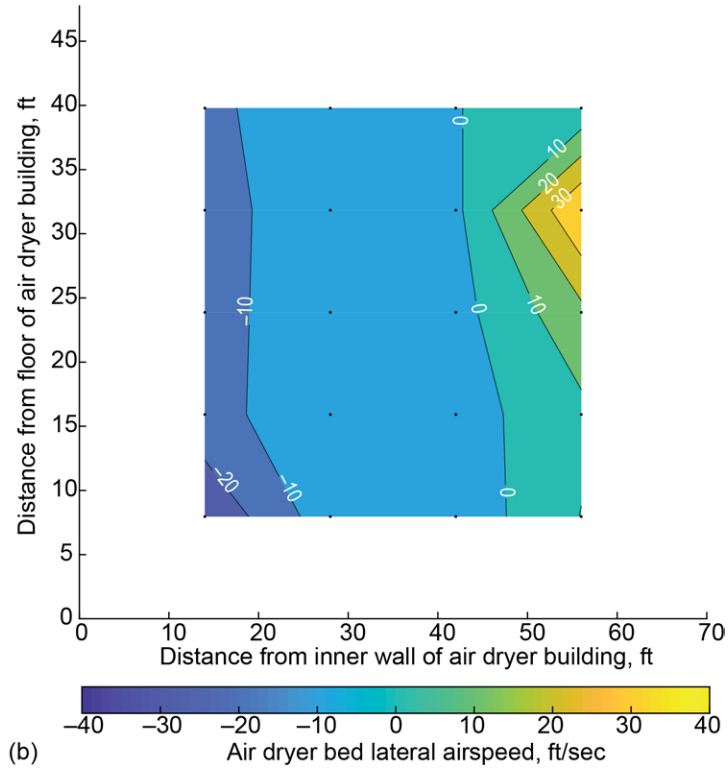

Figure 49.—Contour plot of airspeed at air dryer bed inlet plane during operation of 8- by 6-Foot Supersonic Wind Tunnel (upstream looking aft). Nominally Mach 1.70 (three-motor, closed-loop operating mode). (a) Axial airspeed. (b) Lateral airspeed.

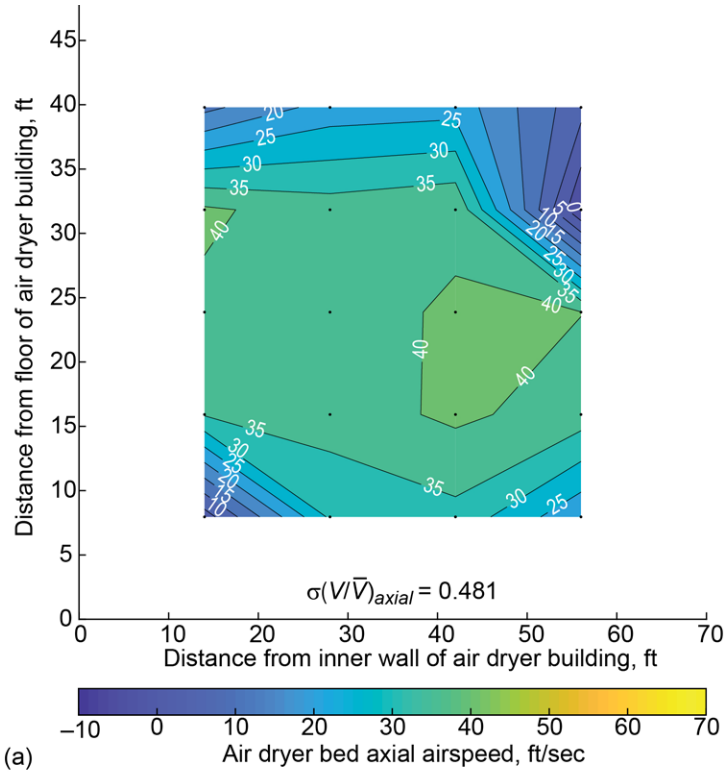

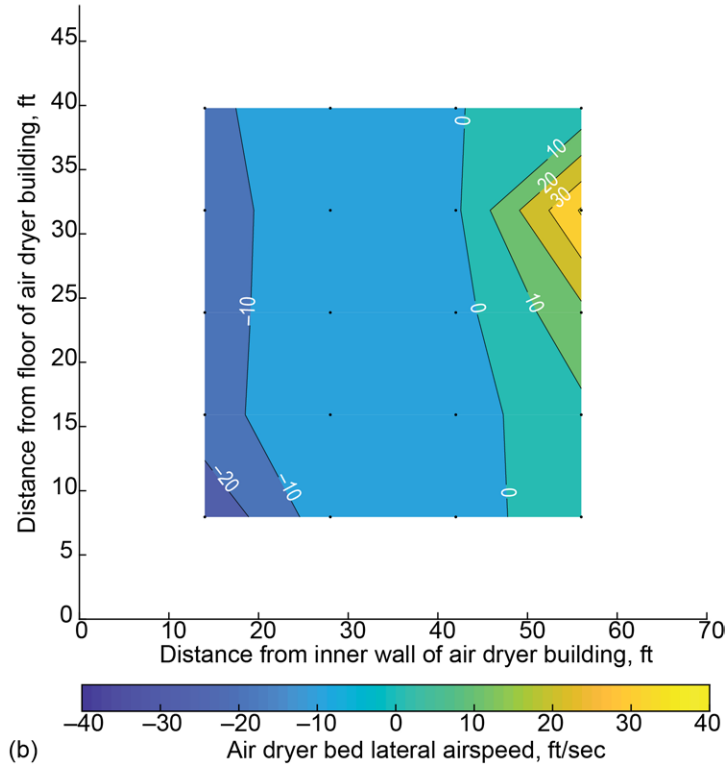

Figure 50.—Contour plot of airspeed at air dryer bed inlet plane during operation of 8- by 6-Foot Supersonic Wind Tunnel (upstream looking aft). Nominally Mach 1.60 (three-motor, closed-loop operating mode). (a) Axial airspeed. (b) Lateral airspeed.

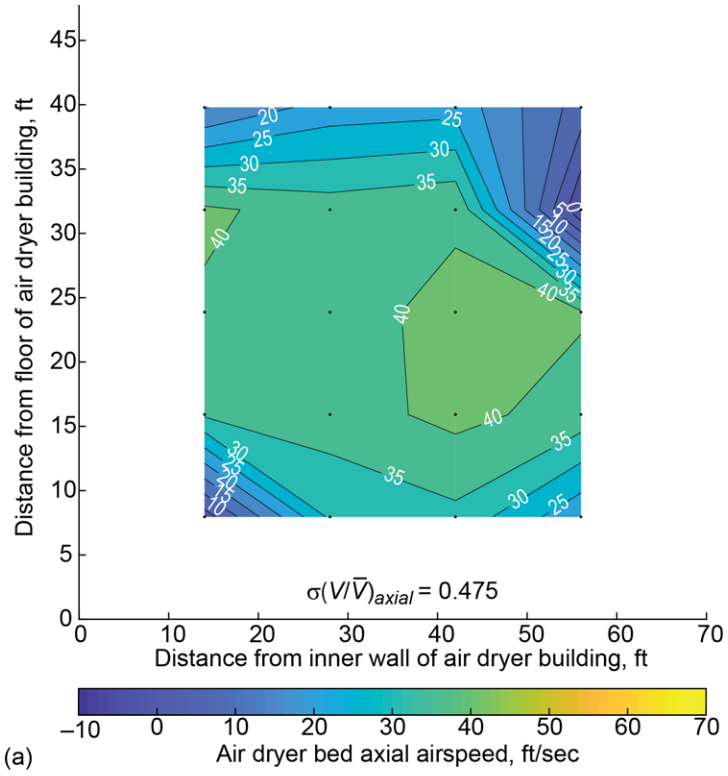

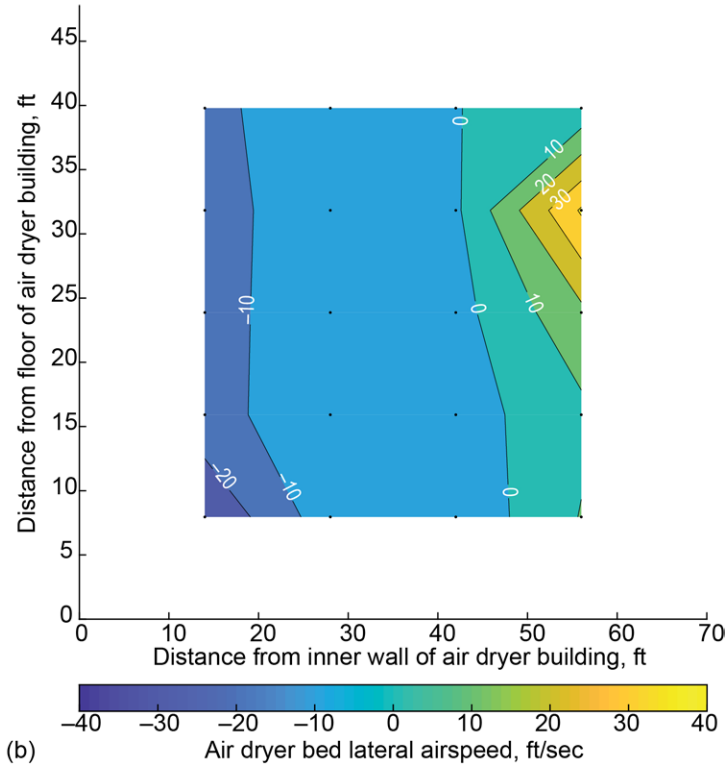

Figure 51.—Contour plot of airspeed at air dryer bed inlet plane during operation of 8- by 6-Foot Supersonic Wind Tunnel (upstream looking aft). Nominally Mach 1.50 (three-motor, closed-loop operating mode). (a) Axial airspeed. (b) Lateral airspeed.

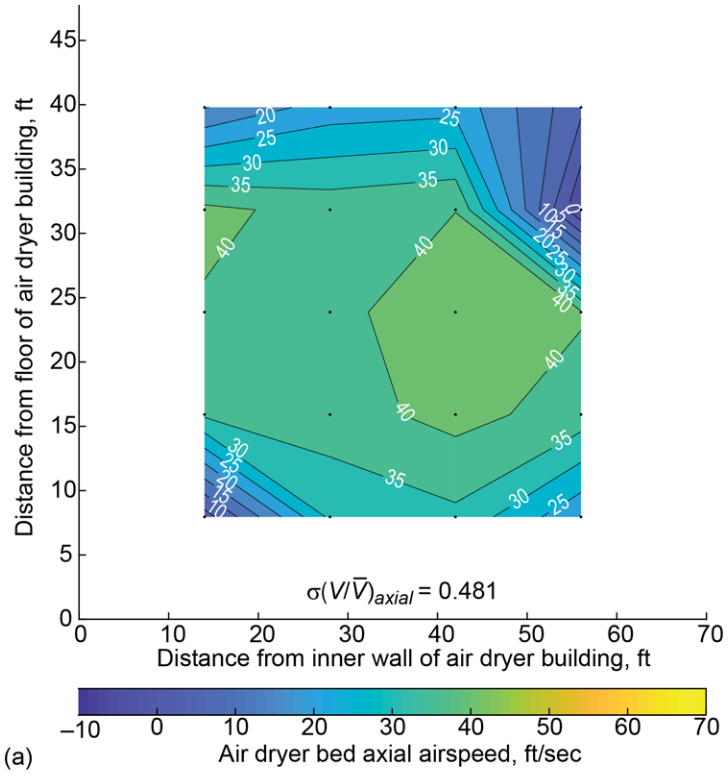

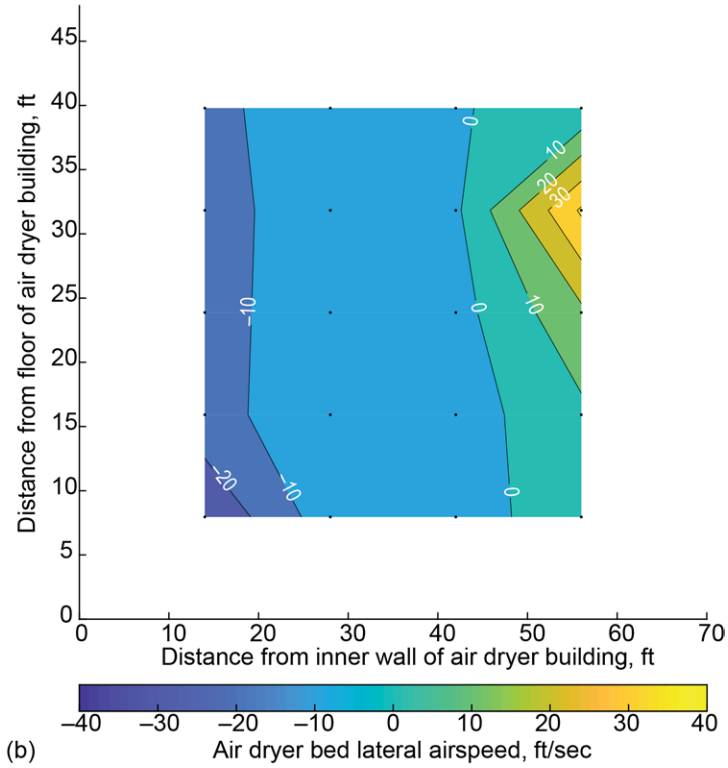

Figure 52.—Contour plot of airspeed at air dryer bed inlet plane during operation of 8- by 6-Foot Supersonic Wind Tunnel (upstream looking aft). Nominally Mach 1.40 (three-motor, closed-loop operating mode). (a) Axial airspeed. (b) Lateral airspeed.

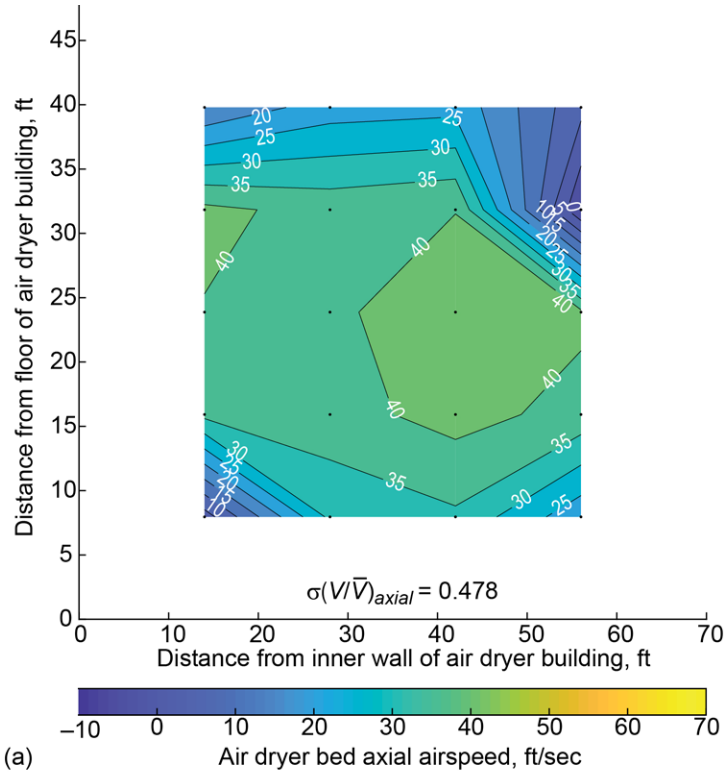

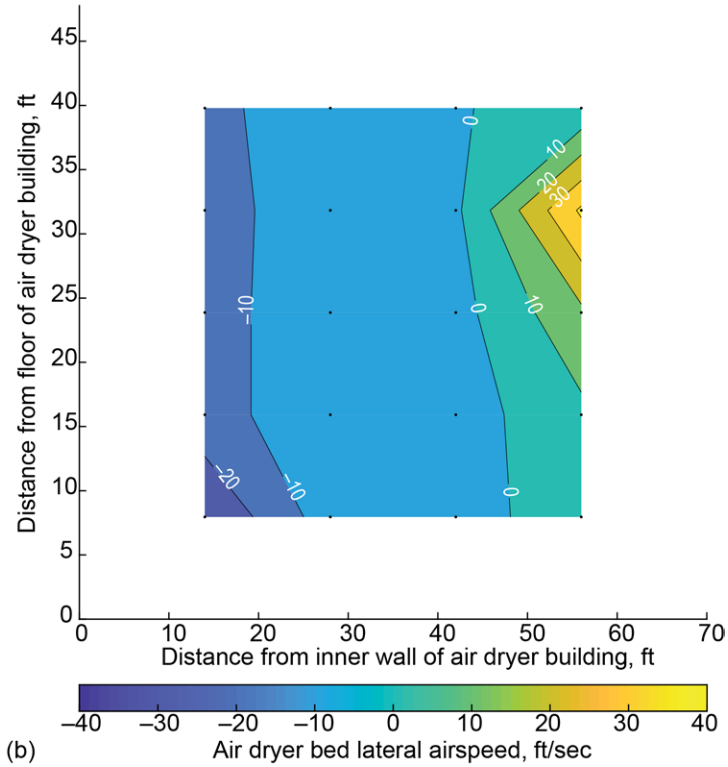

Figure 53.—Contour plot of airspeed at air dryer bed inlet plane during operation of 8- by 6-Foot Supersonic Wind Tunnel (upstream looking aft). Nominally Mach 1.30 (three-motor, closed-loop operating mode with doors 4 and 5 open). (a) Axial airspeed. (b) Lateral airspeed.

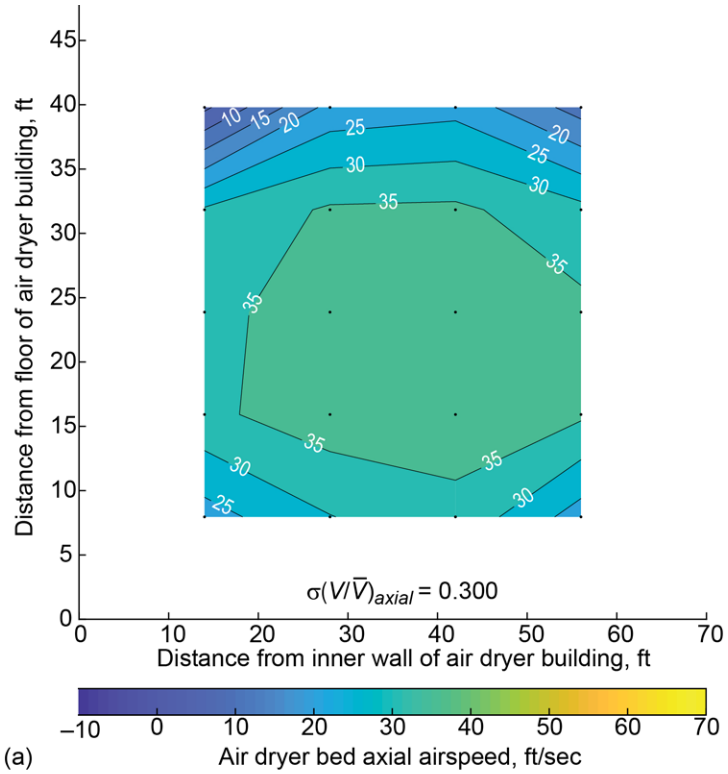

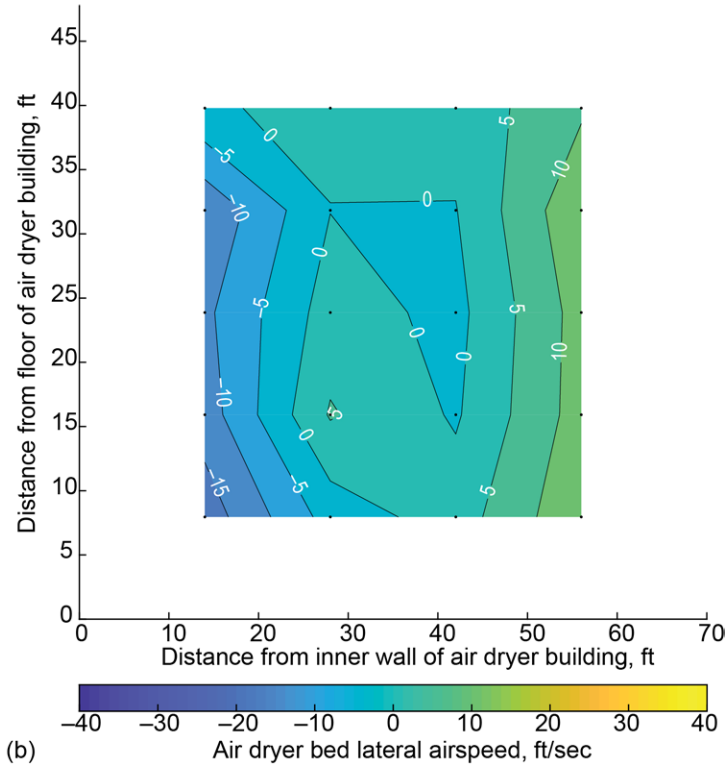

Figure 54.—Contour plot of airspeed at air dryer bed inlet plane during operation of 8- by 6-Foot Supersonic Wind Tunnel (upstream looking aft). Nominally Mach 1.60 (three-motor, open-loop operating mode). (a) Axial airspeed. (b) Lateral airspeed.

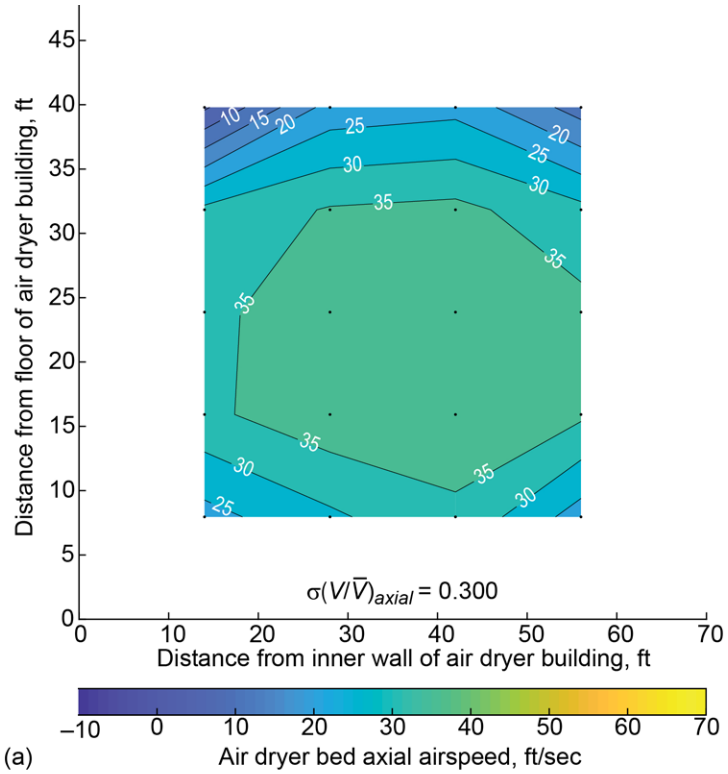

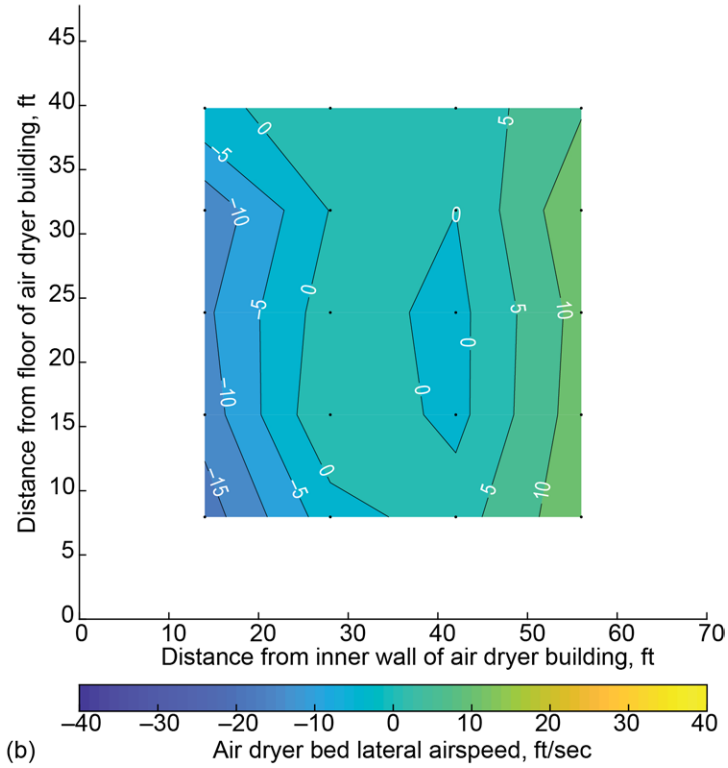

Figure 55.—Contour plot of airspeed at air dryer bed inlet plane during operation of 8- by 6-Foot Supersonic Wind Tunnel (upstream looking aft). Nominally Mach 1.50 (three-motor, open-loop operating mode). (a) Axial airspeed. (b) Lateral airspeed.

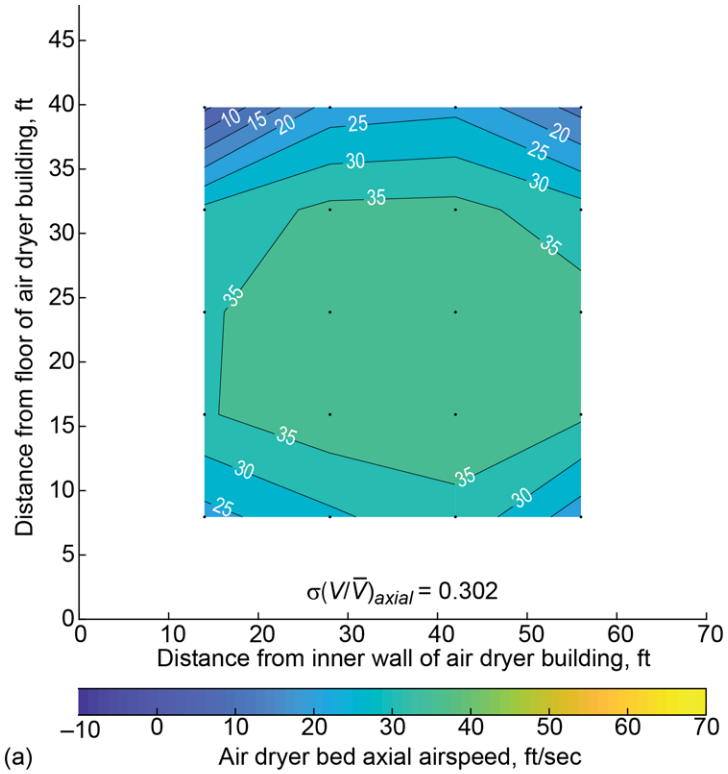

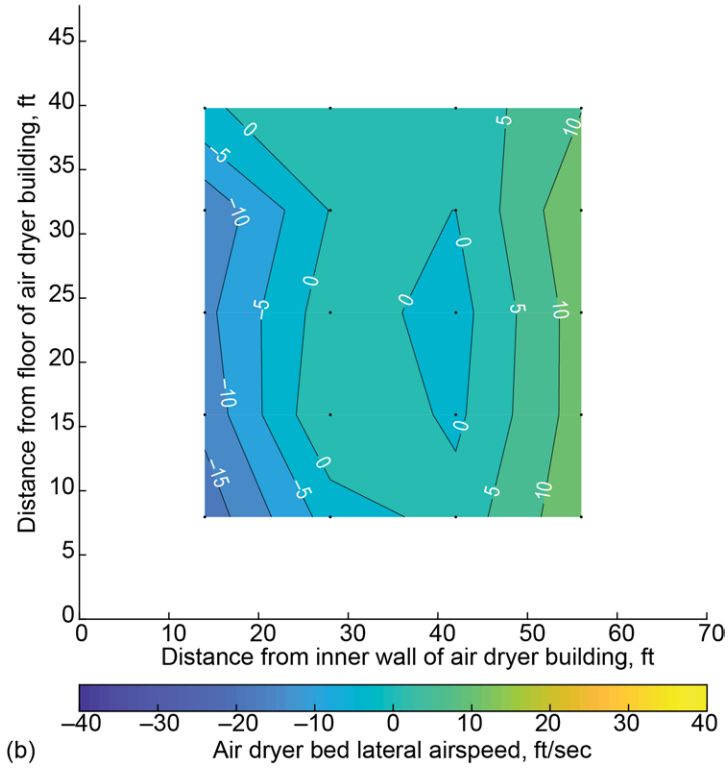

Figure 56.—Contour plot of airspeed at air dryer bed inlet plane during operation of 8- by 6-Foot Supersonic Wind Tunnel (upstream looking aft). Nominally Mach 1.40 (three-motor, open-loop operating mode). (a) Axial airspeed. (b) Lateral airspeed.

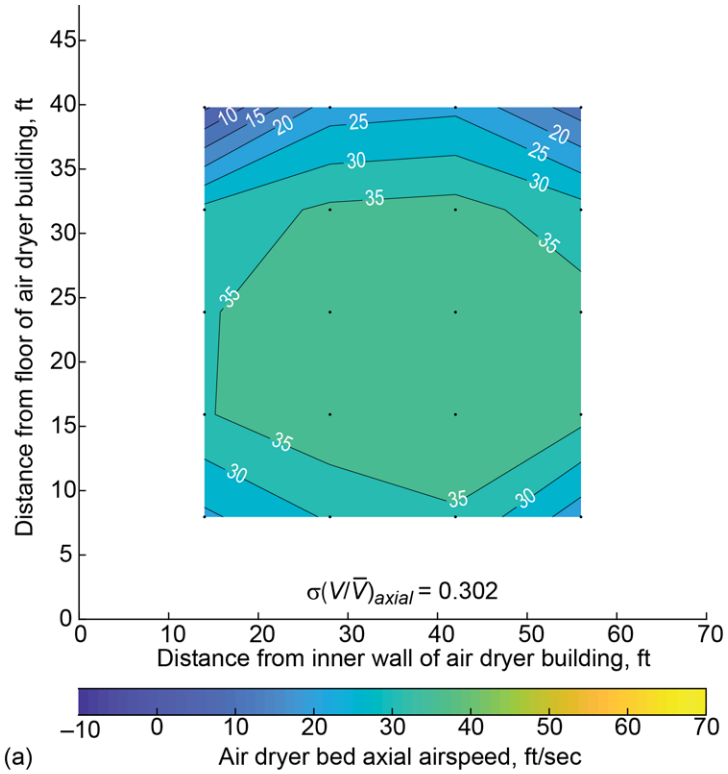

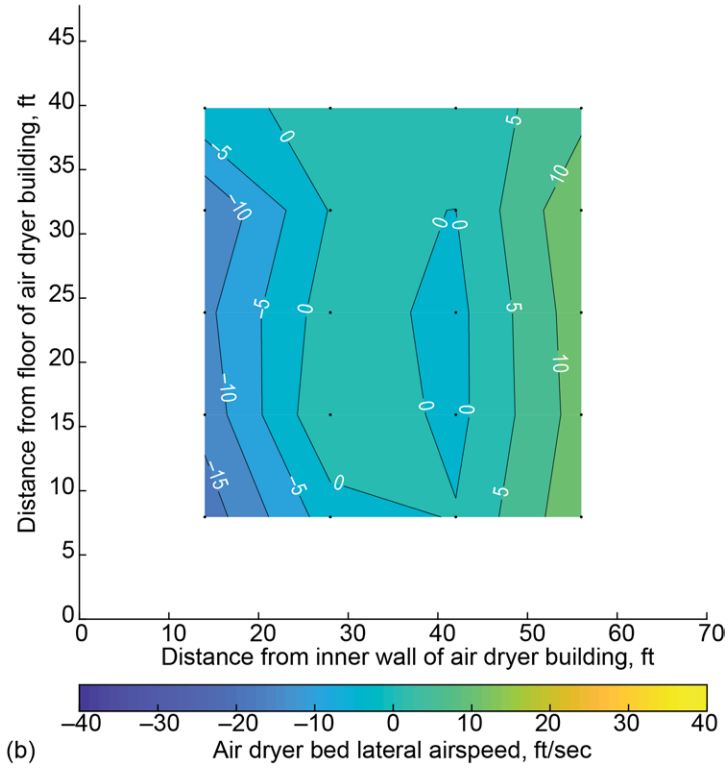

Figure 57.—Contour plot of airspeed at air dryer bed inlet plane during operation of 8- by 6-Foot Supersonic Wind Tunnel (upstream looking aft). Nominally Mach 1.30 (three-motor, open-loop operating mode). (a) Axial airspeed. (b) Lateral airspeed.

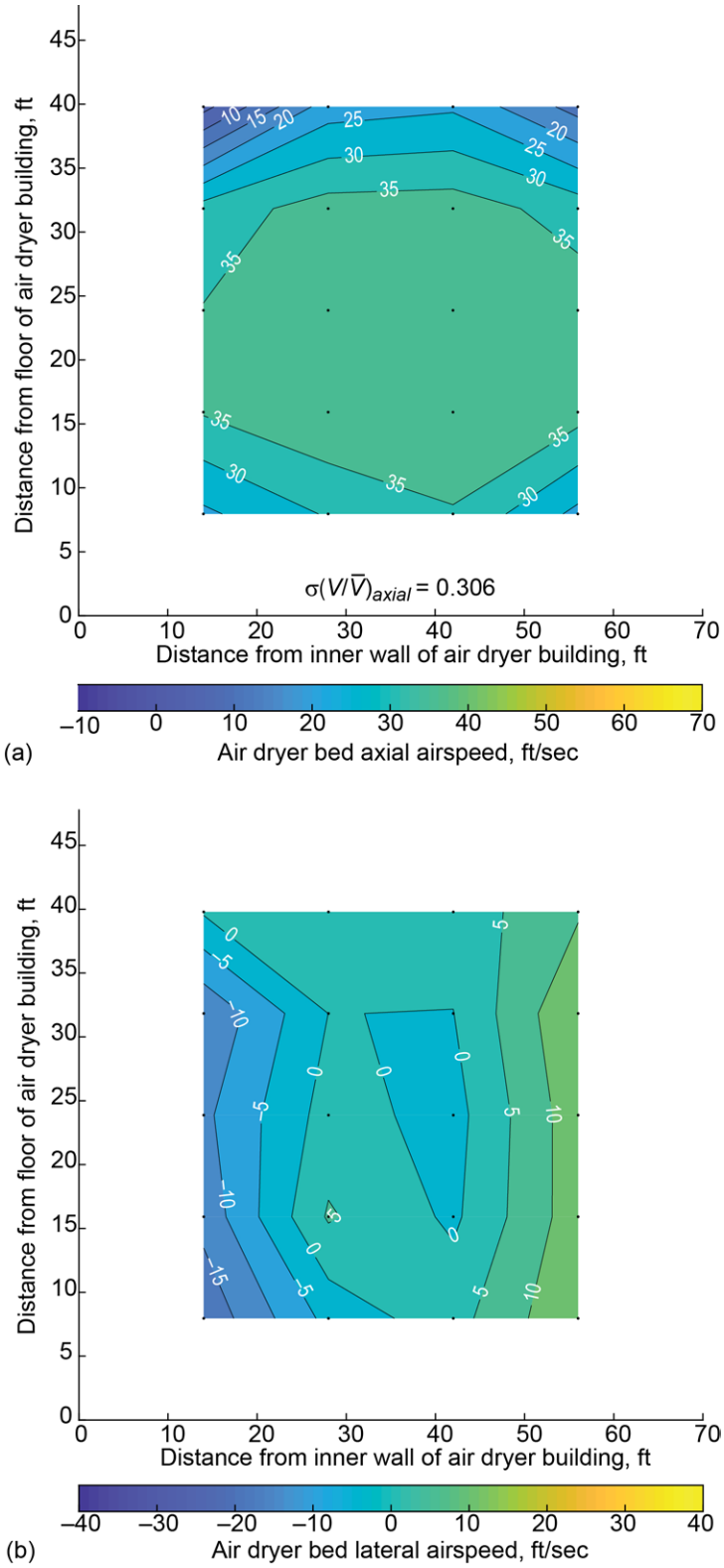

Figure 58.—Contour plot of airspeed at air dryer bed inlet plane during operation of 8- by 6-Foot Supersonic Wind Tunnel (upstream looking aft). Nominally Mach 1.20 (three-motor, open-loop operating mode). (a) Axial airspeed. (b) Lateral airspeed.

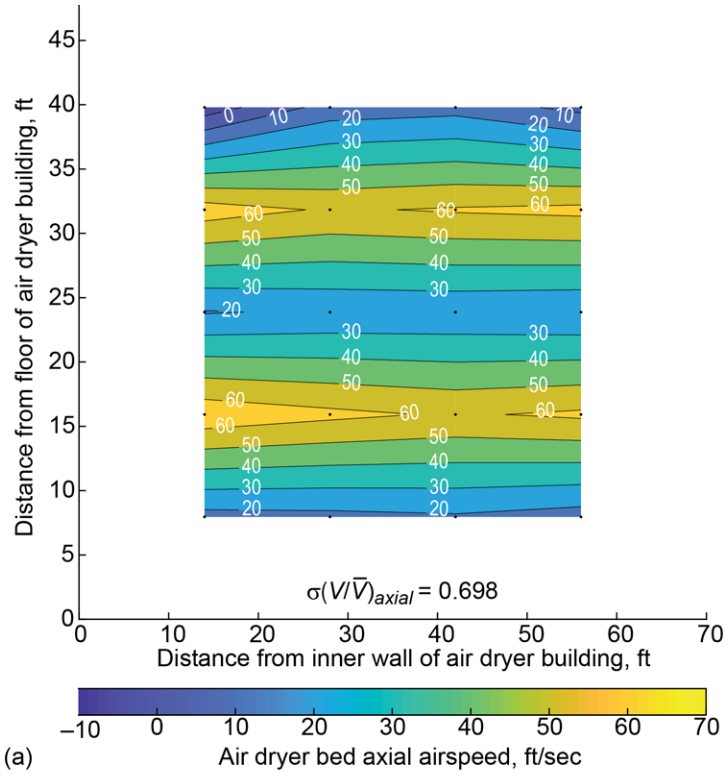

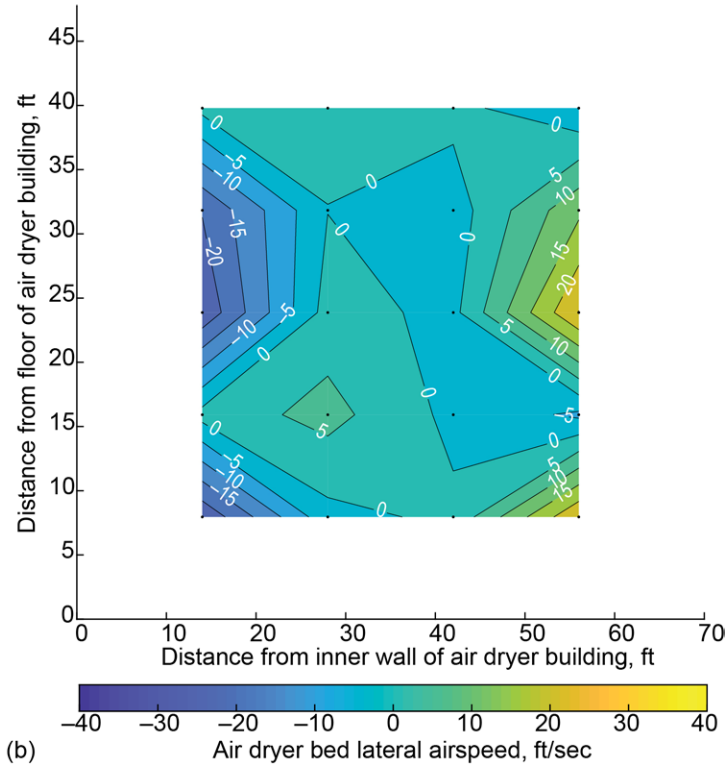

Figure 59.—Contour plot of airspeed at air dryer bed inlet plane during operation of 8- by 6-Foot Supersonic Wind Tunnel (upstream looking aft). Nominally Mach 1.10 (three-motor, open-loop operating mode). (a) Axial airspeed. (b) Lateral airspeed.

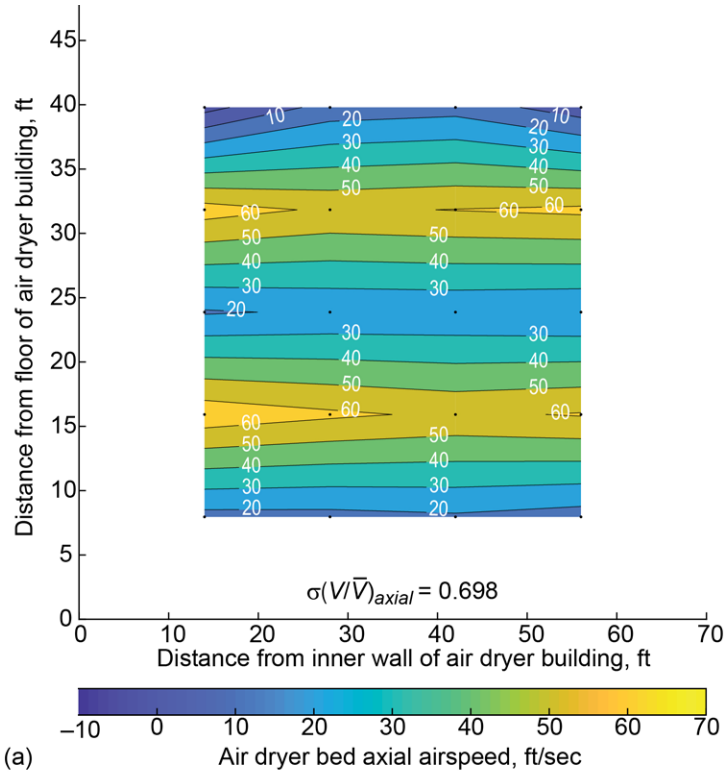

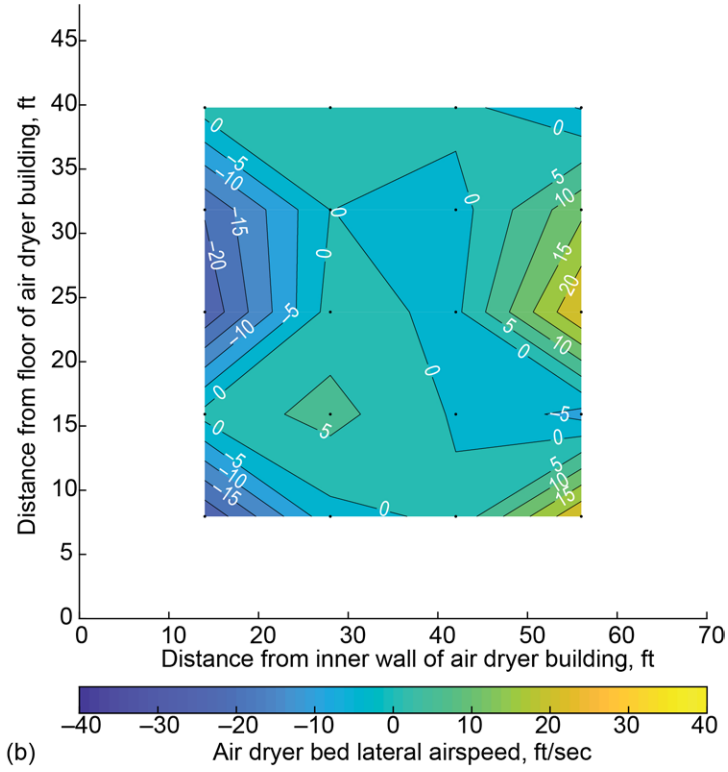

Figure 60.—Contour plot of airspeed at air dryer bed inlet plane during operation of 8- by 6-Foot Supersonic Wind Tunnel (upstream looking aft). Nominally Mach 0.90 (three-motor, open-loop operating mode). (a) Axial airspeed. (b) Lateral airspeed.

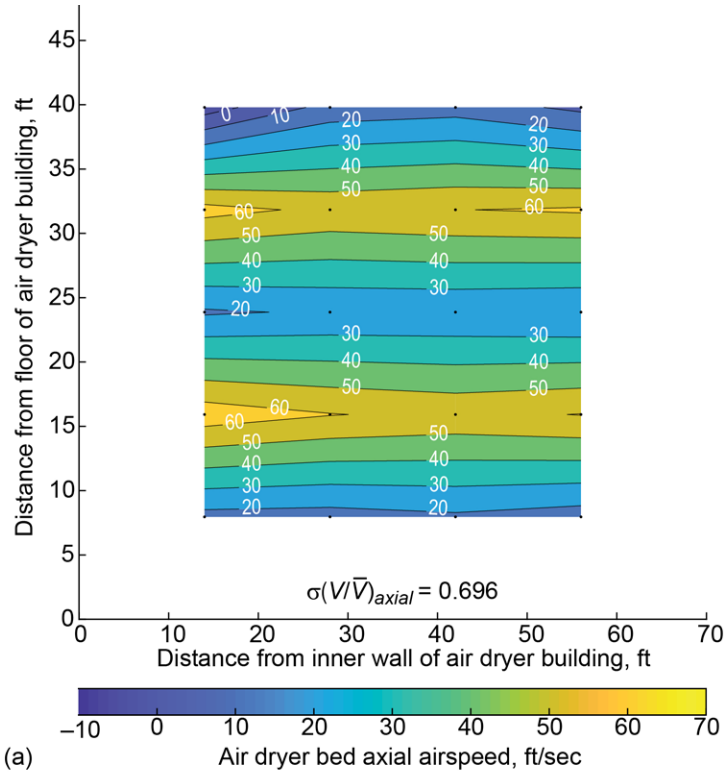

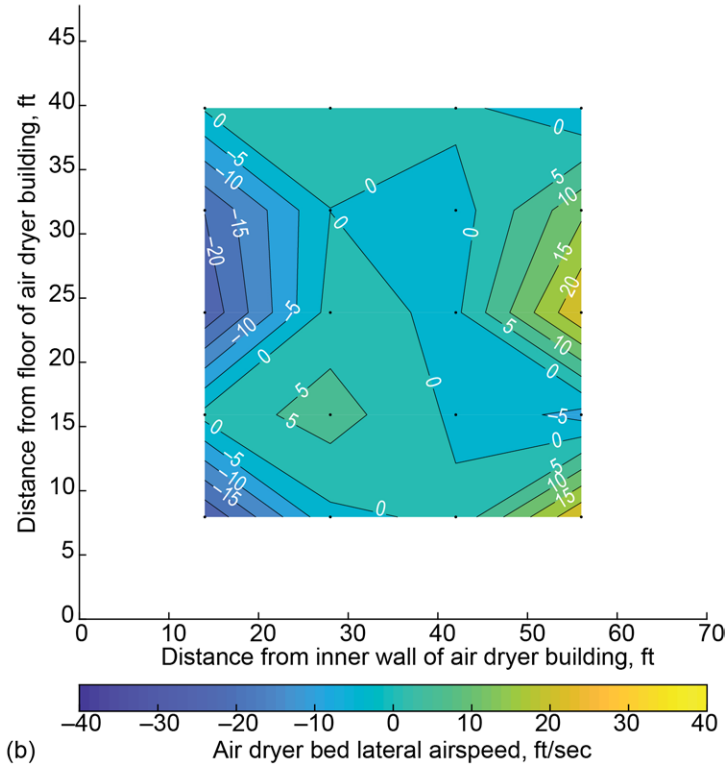

Figure 61.—Contour plot of airspeed at air dryer bed inlet plane during operation of 8- by 6-Foot Supersonic Wind Tunnel (upstream looking aft). Nominally Mach 0.80 (three-motor, open-loop operating mode). (a) Axial airspeed. (b) Lateral airspeed.

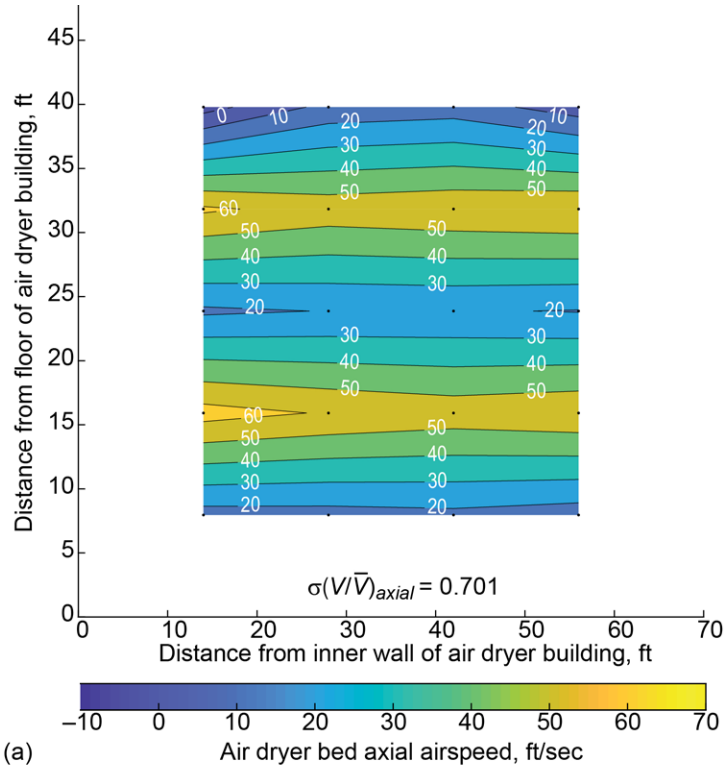

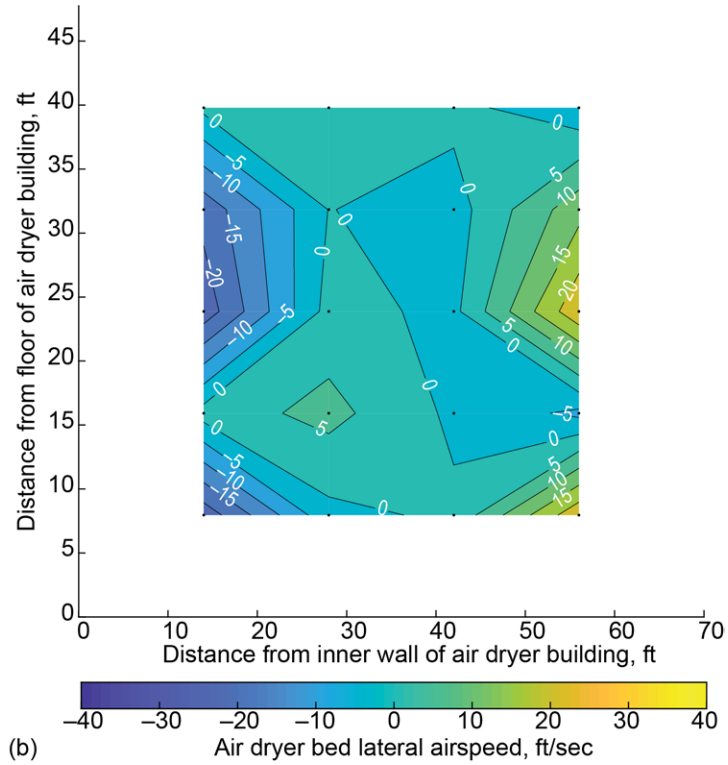

Figure 62.—Contour plot of airspeed at air dryer bed inlet plane during operation of 8- by 6-Foot Supersonic Wind Tunnel (upstream looking aft). Nominally Mach 0.70 (three-motor, open-loop operating mode). (a) Axial airspeed. (b) Lateral airspeed.

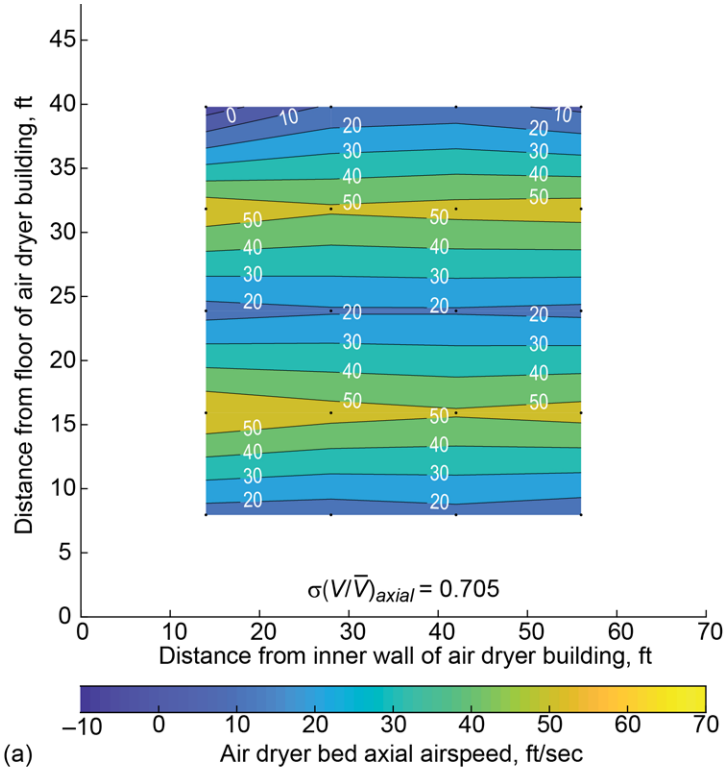

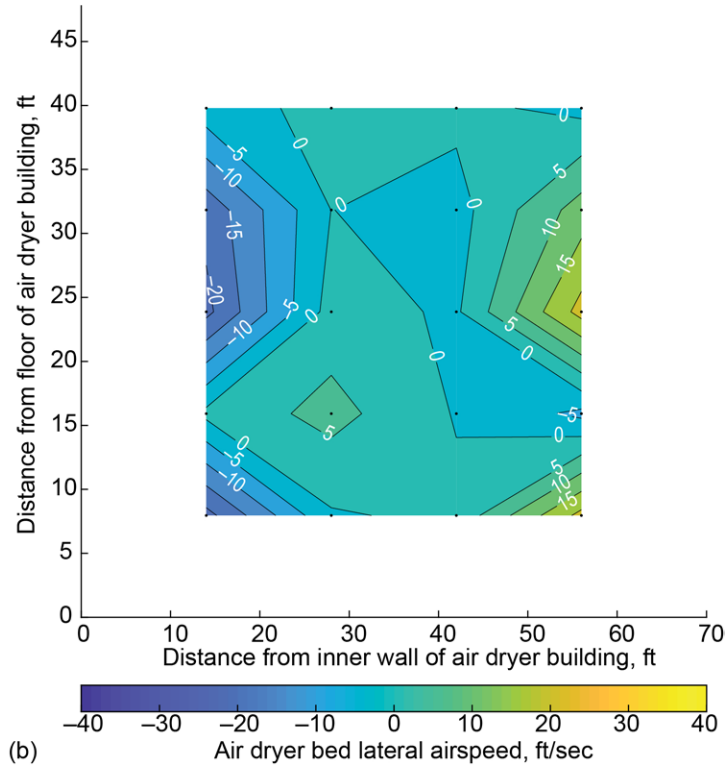

Figure 63.—Contour plot of airspeed at air dryer bed inlet plane during operation of 8- by 6-Foot Supersonic Wind Tunnel (upstream looking aft). Nominally Mach 0.60 (three-motor, open-loop operating mode). (a) Axial airspeed. (b) Lateral airspeed.

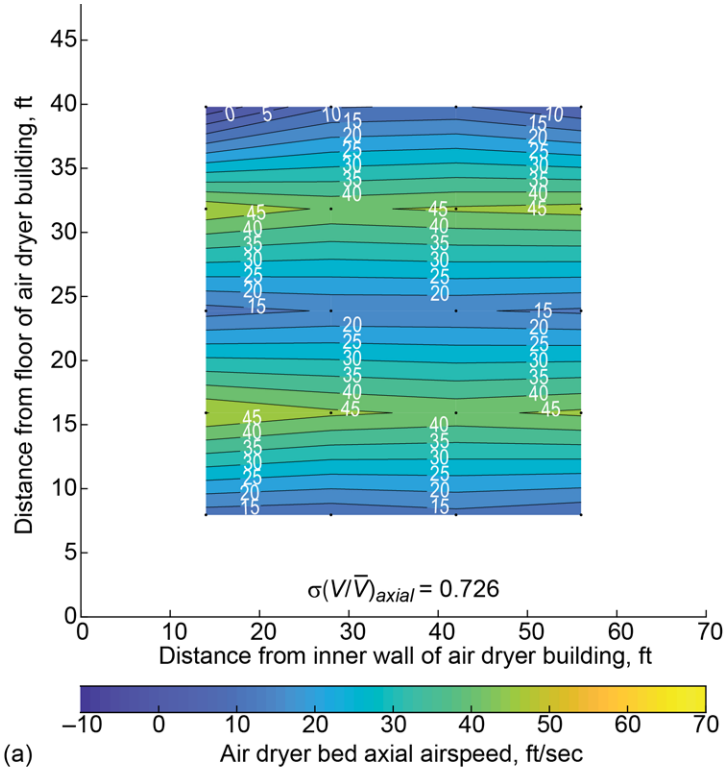

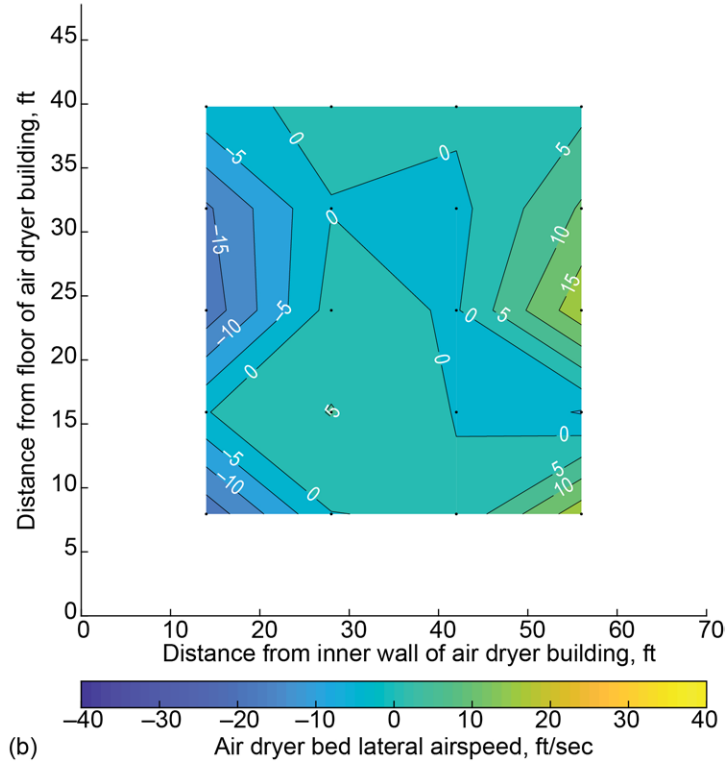

Figure 64.—Contour plot of airspeed at air dryer bed inlet plane during operation of 8- by 6-Foot Supersonic Wind Tunnel (upstream looking aft). Nominally Mach 0.50 (three-motor, open-loop operating mode). (a) Axial airspeed. (b) Lateral airspeed.

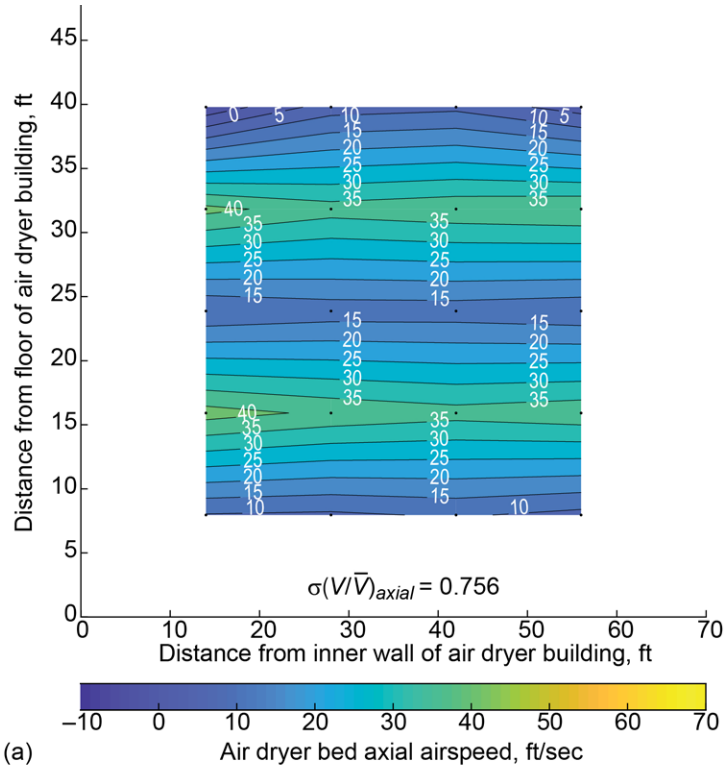

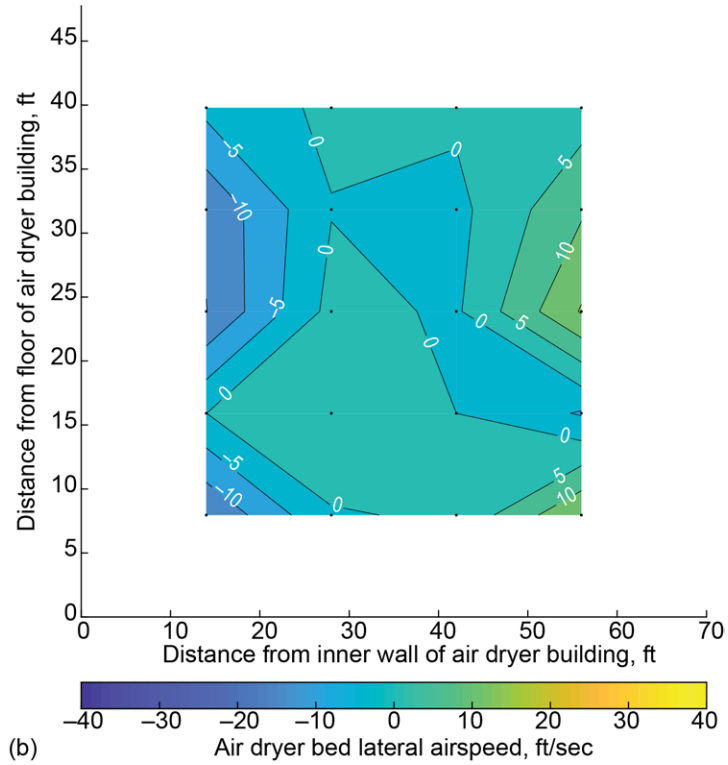

Figure 65.—Contour plot of airspeed at air dryer bed inlet plane during operation of 8- by 6-Foot Supersonic Wind Tunnel (upstream looking aft). Nominally Mach 0.40 (three-motor, open-loop operating mode). (a) Axial airspeed. (b) Lateral airspeed.

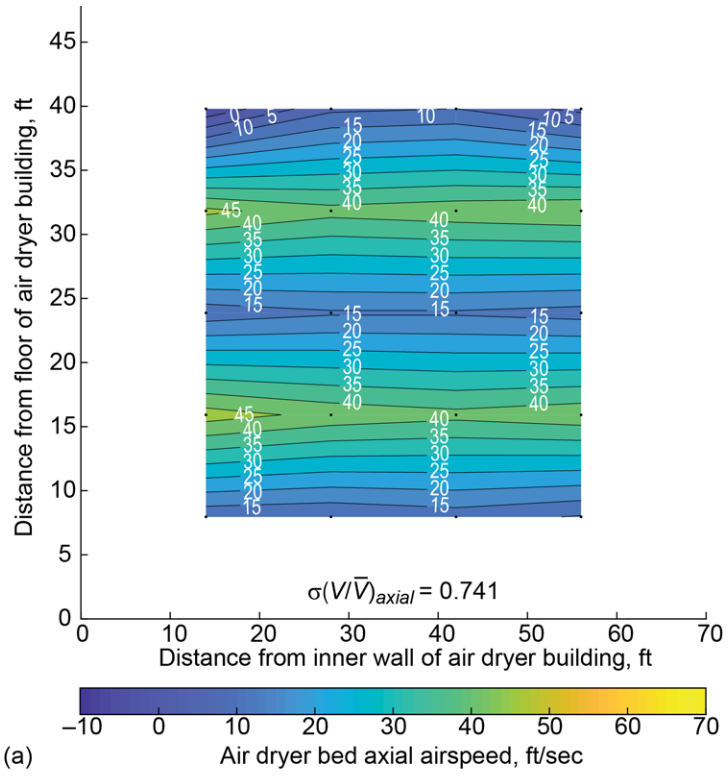

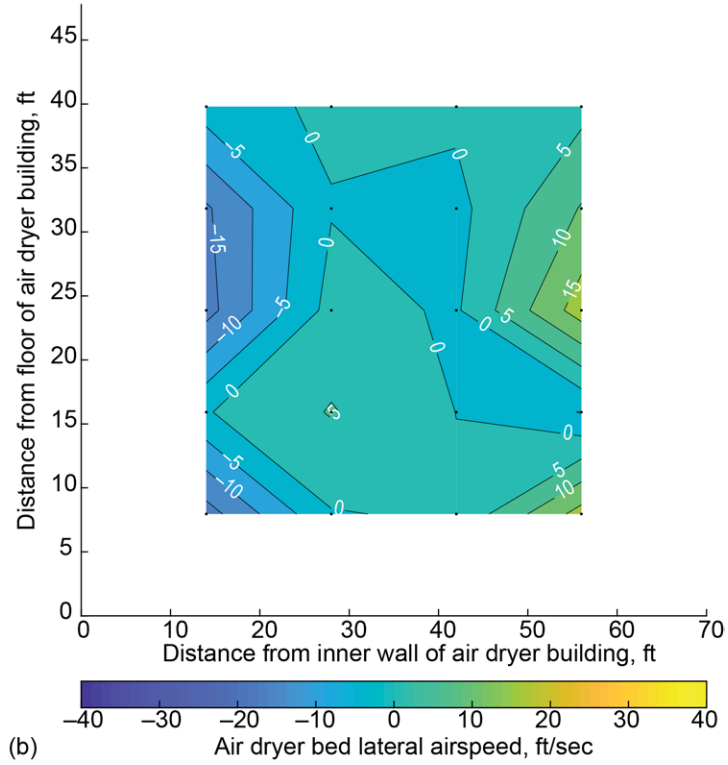

Figure 66.—Contour plot of airspeed at air dryer bed inlet plane during operation of 8- by 6-Foot Supersonic Wind Tunnel (upstream looking aft). Nominally Mach 0.50 (one-motor, open-loop operating mode). (a) Axial airspeed. (b) Lateral airspeed.

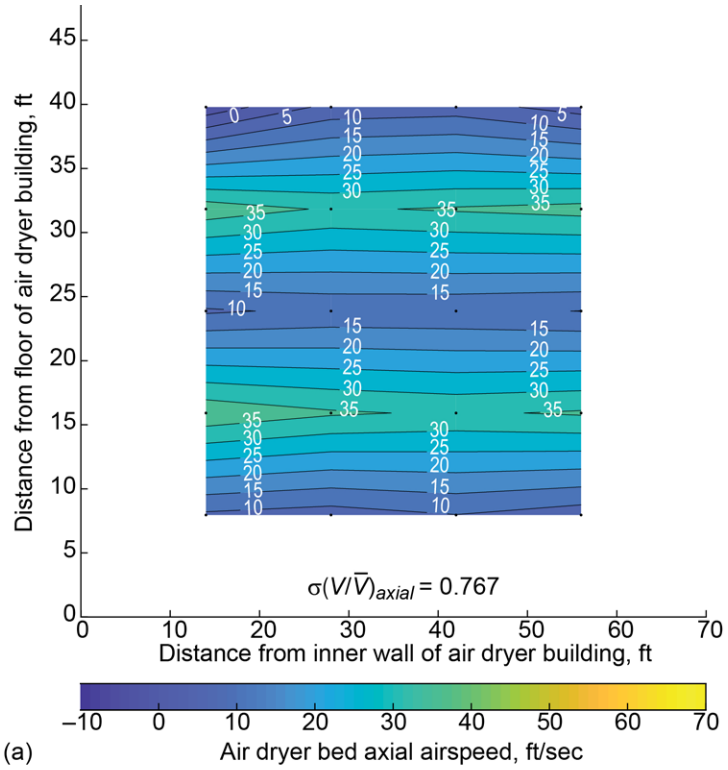

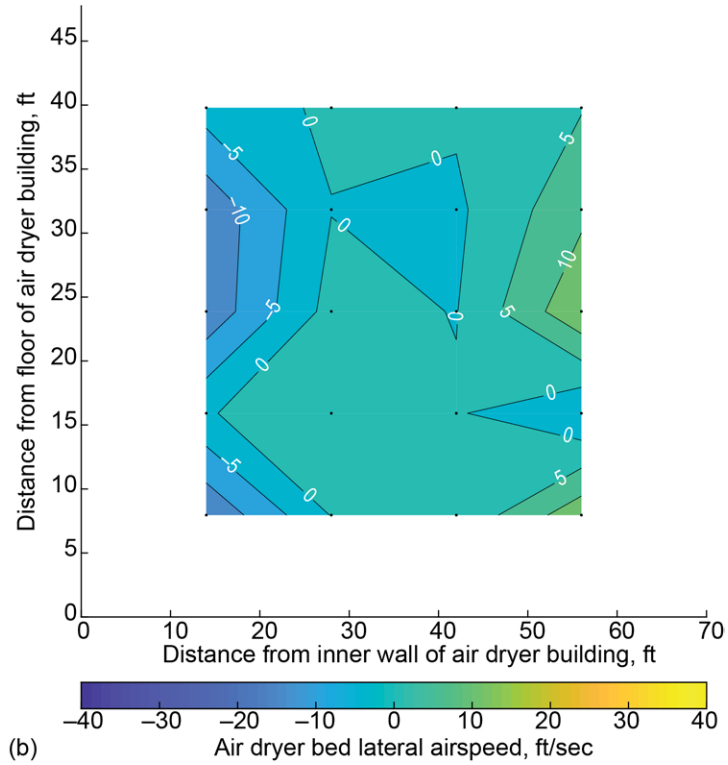

Figure 67.—Contour plot of airspeed at air dryer bed inlet plane during operation of 8- by 6-Foot Supersonic Wind Tunnel (upstream looking aft). Nominally Mach 0.40 (one-motor, open-loop operating mode). (a) Axial airspeed. (b) Lateral airspeed.

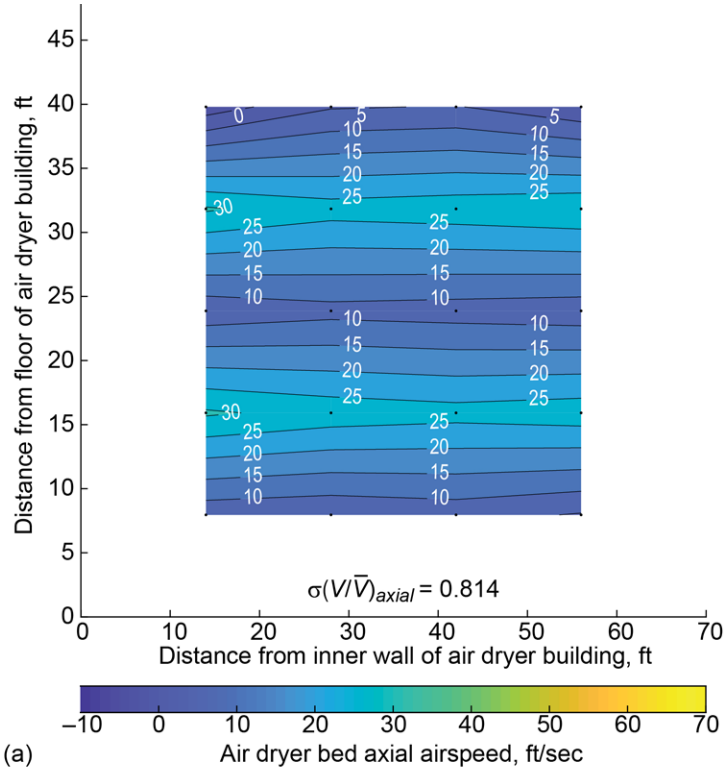

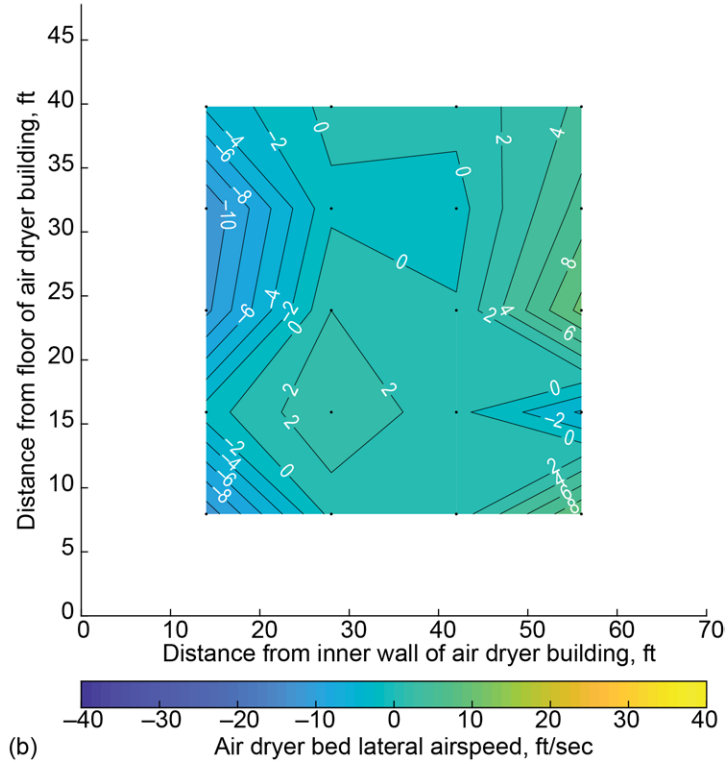

Figure 68.—Contour plot of airspeed at air dryer bed inlet plane during operation of 8- by 6-Foot Supersonic Wind Tunnel (upstream looking aft). Nominally Mach 0.30 (one-motor, open-loop operating mode). (a) Axial airspeed. (b) Lateral airspeed.

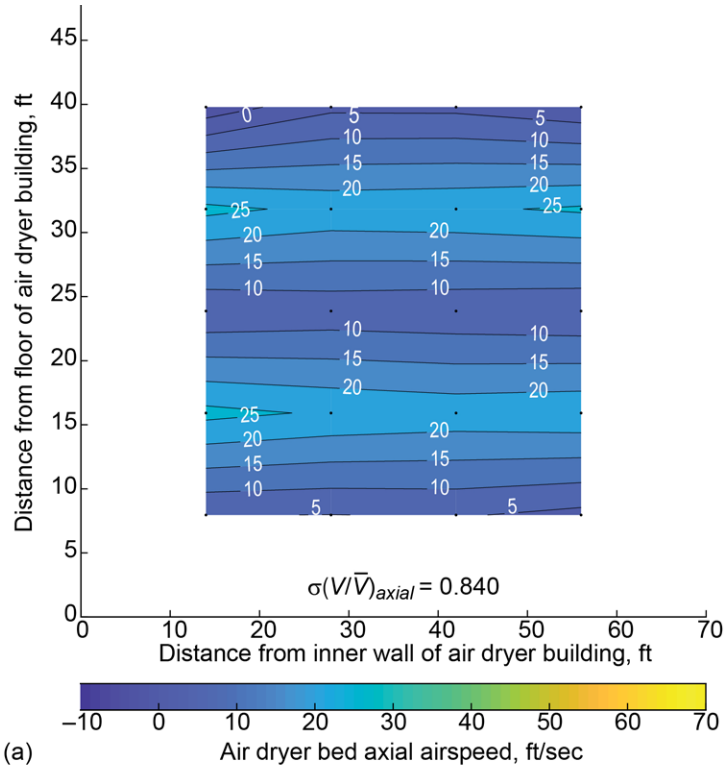

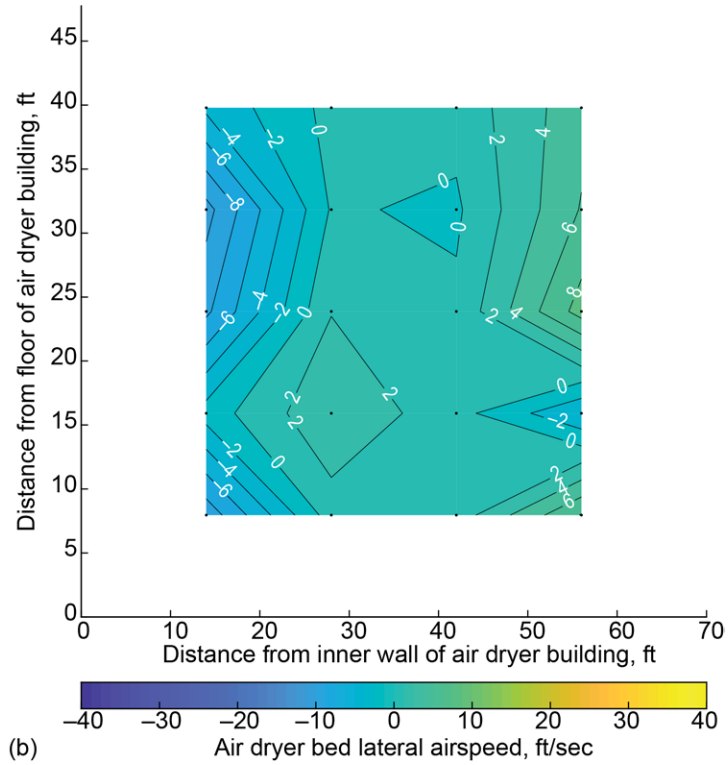

Figure 69.—Contour plot of airspeed at air dryer bed inlet plane during operation of 8- by 6-Foot Supersonic Wind Tunnel (upstream looking aft). Nominally Mach 0.25 (one-motor, open-loop operating mode). (a) Axial airspeed. (b) Lateral airspeed.

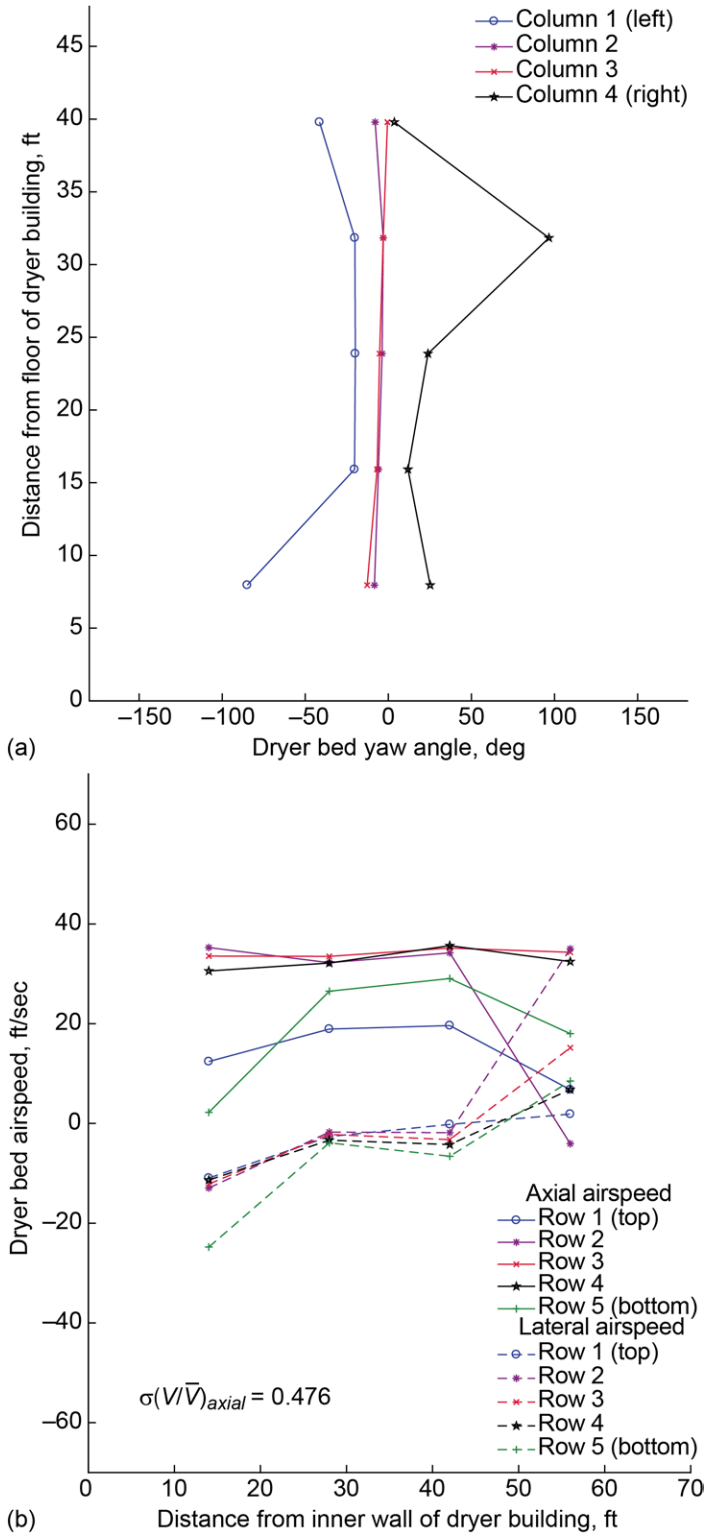

Figure 70.—Measurements from each of the 20 dryer bed wind anemometers at dryer bed inlet plane during operation of 8- by 6-Foot Supersonic Wind Tunnel (upstream looking aft). Nominally Mach 2.00 (three-motor, closed-loop operating mode). (a) Yaw flow angle. (b) Axial and lateral airspeed.

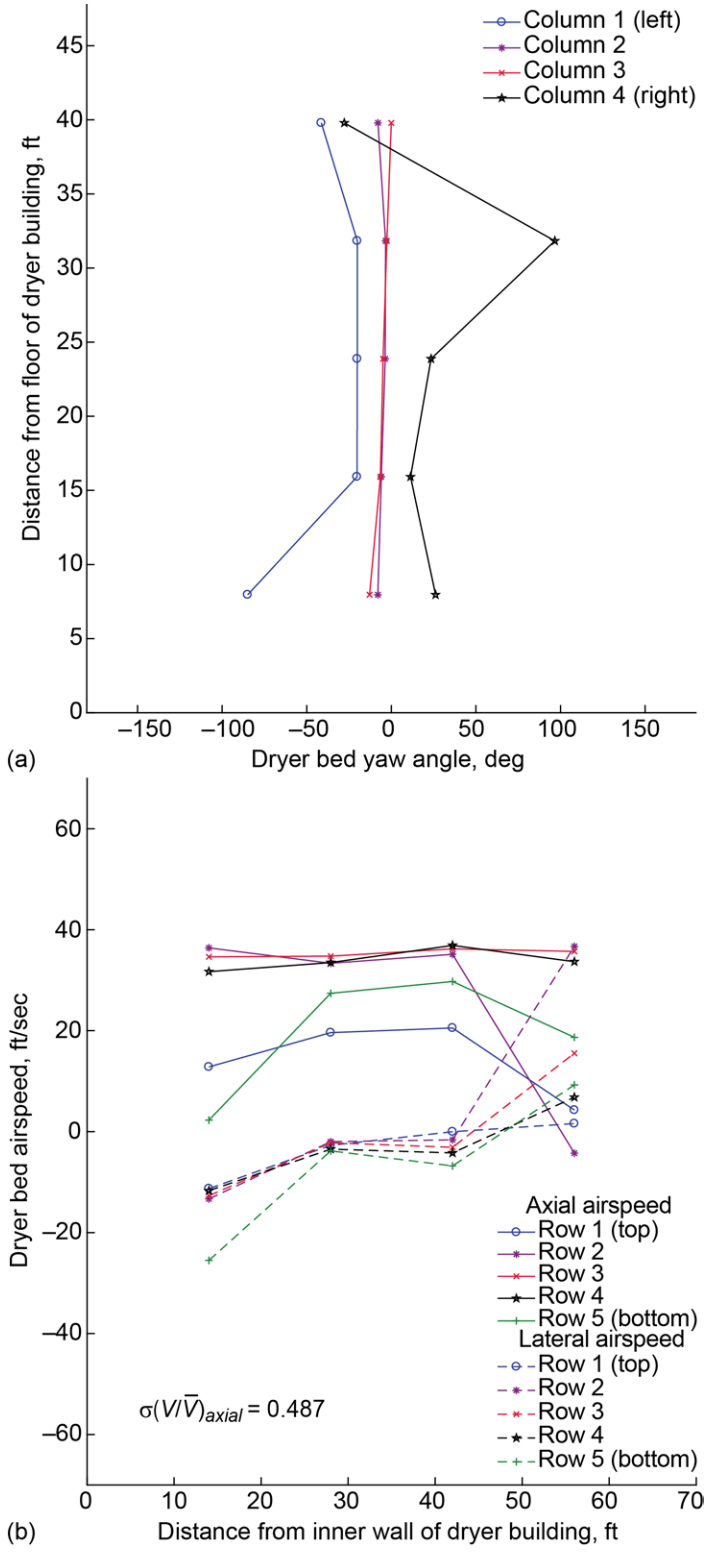

Figure 71.—Measurements from each of the 20 dryer bed wind anemometers at dryer bed inlet plane during operation of 8- by 6-Foot Supersonic Wind Tunnel (upstream looking aft). Nominally Mach 1.90 (three-motor, closed-loop operating mode). (a) Yaw flow angle. (b) Axial and lateral airspeed.

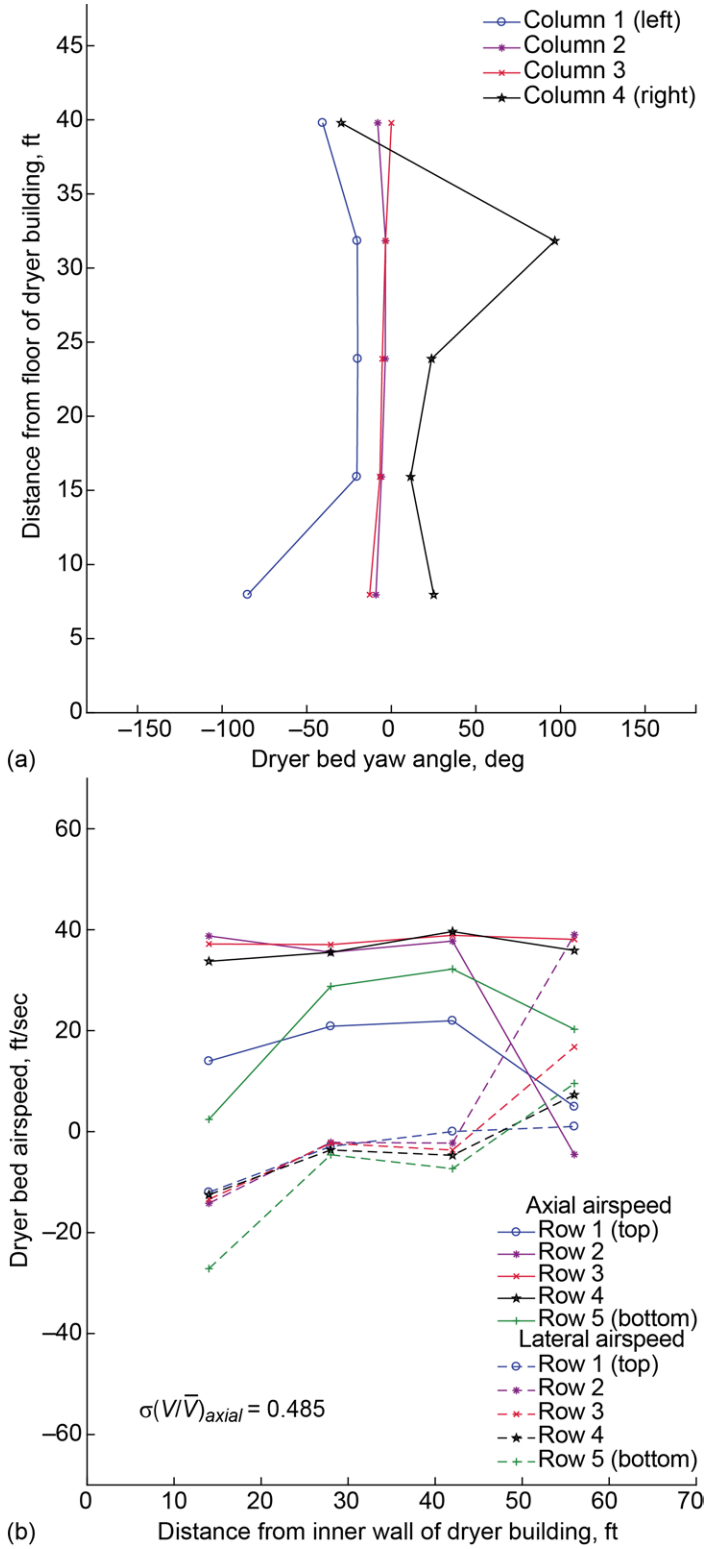

Figure 72.—Measurements from each of the 20 dryer bed wind anemometers at dryer bed inlet plane during operation of 8- by 6-Foot Supersonic Wind Tunnel (upstream looking aft). Nominally Mach 1.80 (three-motor, closed-loop operating mode). (a) Yaw flow angle. (b) Axial and lateral airspeed.

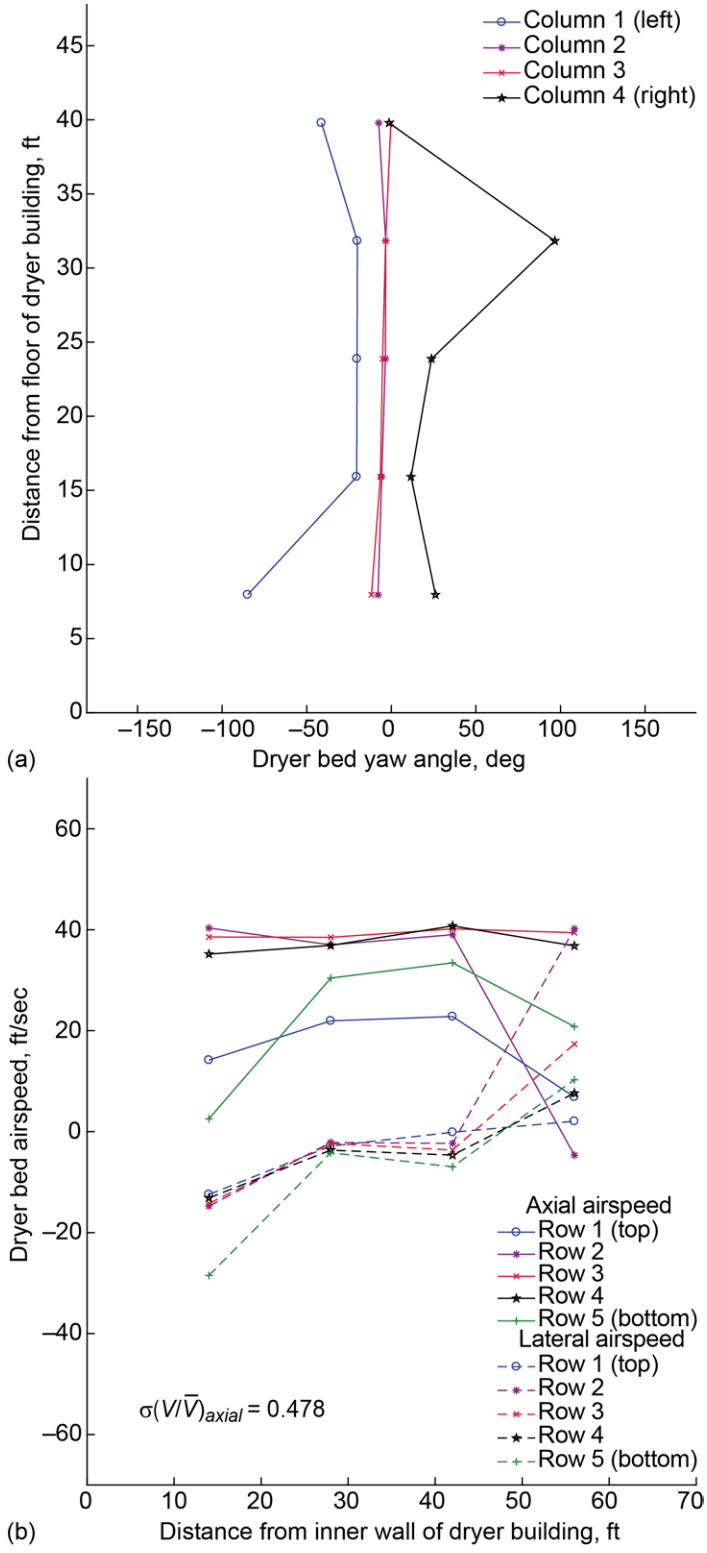

Figure 73.—Measurements from each of the 20 dryer bed wind anemometers at dryer bed inlet plane during operation of 8- by 6-Foot Supersonic Wind Tunnel (upstream looking aft). Nominally Mach 1.70 (three-motor, closed-loop operating mode). (a) Yaw flow angle. (b) Axial and lateral airspeed.

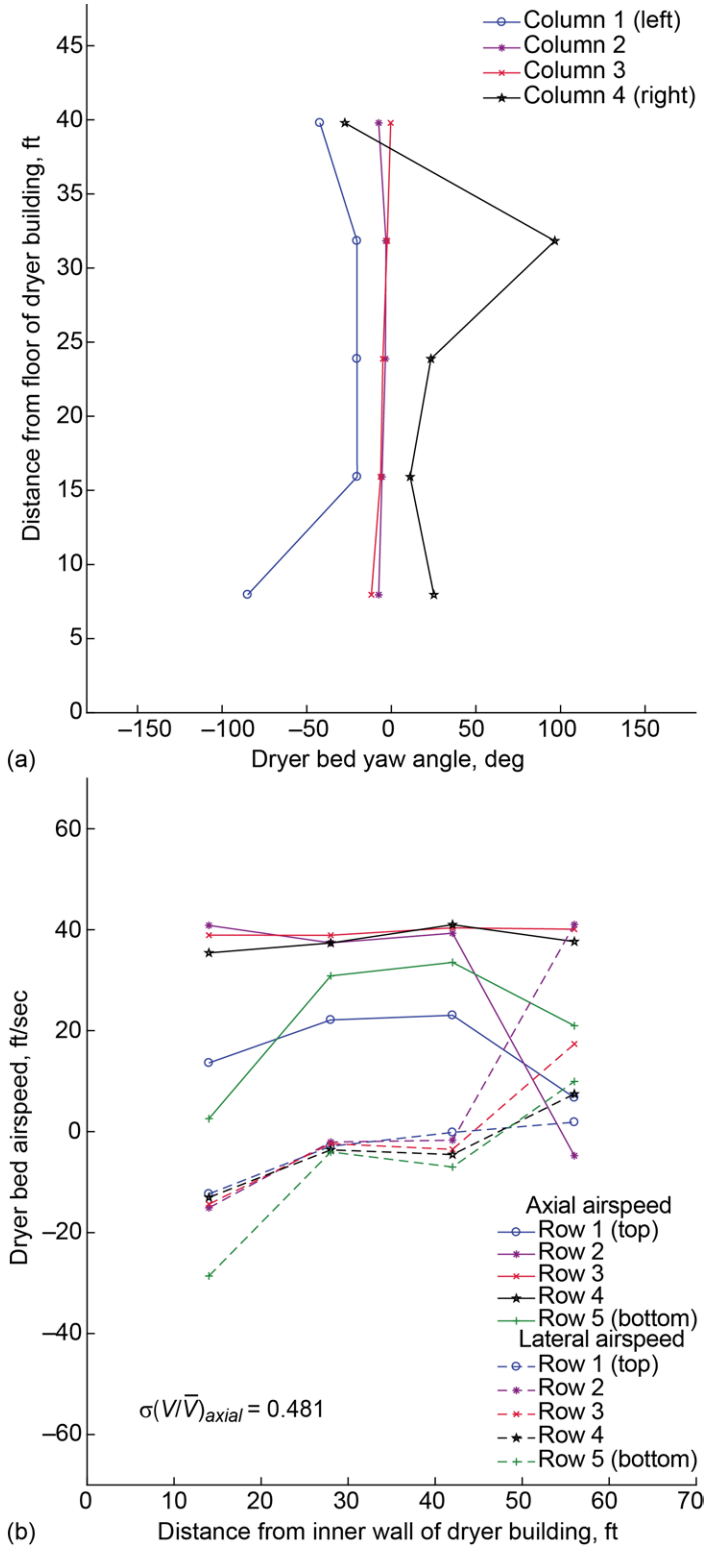

Figure 74.—Measurements from each of the 20 dryer bed wind anemometers at dryer bed inlet plane during operation of 8- by 6-Foot Supersonic Wind Tunnel (upstream looking aft). Nominally Mach 1.60 (three-motor, closed-loop operating mode). (a) Yaw flow angle. (b) Axial and lateral airspeed.

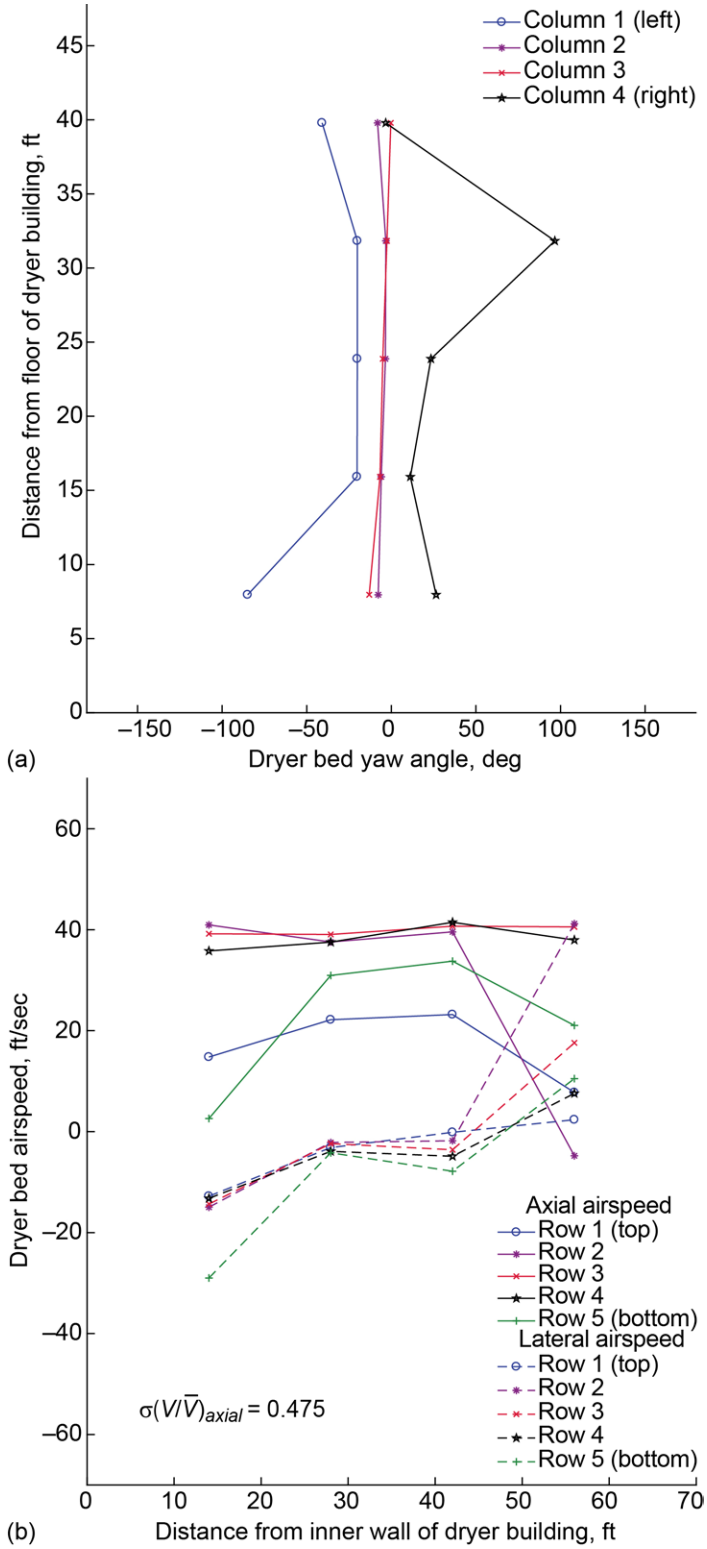

Figure 75.—Measurements from each of the 20 dryer bed wind anemometers at dryer bed inlet plane during operation of 8- by 6-Foot Supersonic Wind Tunnel (upstream looking aft). Nominally Mach 1.50 (three-motor, closed-loop operating mode). (a) Yaw flow angle. (b) Axial and lateral airspeed.

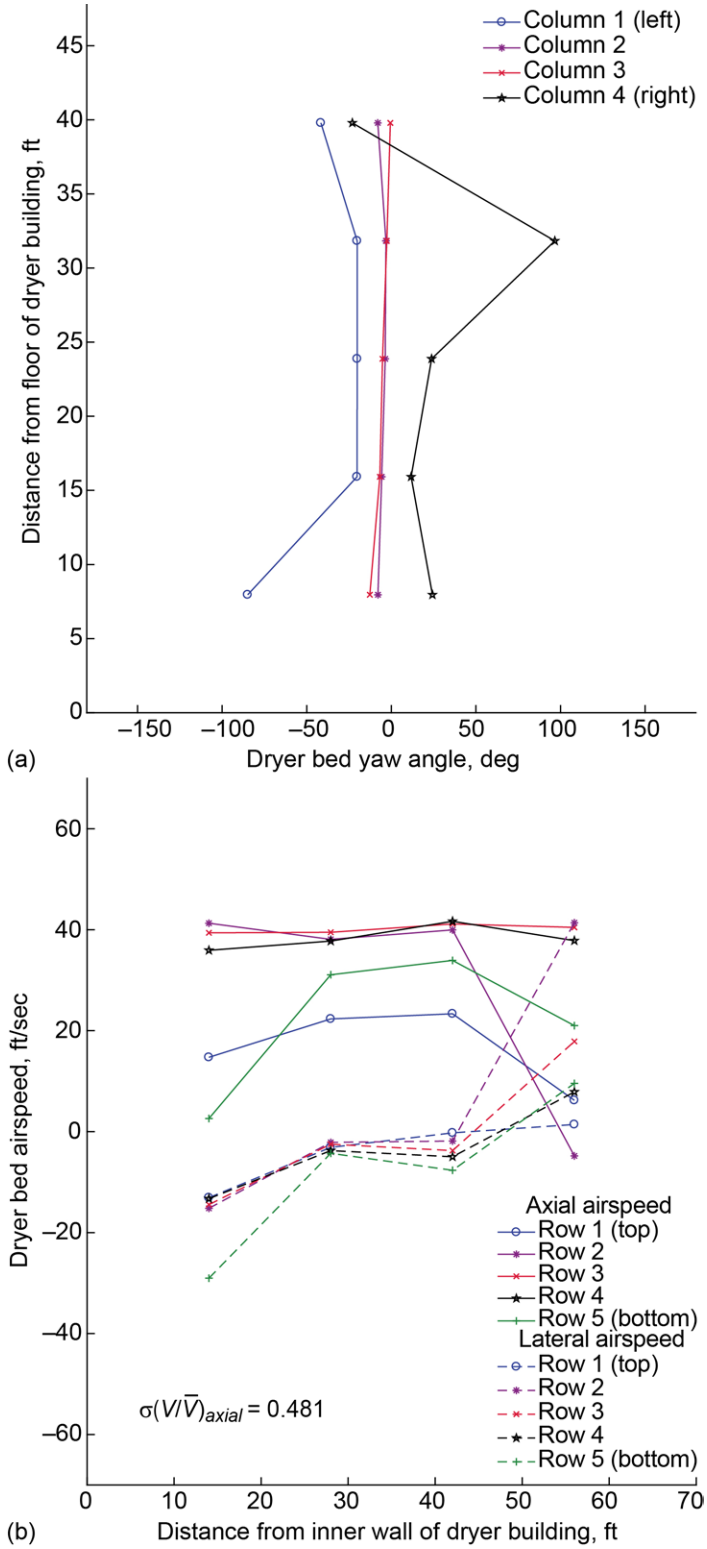

Figure 76.—Measurements from each of the 20 dryer bed wind anemometers at dryer bed inlet plane during operation of 8- by 6-Foot Supersonic Wind Tunnel (upstream looking aft). Nominally Mach 1.40 (three-motor, closed-loop operating mode). (a) Yaw flow angle. (b) Axial and lateral airspeed.

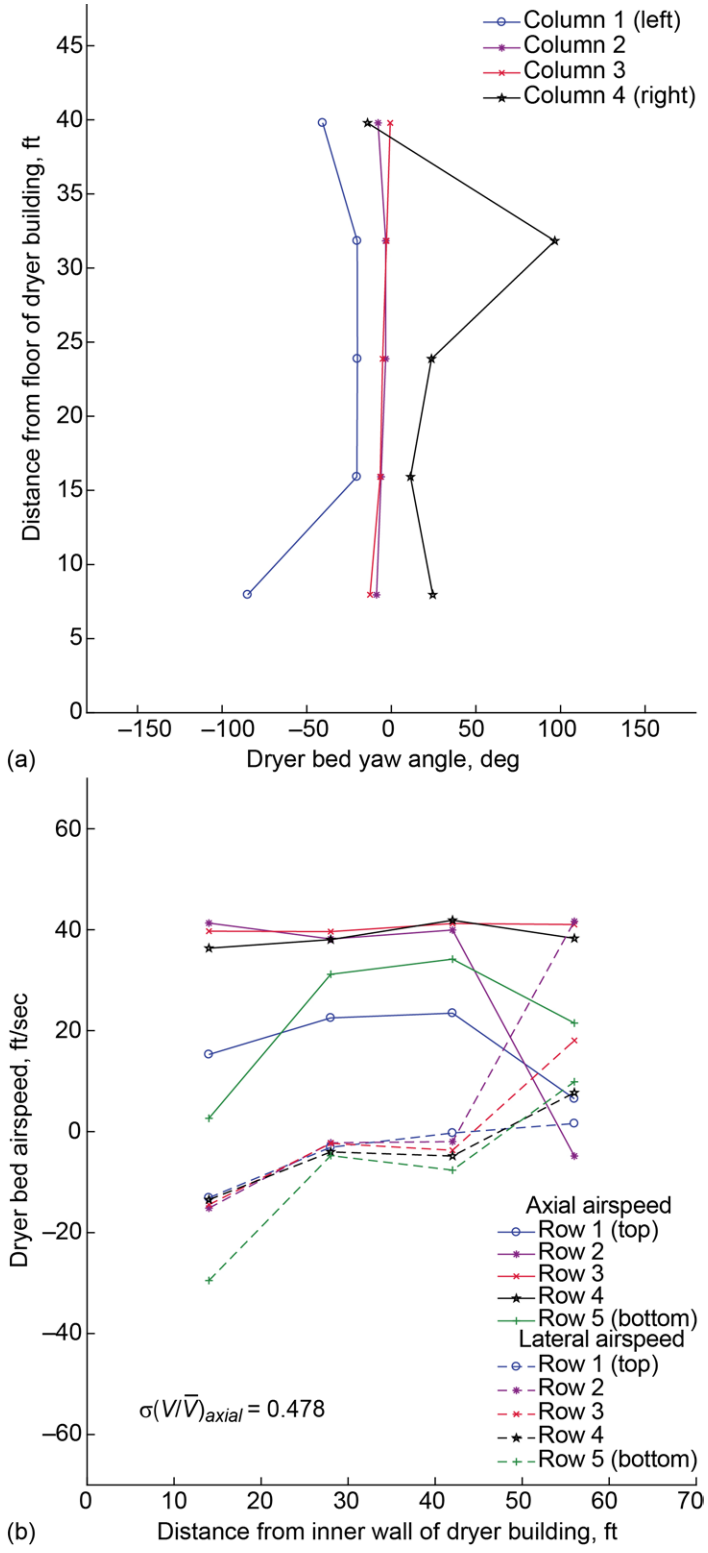

Figure 77.—Measurements from each of the 20 dryer bed wind anemometers at dryer bed inlet plane during operation of 8- by 6-Foot Supersonic Wind Tunnel (upstream looking aft). Nominally Mach 1.30 (three-motor, closed-loop operating mode with doors 4 and 5 open). (a) Yaw flow angle. (b) Axial and lateral airspeed.

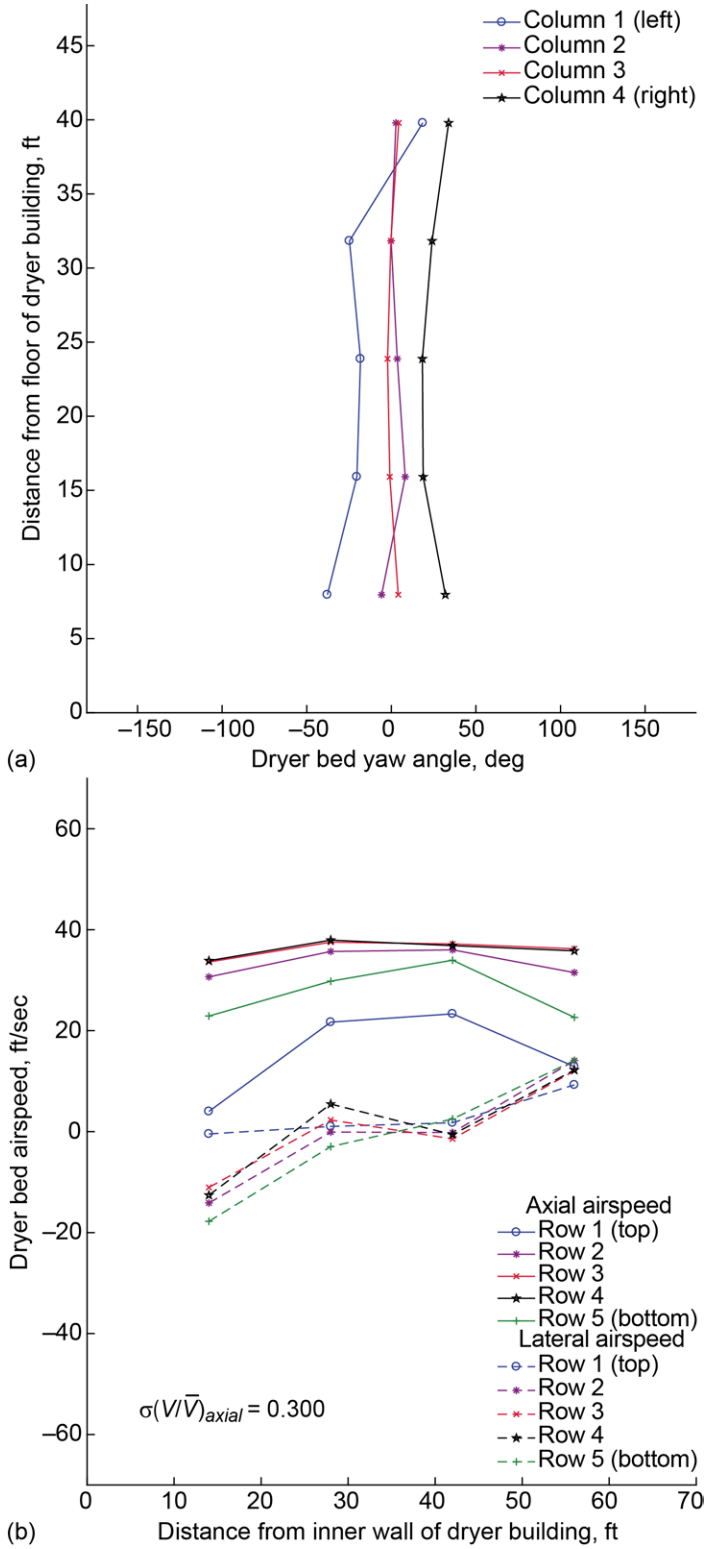

Figure 78.—Measurements from each of the 20 dryer bed wind anemometers at dryer bed inlet plane during operation of 8- by 6-Foot Supersonic Wind Tunnel (upstream looking aft). Nominally Mach 1.60 (three-motor, open-loop operating mode). (a) Yaw flow angle. (b) Axial and lateral airspeed.

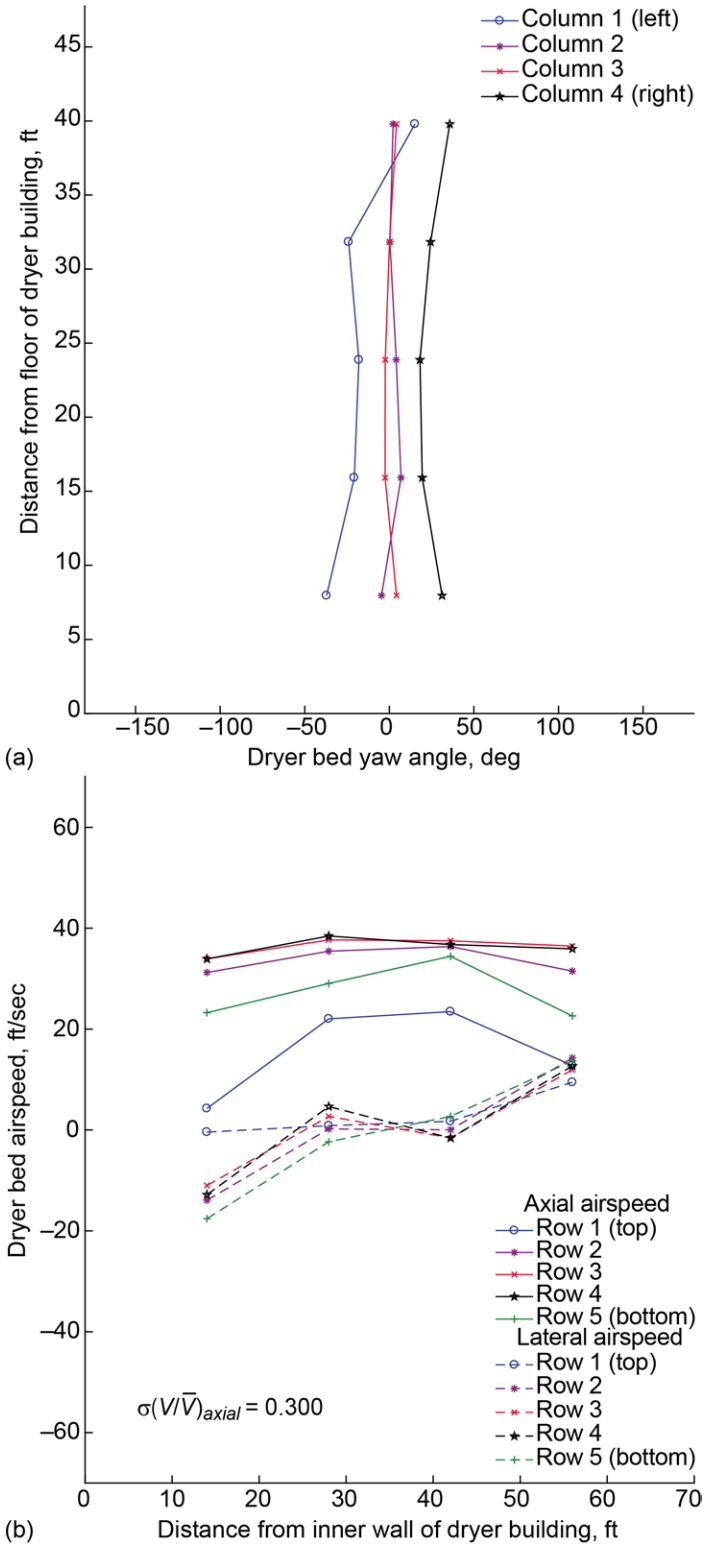

Figure 79.—Measurements from each of the 20 dryer bed wind anemometers at dryer bed inlet plane during operation of 8- by 6-Foot Supersonic Wind Tunnel (upstream looking aft). Nominally Mach 1.50 (three-motor, open-loop operating mode). (a) Yaw flow angle. (b) Axial and lateral airspeed.

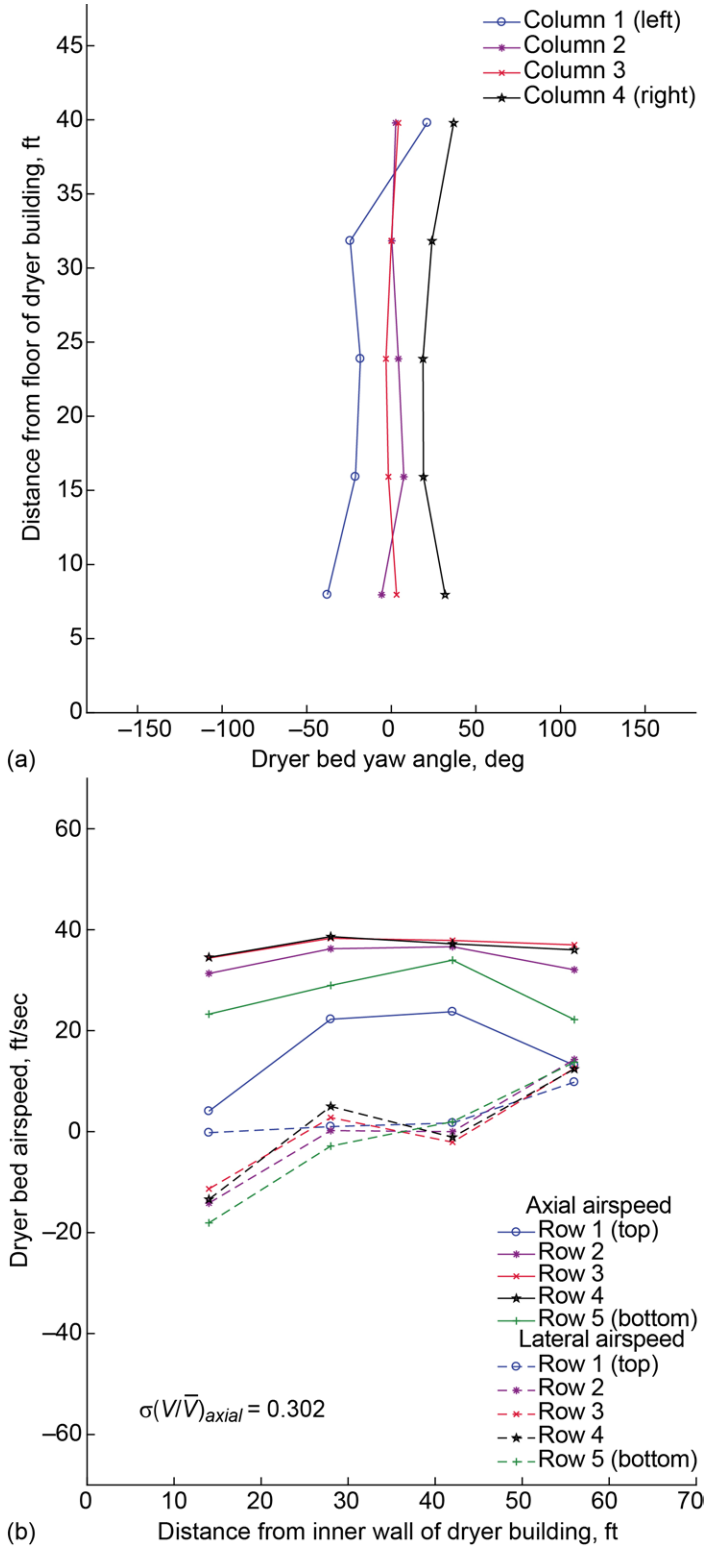

Figure 80.—Measurements from each of the 20 dryer bed wind anemometers at dryer bed inlet plane during operation of 8- by 6-Foot Supersonic Wind Tunnel (upstream looking aft). Nominally Mach 1.40 (three-motor, open-loop operating mode). (a) Yaw flow angle. (b) Axial and lateral airspeed.

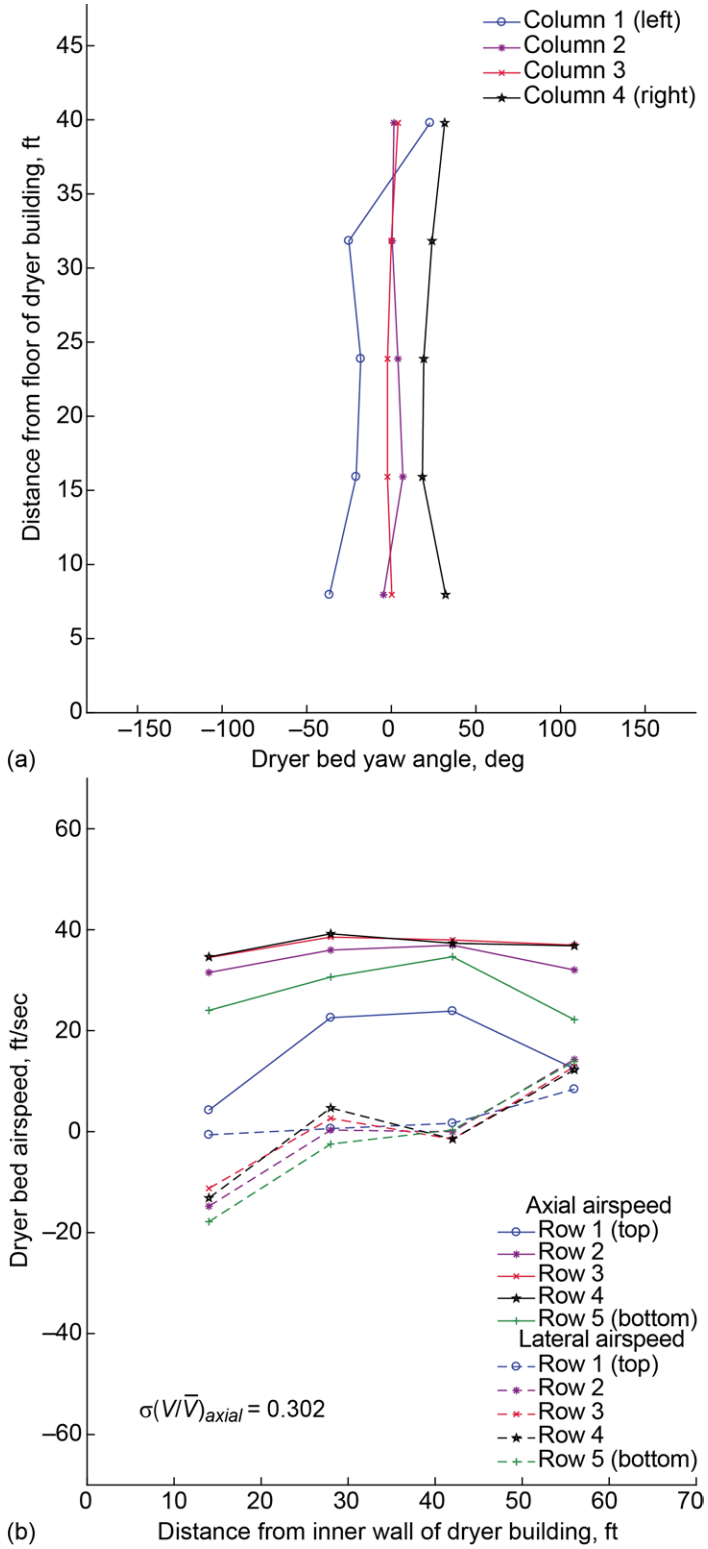

Figure 81.—Measurements from each of the 20 dryer bed wind anemometers at dryer bed inlet plane during operation of 8- by 6-Foot Supersonic Wind Tunnel (upstream looking aft). Nominally Mach 1.30 (three-motor, open-loop operating mode). (a) Yaw flow angle. (b) Axial and lateral airspeed.

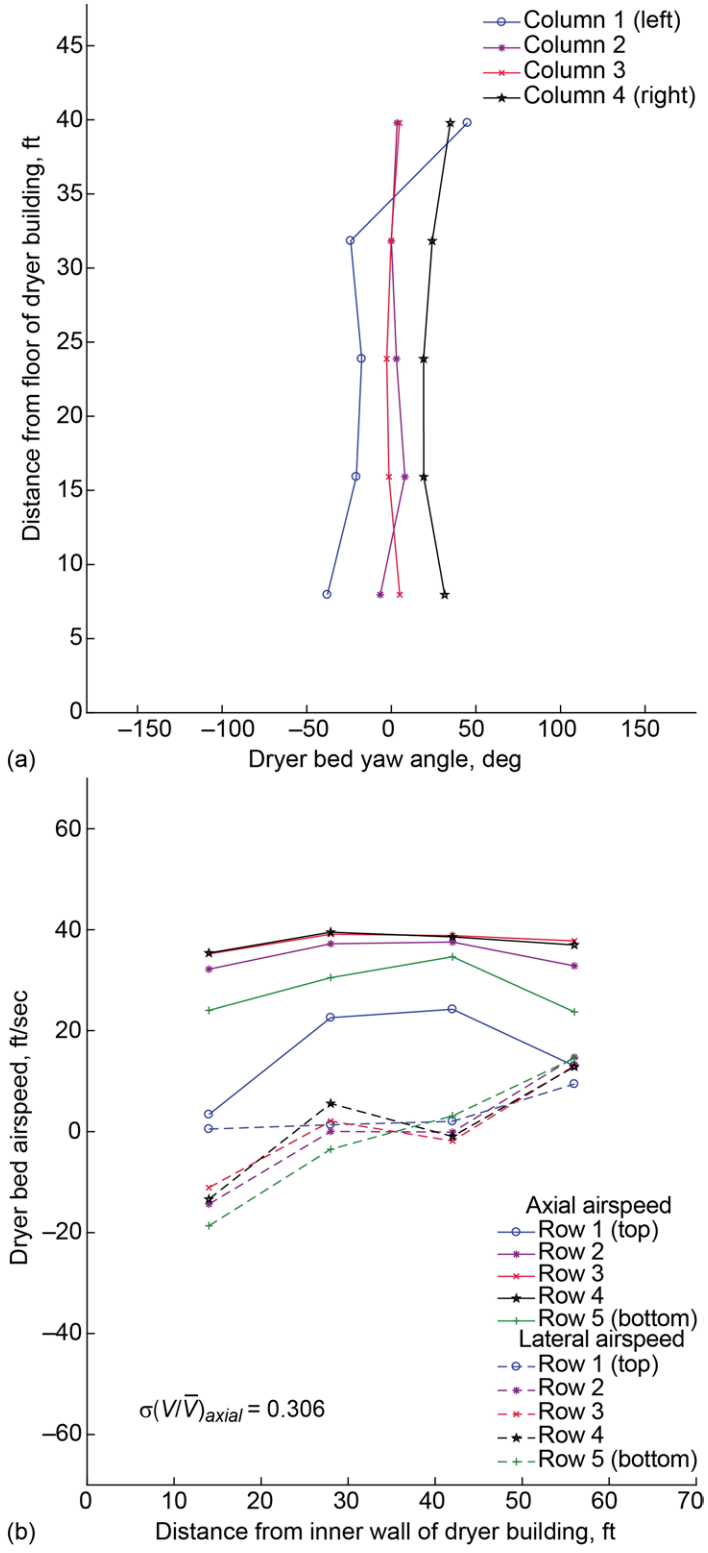

Figure 82.—Measurements from each of the 20 dryer bed wind anemometers at dryer bed inlet plane during operation of 8- by 6-Foot Supersonic Wind Tunnel (upstream looking aft). Nominally Mach 1.20 (three-motor, open-loop operating mode). (a) Yaw flow angle. (b) Axial and lateral airspeed.

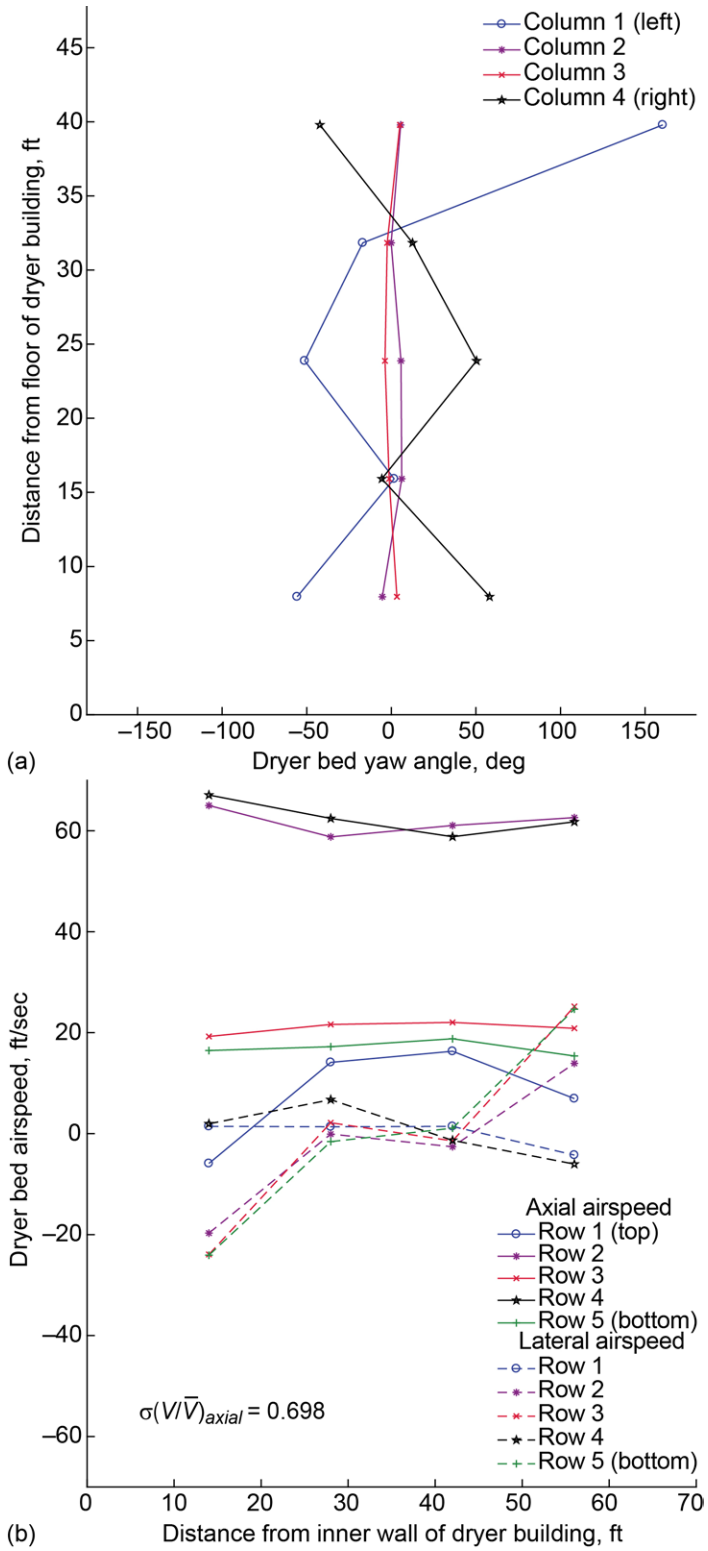

Figure 83.—Measurements from each of the 20 dryer bed wind anemometers at dryer bed inlet plane during operation of 8- by 6-Foot Supersonic Wind Tunnel (upstream looking aft). Nominally Mach 1.10 (three-motor, open-loop operating mode). (a) Yaw flow angle. (b) Axial and lateral airspeed.

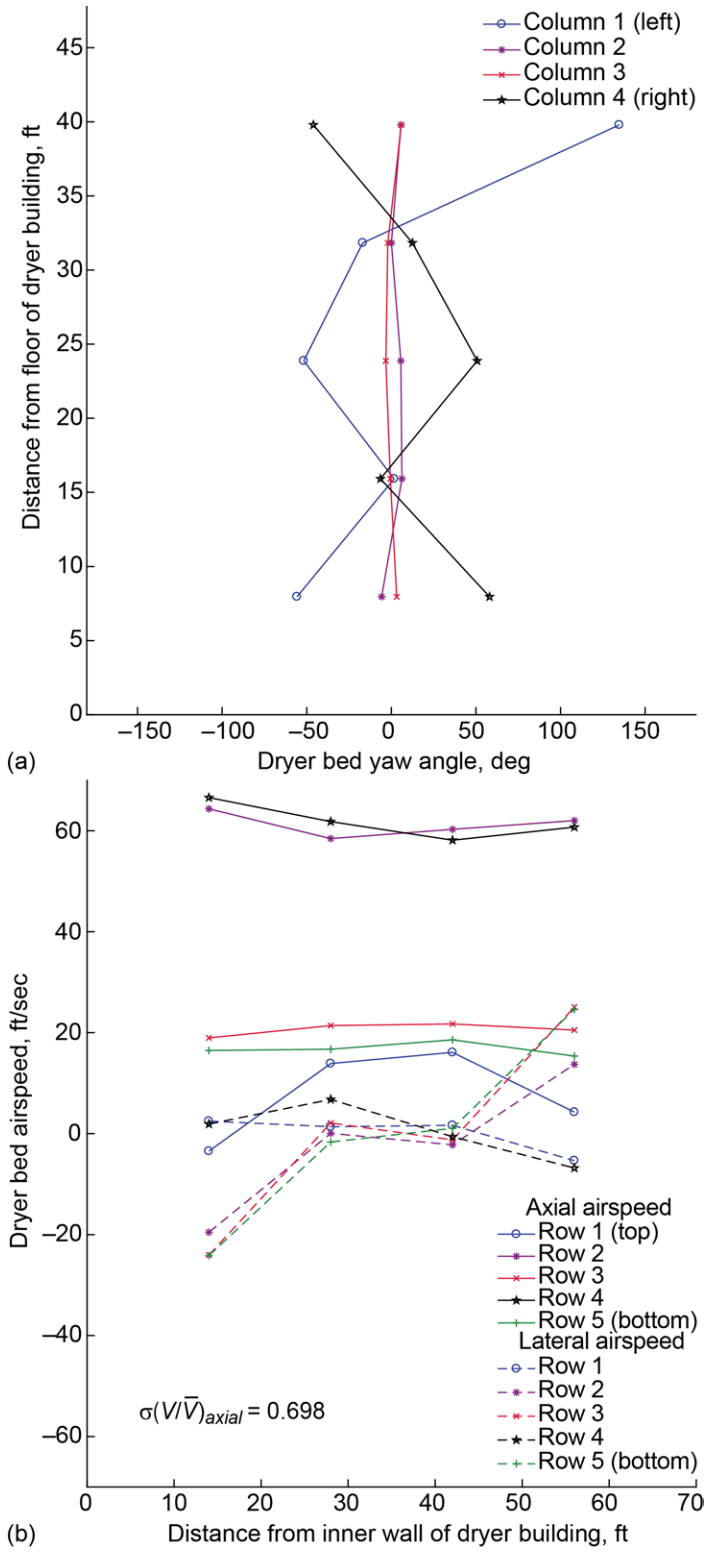

Figure 84.—Measurements from each of the 20 dryer bed wind anemometers at dryer bed inlet plane during operation of 8- by 6-Foot Supersonic Wind Tunnel (upstream looking aft). Nominally Mach 0.90 (three-motor, open-loop operating mode). (a) Yaw flow angle. (b) Axial and lateral airspeed.

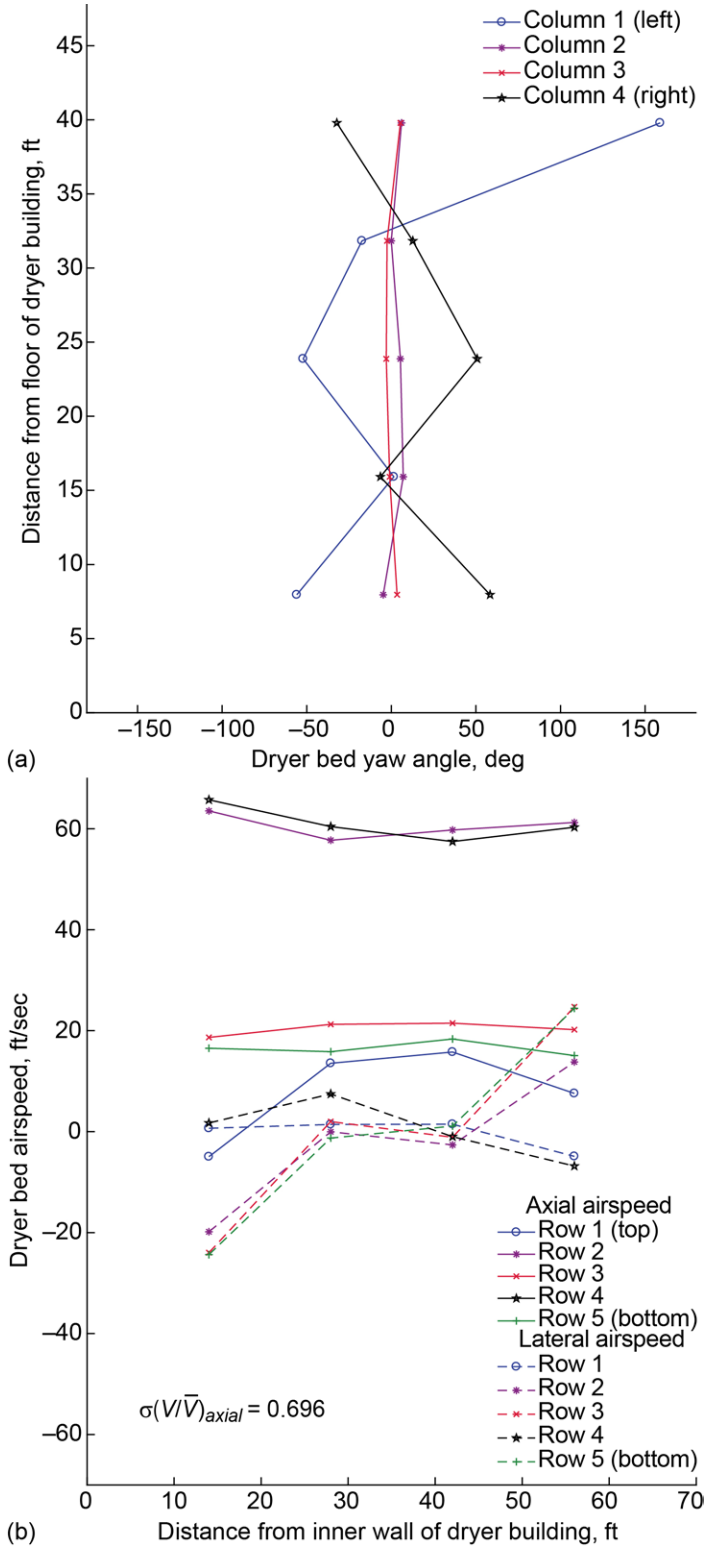

Figure 85.—Measurements from each of the 20 dryer bed wind anemometers at dryer bed inlet plane during operation of 8- by 6-Foot Supersonic Wind Tunnel (upstream looking aft). Nominally Mach 0.80 (three-motor, open-loop operating mode). (a) Yaw flow angle. (b) Axial and lateral airspeed.

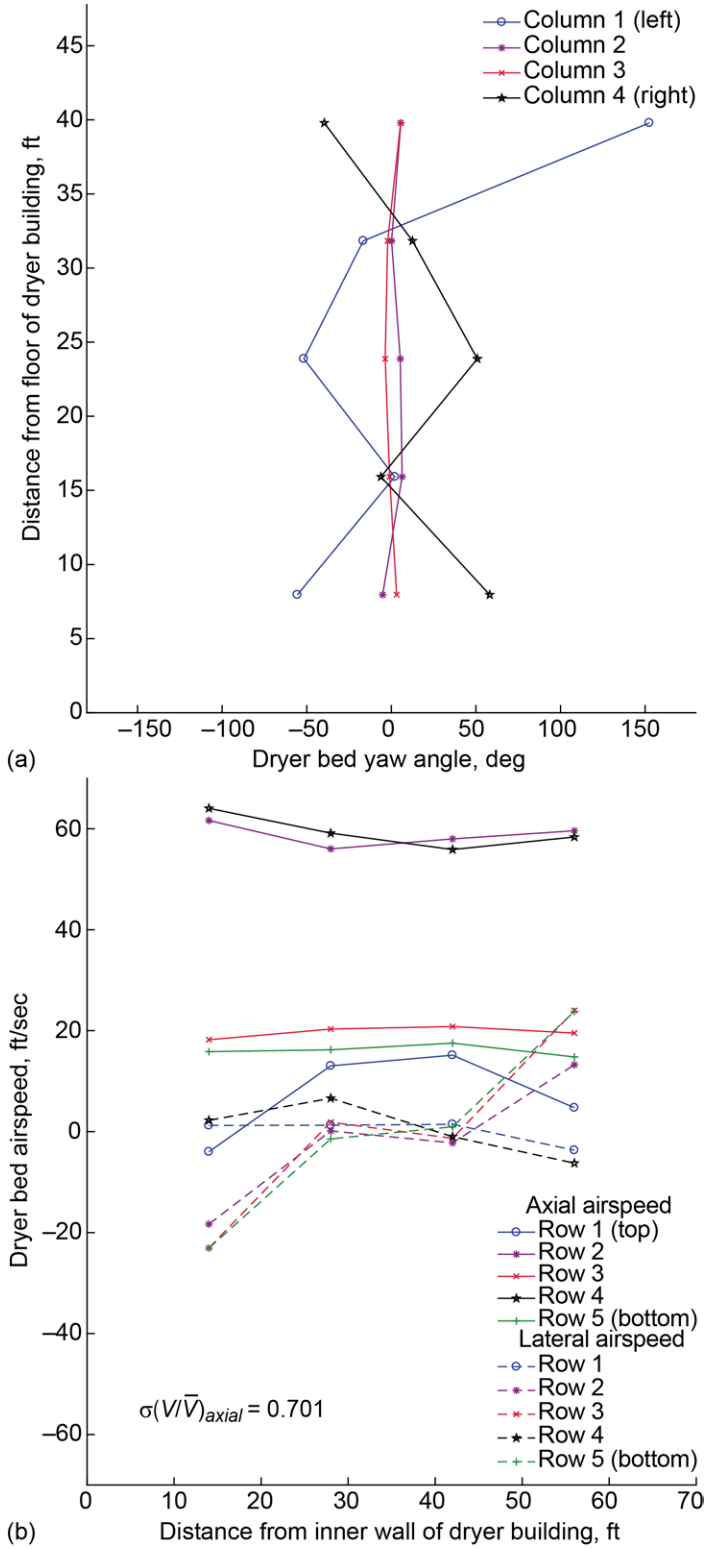

Figure 86.—Measurements from each of the 20 dryer bed wind anemometers at dryer bed inlet plane during operation of 8- by 6-Foot Supersonic Wind Tunnel (upstream looking aft). Nominally Mach 0.70 (three-motor, open-loop operating mode). (a) Yaw flow angle. (b) Axial and lateral airspeed.

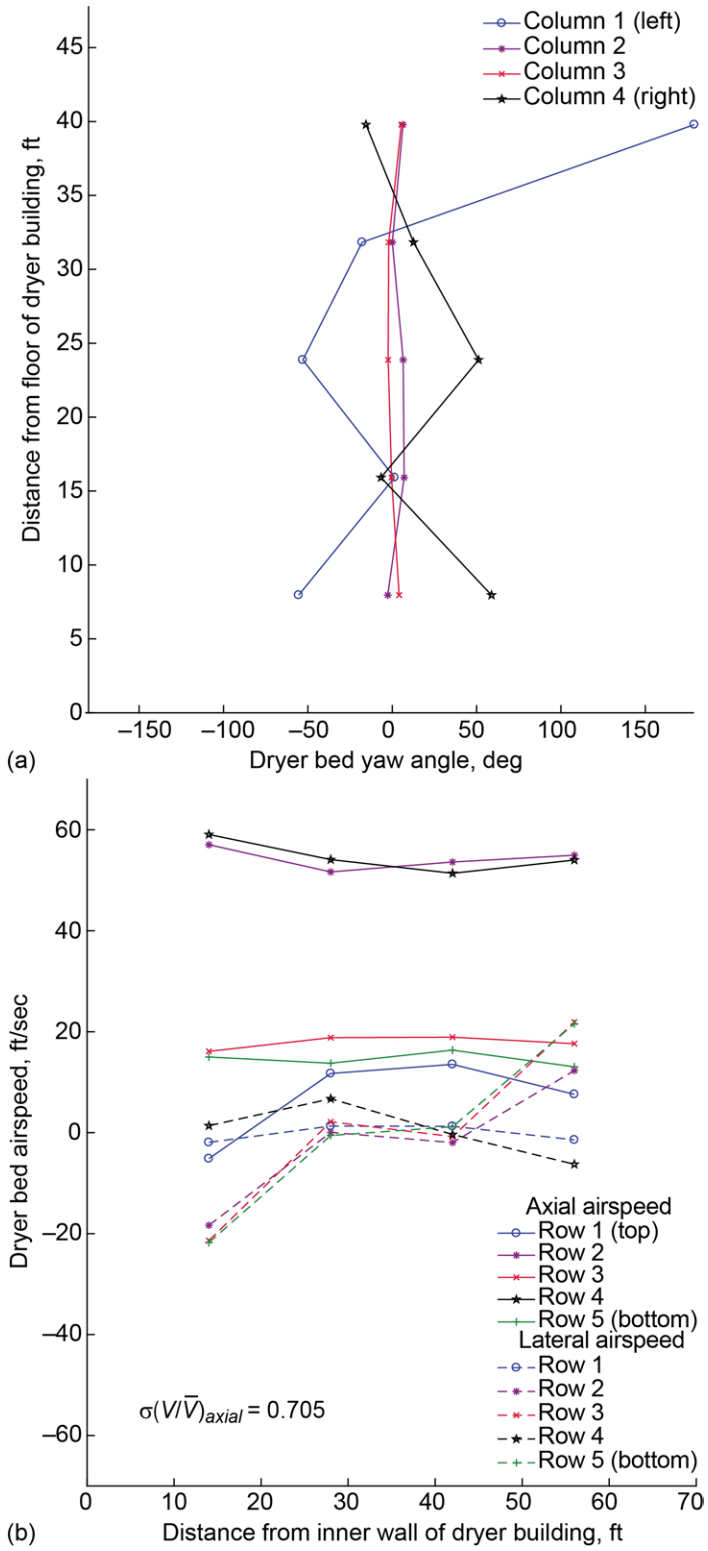

Figure 87.—Measurements from each of the 20 dryer bed wind anemometers at dryer bed inlet plane during operation of 8- by 6-Foot Supersonic Wind Tunnel (upstream looking aft). Nominally Mach 0.60 (three-motor, open-loop operating mode). (a) Yaw flow angle. (b) Axial and lateral airspeed.

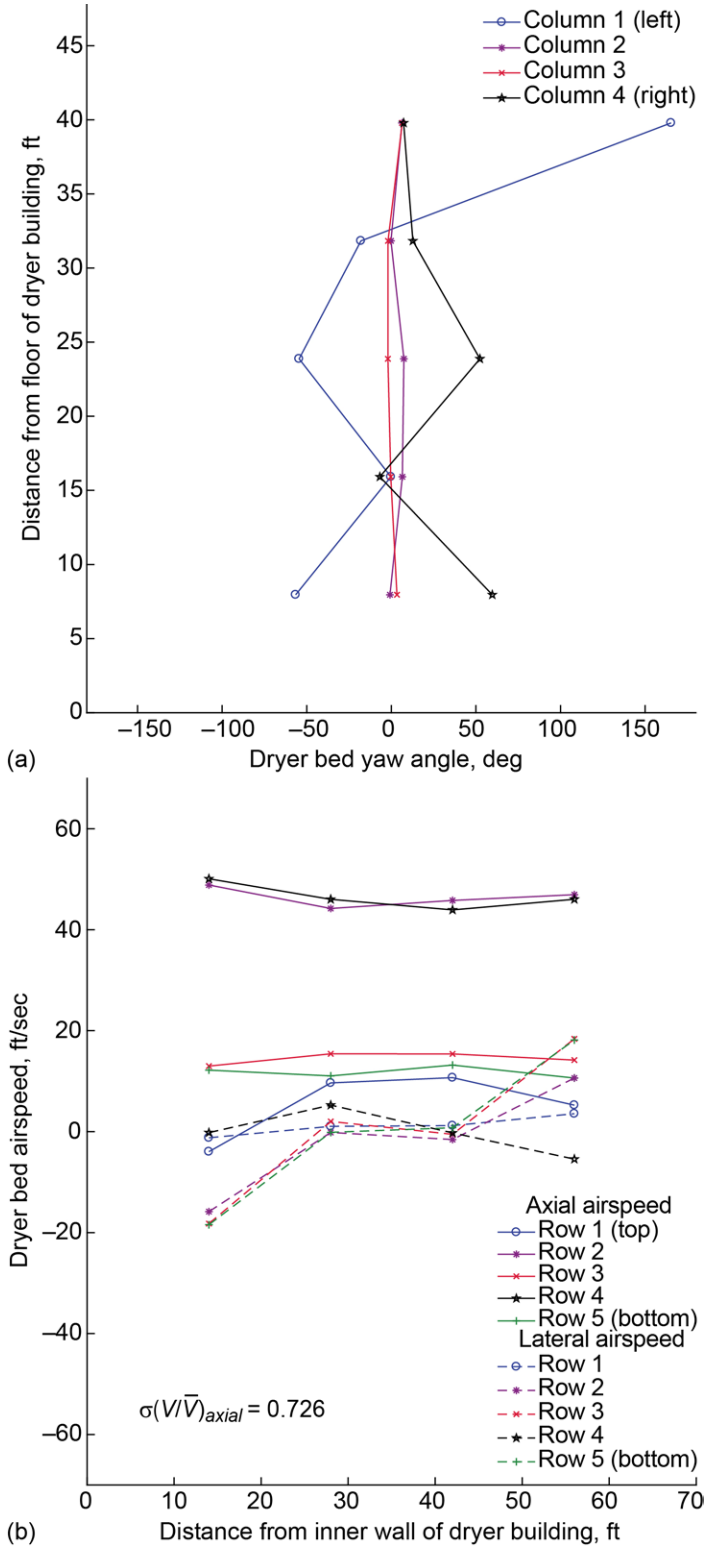

Figure 88.—Measurements from each of the 20 dryer bed wind anemometers at dryer bed inlet plane during operation of 8- by 6-Foot Supersonic Wind Tunnel (upstream looking aft). Nominally Mach 0.50 (three-motor, open-loop operating mode). (a) Yaw flow angle. (b) Axial and lateral airspeed.

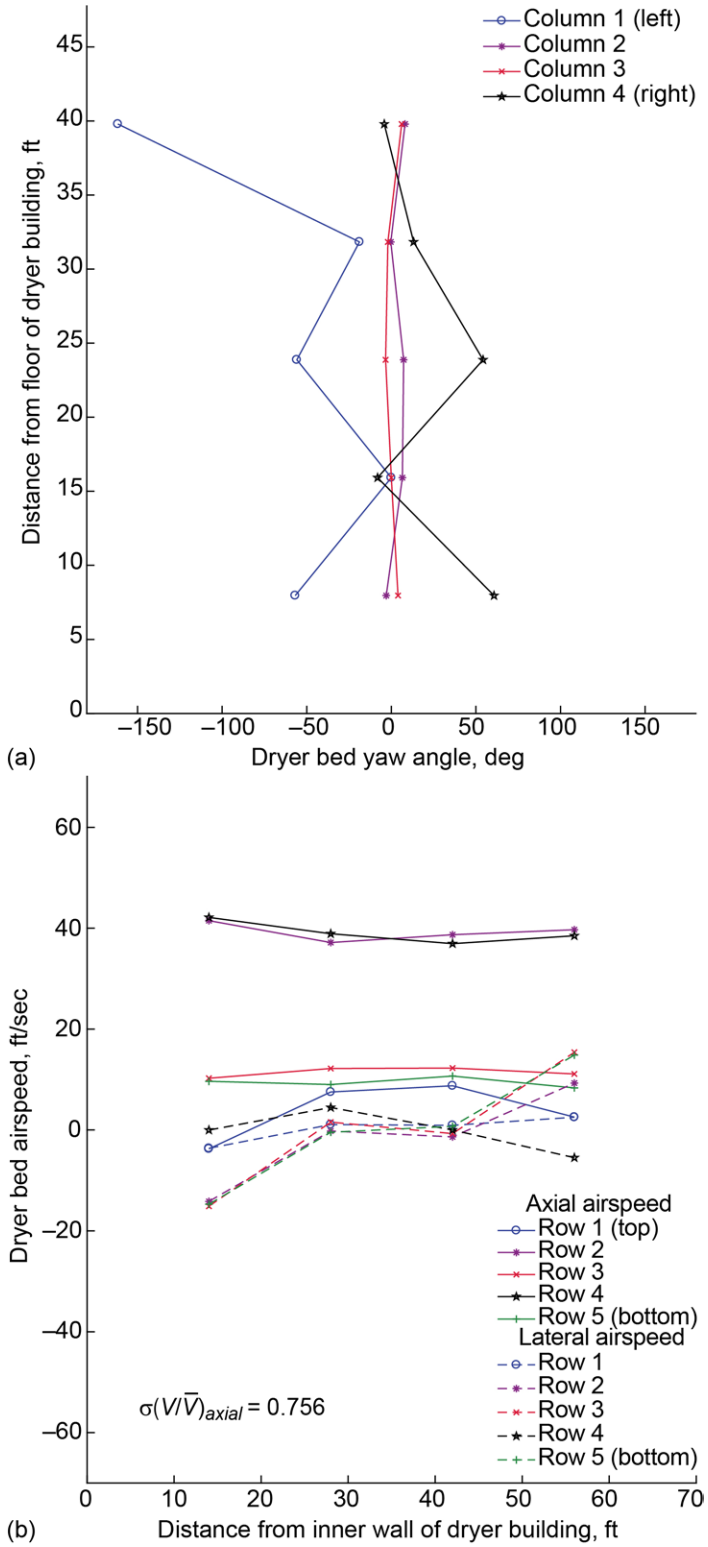

Figure 89.—Measurements from each of the 20 dryer bed wind anemometers at dryer bed inlet plane during operation of 8- by 6-Foot Supersonic Wind Tunnel (upstream looking aft). Nominally Mach 0.40 (three-motor, open-loop operating mode). (a) Yaw flow angle. (b) Axial and lateral airspeed.

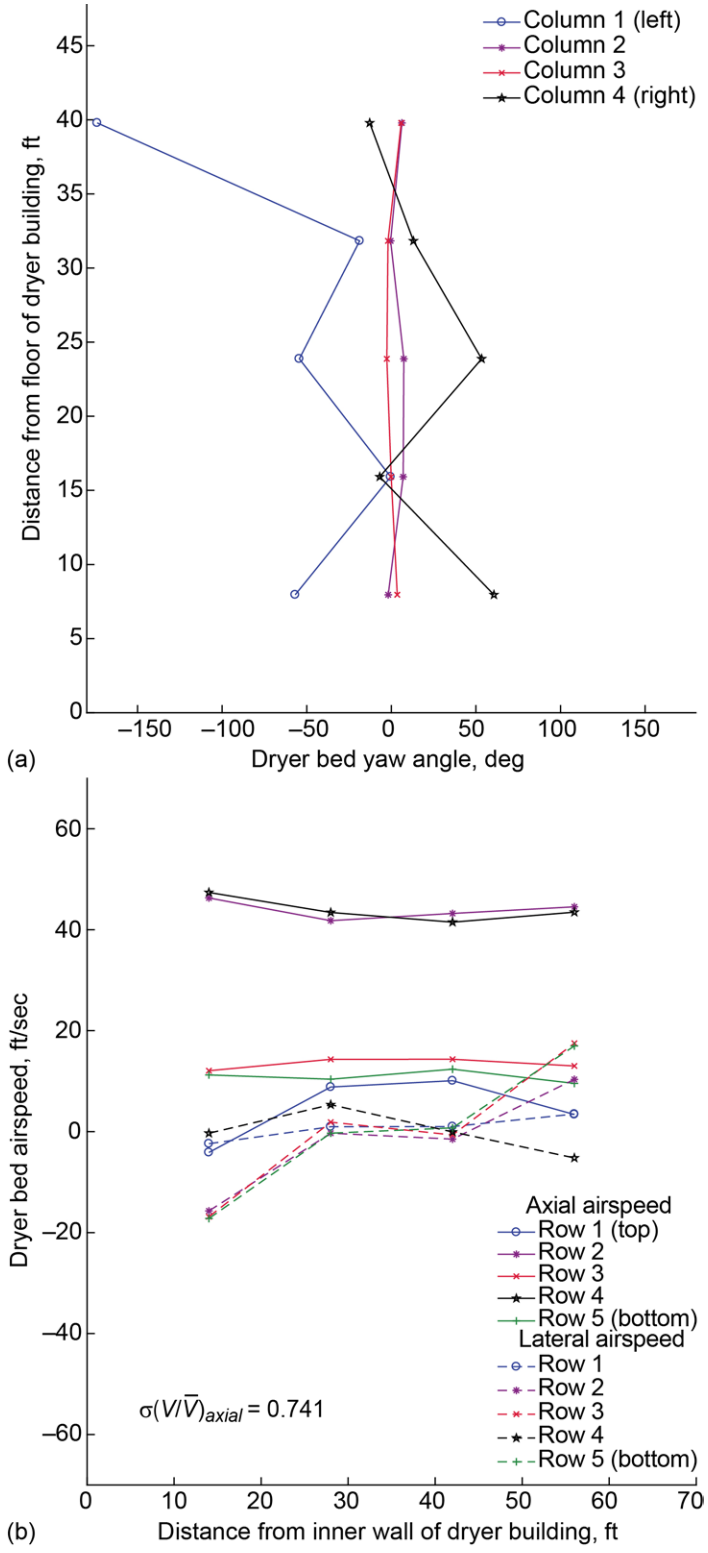

Figure 90.—Measurements from each of the 20 dryer bed wind anemometers at dryer bed inlet plane during operation of 8- by 6-Foot Supersonic Wind Tunnel (upstream looking aft). Nominally Mach 0.50 (one-motor, open-loop operating mode). (a) Yaw flow angle. (b) Axial and lateral airspeed.

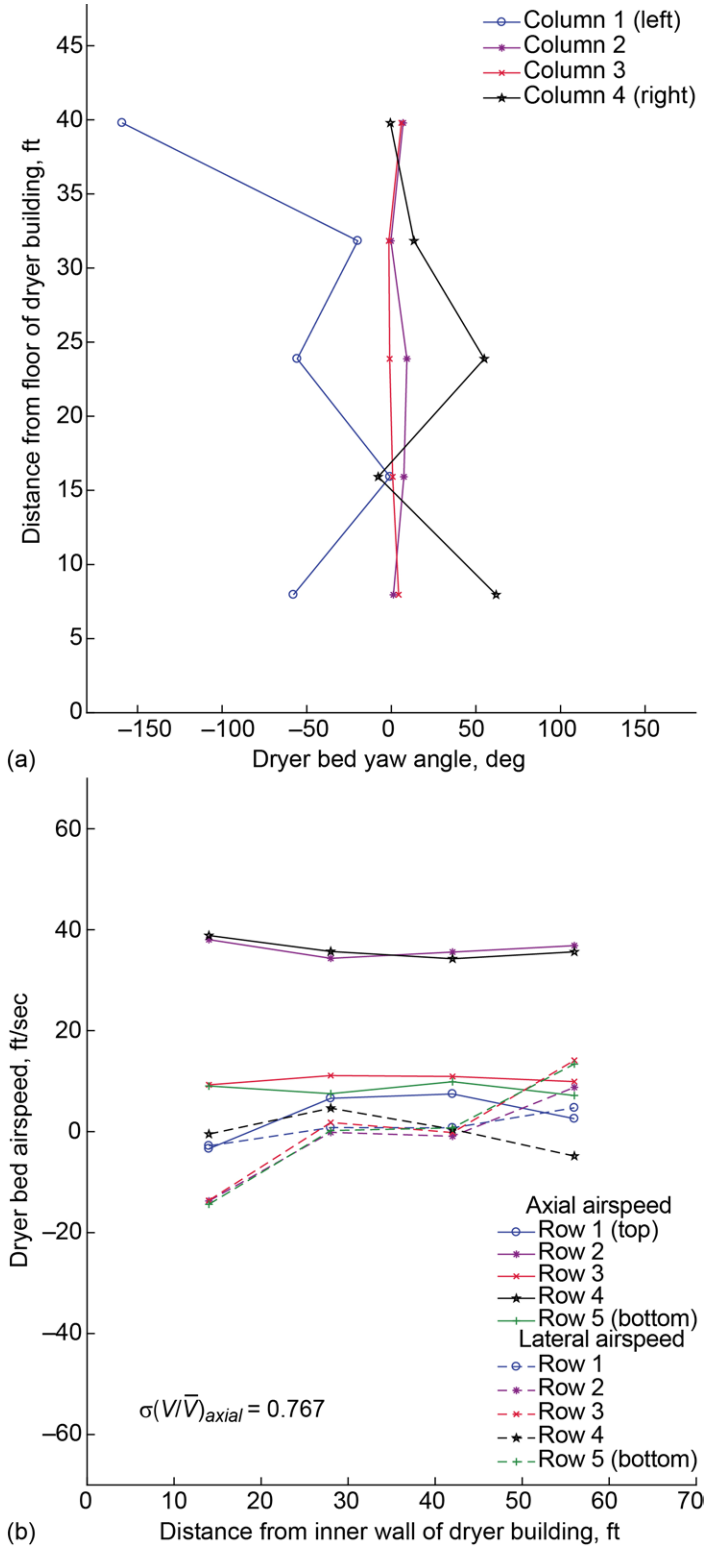

Figure 91.—Measurements from each of the 20 dryer bed wind anemometers at dryer bed inlet plane during operation of 8- by 6-Foot Supersonic Wind Tunnel (upstream looking aft). Nominally Mach 0.40 (one-motor, open-loop operating mode). (a) Yaw flow angle. (b) Axial and lateral airspeed.

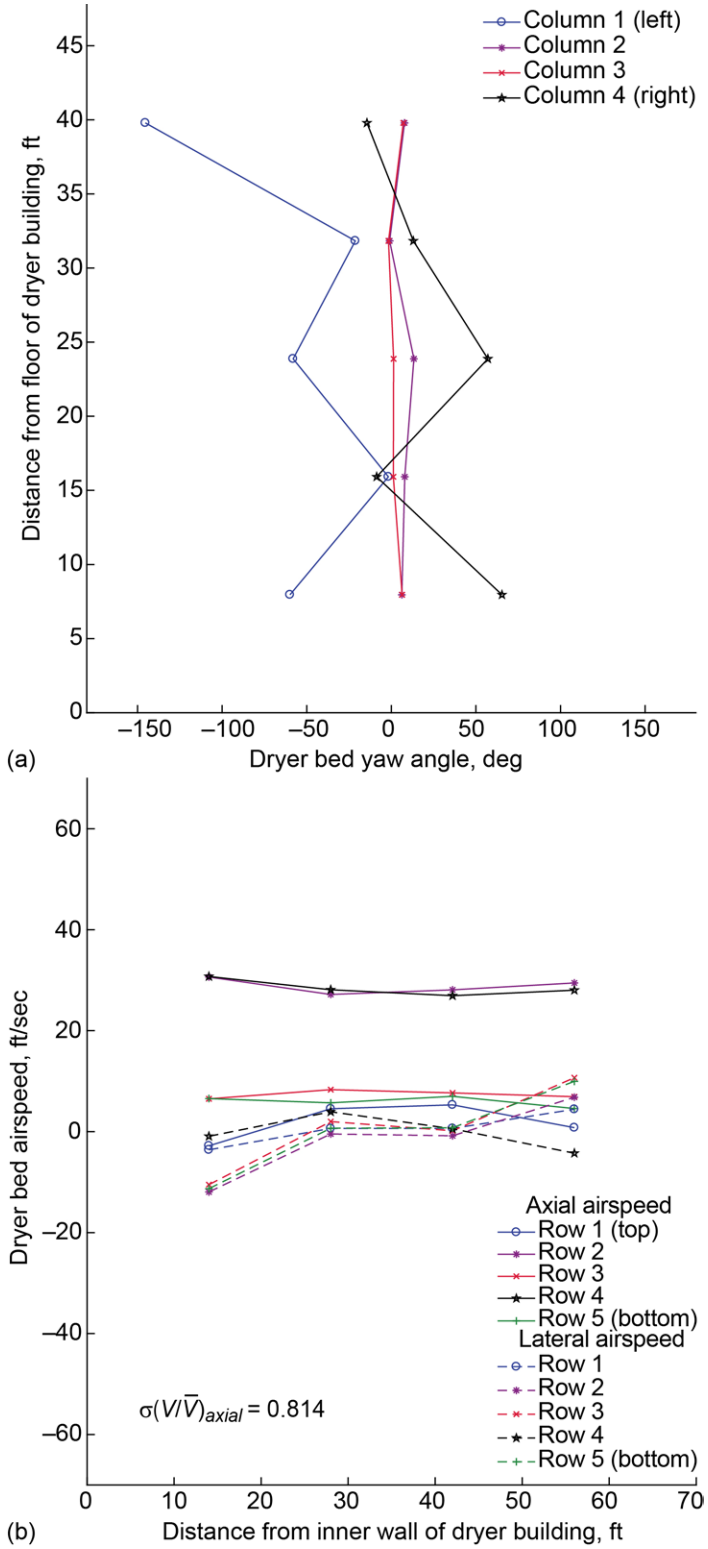

Figure 92.—Measurements from each of the 20 dryer bed wind anemometers at dryer bed inlet plane during operation of 8- by 6-Foot Supersonic Wind Tunnel (upstream looking aft). Nominally Mach 0.30 (one-motor, open-loop operating mode). (a) Yaw flow angle. (b) Axial and lateral airspeed.

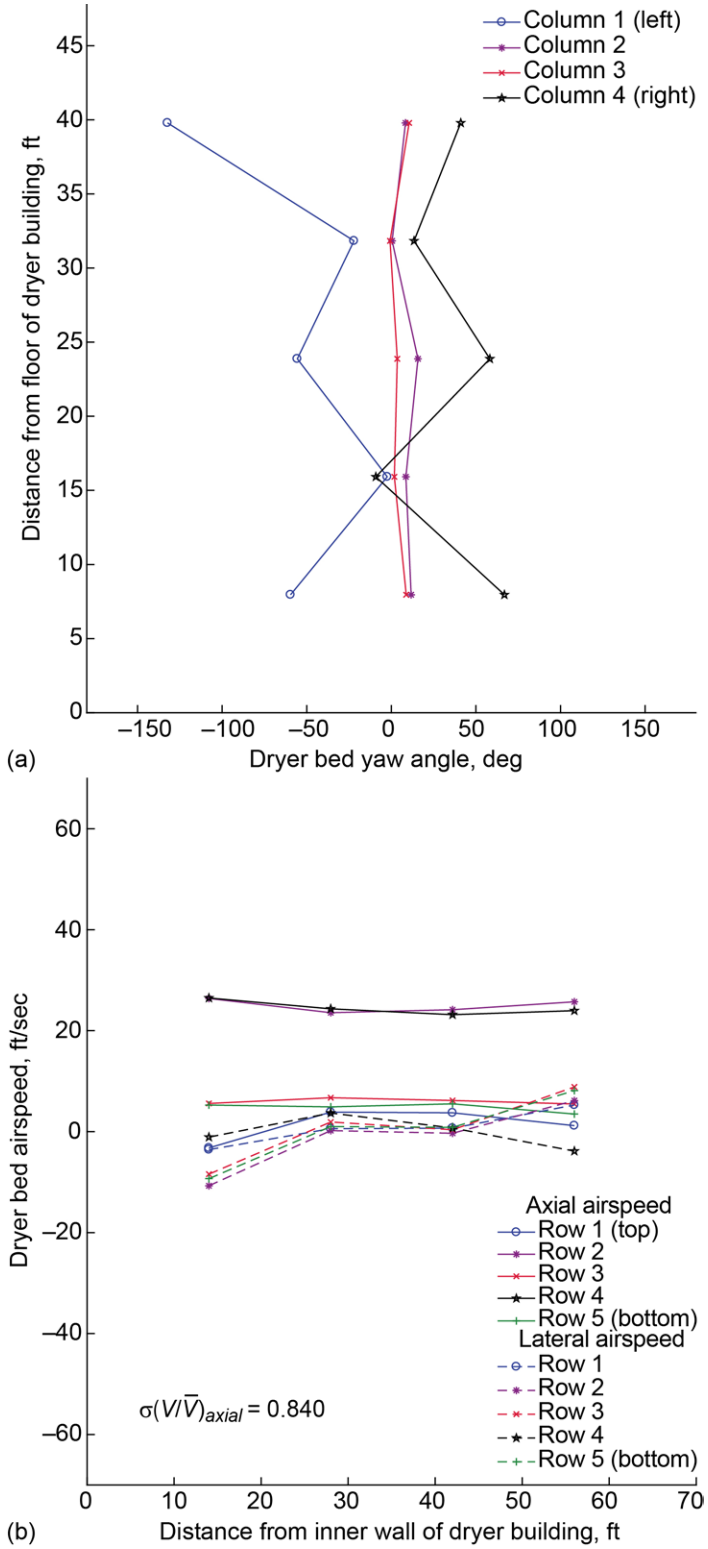

Figure 93.—Measurements from each of the 20 dryer bed wind anemometers at dryer bed inlet plane during operation of 8- by 6-Foot Supersonic Wind Tunnel (upstream looking aft). Nominally Mach 0.25 (one-motor, open-loop operating mode). (a) Yaw flow angle. (b) Axial and lateral airspeed.